MIKES Metrology
Espoo 2007

Measurement Traceability and Uncertainty in Machine Vision Applications

Björn Hemming

Dissertation for the degree of Doctor of Science in Technology to be presented with due permission of the Department of Electrical and Communications Engineering, for public examination and debate in Auditorium S1 at Helsinki University of Technology (Espoo, Finland) on the 17th of December 2007, at 12 noon.

Abstract

During the past decades increasing use of machine vision in dimensional measurements has been seen. From a metrological view every serious measurement should be traceable to SI units and have a stated measurement uncertainty. The first step to ensure this is the calibration of the measurement instruments. Quality systems in manufacturing industry require traceable calibrations and measurements. This has lead to a good knowledge of measurement accuracy for traditional manual hand-held measurement instruments. The entrance of rather complex computerised machine vision instruments and optical coordinate measuring machines, at the production lines and measurement rooms, is a threat or at least a challenge, to the understanding of the accuracy of the measurement. Accuracies of algorithms for edge detection and camera calibration are studied in the field of machine vision, but uncertainty evaluations of complete systems are seldom seen. In real applications the final measurement uncertainty is affected by many factors such as illumination, edge effects, the operator, and non-idealities of the object to be measured.

In this thesis the use of the GUM (Guide to the Expression of Uncertainty in Measurement) method is applied for the estimation of measurement uncertainty in two machine vision applications. The work is mainly limited to two-dimensional applications where a gray-scale camera is used. The described equipment for calibration of micrometers using machine vision is unique. The full evaluation of measurement uncertainty in aperture diameter measurements using an optical coordinate measuring machine is presented for the first time.

In the presented applications the uncertainty budgets are very different. This confirms the conclusion, that a detailed uncertainty budget is the only way to achieve an understanding of the reliability of dimensional measurements in machine vision. Uncertainty budgets for the type of the two described machine vision applications have never previously been published.

Tiivistelmä

Viime vuosikymmenien aikana konenäkö on yleistynyt yhä enemmän geometrisissä mittauksissa. Metrologisesta näkökulmasta jokaisen mittauksen olisi oltava jäljitettävissä SI-yksikköjärjestelmään ja jokaisella mittauksella tulisi olla tunnettu mittausepävarmuus. Kaupallisesta näkökulmasta on tärkeää, että tavaran mitattavista ominaisuuksista ei synny mittausvirheistä johtuvia kiistoja ostajan ja myyjän välillä. Jos mittausepävarmuus on tunnettu, niin kalibroinnilla saadaan aikaan jäljitettävyys perussuureeseen. Jäljitettävyys konenäkösovelluksissa pituuden SI-yksikköön metriin saadaan aikaan pitkällä katkeamattomalla jäljitettävyysketjulla. Konepajoissa laatujärjestelmät ovat jo pitkään edellyttäneet, että mittalaitteet ovat jäljitettävästi kalibroitu. Jokaiseen kalibrointiin liittyy myös mittausepävarmuuslaskelma, jossa tärkeimmät epävarmuuslähteet ovat mallinnettu. Optisten koordinaattimittauskoneiden sekä muiden konenäköön perustuvien mittausjärjestelmien mutkikkuus on suuri haaste mittausepävarmuuslaskelman laatimiselle. Konenäkö sekä tarkkuuskysymykset konenäössä ovat paljon tutkittuja aiheita, mutta kokonaisten mittausjärjestelmien epävarmuuslaskelmia laaditaan edelleenkin erittäin harvoin. Epävarmuustekijöitä, jotka olisi otettava huomioon, ovat valaistuksen, reunojen ja käyttäjän valintojen vaikutus yhdessä mitattavan kappaleen mahdollisten puutteellisuuksien kanssa.

Tässä työssä tutkitaan GUM-menetelmän (Guide to the Expression of Uncertainty in Measurement) käyttöä kolmessa konenäkösovelluksessa, joille esitetään epävarmuuslaskelma. Neljäs esitettävä sovellus on apertuurien halkaisijan mittaaminen optisella koordinaattimittauskoneella. Ensimmäistä kertaa tällaiselle sovellukselle esitetään mittausepävarmuuslaskelma. Työn johtopäätöksenä on, että yksityiskohtaisen epävarmuuslaskelman laatiminen on ainut keino saada käsitys mittauksen virhelähteistä. Työ on rajattu kaksidimensionaalisiin mittauksiin, joissa käytetään yhtä harmaasävykameraa.

Preface

The research work behind this thesis is done at MIKES (Centre for Metrology and Accreditation) as several research and development projects. A part of work described in this thesis began when the author worked at VTT (Technical Research Centre of Finland) during 1989 to 2000. The dimensional measurement group at VTT moved to MIKES in 2000, due to a re-organization and strengthening of metrology in Finland.

The author is in gratitude to Prof. Timo Hirvi and Prof. Ulla Lähteenmäki for offering research possibilities to the author. The author also wants to thank Dr Heikki Isotalo for giving the initial inspiration to write this thesis. The author also greatly indebted to his supervisor Prof. Erkki Ikonen for encouragement and inspiration. I thank the Academy of Finland for financial support for this project.

The author wishes to thank Lic.Sc (Tech) Heikki Lehto for ideas and advice. The author wishes also to thank Dr Antti Lassila for ideas and support. The author is grateful to Mrs Jenni Kuva for proofreading this thesis. The author is grateful to M.Sc. (Tech.) Ilkka Palosuo, Mr Asko Rantanen, M.Sc. Anu Fagerholm (former Tanninen) and Mr Hannu Sainio at VTT for substantial co-work in projects related to this dissertation. In the last phase of this work the author received spiritual support and many helpful hints from M.Sc. Virpi Korpelainen, Dr Kaj Nyholm and Dr Mikko Merimaa. The author thanks Mrs. Kirsi Tuomisto and M.Sc. (Tech.) Milla Kaukonen for help with the final editing of the thesis. The author also thanks Prof. Henrik Haggrén at the laboratory of Photogrammetry at TKK (Helsinki University of Technology) for views and ideas

Furthermore I want to thank all my colleagues at MIKES and especially my colleagues Ilkka, Raimo, Jarkko and Veli-Pekka, in the length group for help, patience and support during the years at the new MIKES.

Last but not least I thank my wife Marja-Riitta and daughters Ella and Malin.

Björn Hemming

List of Publications

This thesis consists of an overview and the following selection of the author's publications.

Publ. I

B. Hemming, I. Palosuo, and A. Lassila, "Design of Calibration Machine for Optical Two-Dimensional Length Standards", in Proc. SPIE, Optomechatronical Systems III, Vol. 4902, pp. 670-678 (2002).

Publ. II

B. Hemming, E. Ikonen, and M. Noorma, "Measurement of Aperture Diameters using an Optical Coordinate Measuring Machine", *International Journal of Optomechatronics*, **1**, 297–311 (2007).

Publ. III

B. Hemming and H. Lehto, "Calibration of Dial Indicators using Machine Vision," *Meas. Sci. Technol.* **13,** 45-49 (2002).

Publ. IV

B. Hemming, A. Fagerholm, and A. Lassila, "High-accuracy Automatic Machine Vision Based Calibration of Micrometers", *Meas. Sci. Technol.* **18**, 1655-1660 (2007).

Authors Contribution

The development of the equipment described in Publ. I was a team project, where the responsibility of the author was the machine vision hardware and software development. The software was written with the assistance of M.Sc. (Tech.) Ilkka Palosuo. The role of M.Sc. (Tech.) Ilkka Palosuo was the design of the mechanics of the instrument. For Publ. I the author prepared the manuscript and the uncertainty budget.

For Publ. II the author performed all measurements and analyses alone with the exception of the verification with probing CMM (Coordinate Measuring Machine), which was carried out together with M.Sc. (Tech.) Ilkka Palosuo. For Publ. II the author prepared the manuscript.

For Publ. III the author designed and built the instrument and wrote the software. The author also carried out all of the measurements and the uncertainty analysis. For Publ. III the author prepared the manuscript.

For Publ. IV the author designed and built the instrument. The software was written with the assistance of M.Sc. Anu Fagerholm. The author made all of the measurements and all of the research work including the uncertainty analysis. For Publ. IV the author prepared the manuscript.

The spread of the years of publication was partly due to the moving process to the new MIKES building in 2005.

List of abbreviations

1D	One dimensional
2D	Two dimensional
3D	Three dimensional
BIPM	International Bureau of Weights and Measures/ Bureau International des Poids et Mesures
CCD	Charged coupled device
CCIR	Comité International des Radiocommunications
CMC	Calibration and Measurement Capability
CMM	Coordinate Measuring Machine
EAL	European Cooperation for Accreditation of Laboratories
GUM	Guide to the Expression of Uncertainty in Measurement
LED	Light-emitting diode
METAS	Bundesamt für Metrologie
MIKES	Centre for Metrology and Accreditation/ Mittatekniikan keskus
NIST	National Institute of Standards and Technology
NMI	National Measurement Institute
NPL	National Physical Laboratory
PTB	Physikalisch Technische Bundesanstalt
SPIE	The International Society for Optical Engineering
TKK	Helsinki University of Technology (formerly abbreviated HUT)
VDI/VDE	Verein Deutscher Ingenieure/Verband der Elektrotechnik,
VTT	Technical Research Centre of Finland

List of symbols

dx	Distortion in x-axis
dy	Distortion in y-axis
k	Coverage factor
k_1	Coefficient for 2nd order radial distortion
k_2	Coefficient for 4th order radial distortion
ρ	Distance from image centre
S_x	Scale factor for x-axis
S_y	Scale factor for y-axis
$u(x)$	Standard uncertainty for the input estimate
$u_c(y)$	Combined standard uncertainty
x	Input estimate
X	Input quantity
Xp	Undistorted x-coordinate of a point in the image
y	Estimate of measurand
Y	Measurand
Yp	Undistorted y-coordinate of a point in the image

Table of contents

Abstract i
Tiivistelmä ii
Preface iii
List of publications iv
Authors contribution v
List of abbreviations vi
List of symbols vii

1. Introduction 1
2. Measurement Traceability and Uncertainty 4
   2.1. Measurement Traceability 4
   2.2. Measurement Uncertainty 7
   2.3. Research Question 9
   2.4. Progress in this work 10
3. Calibration of Reference Standards for Machine vision 13
   3.1. Calibration of 2D standards 13
   3.2. Development of equipment for calibration of 2D standards 15
   3.3. Discussion 18
4. The Use of Optical Coordinate Measuring Machines 20
   4.1. Introduction to CMM 20
   4.2. Task specified uncertainty for CMM 22
      Sensitivity analysis 23
      Experimental method using calibrated objects 23
      Computer simulation and virtual CMM 24
   4.3. Measurement of apertures using an optical CMM 25
      Verification measurements 28
   4.4. Discussion 29
5. Machine Vision Based Calibration Equipment 30
   5.1. Introduction to Machine Vision 30
   5.2. Camera Calibration in Machine Vision 33
      An example of camera calibration 34
   5.3. Calibration of Dial Indicators with Machine Vision 35
   5.4. Calibration of Micrometers with Machine Vision 37
   5.5. Discussion 41
6. Conclusions 44

References 47

1. Introduction

In the manufacturing industry the tradition of systematic measurements is long. At the time of the first industrial revolution, James Watt invented the screw micrometer in 1772 [1]. One important step was the invention of gauge blocks in 1896 by C. E. Johansson in Sweden [2]. For the manufacturing industry the gauge blocks have been the basic reference in the calibration of simple handheld instruments such as callipers and micrometers. The first coordinate measuring machine (CMM) with three axes was manufactured by the Swiss company SIP already in 1930. An important invention for machine vision was the CCD camera, developed in the 1960s.

Systematic measurement with known uncertainty is one of the foundations of science and technology. Measurements are central in industrial quality control and in most modern industries the costs bound up in taking measurements constitute 10-15 % of production costs [3]. Quality management is important in any industry where the product is assembled from hundreds of parts, which have to fit together. Therefore, the measuring instruments are calibrated and the users must have knowledge of the measuring uncertainties when they verify that the products are within specified tolerances. If the product is not within specified tolerances, it is useless to send it to the customer. If the product seems to be within specifications, but rejected by the customer, the economic loss is even bigger. Therefore, there is a clear connection between understanding of measurement errors and economics.

In addition to the aforementioned requirements, another challenge is the demand for more accurate measurements. In figure 1 this demand, as seen by the National Physical laboratory (NPL) is illustrated. This increasing demand of accuracy is not narrowed to special cases or small volume production. An example from mass production where high accuracy is needed is the manufacturing of hard disk components and fuel injection systems [4].

During the last 20 years many advances in measurement instruments have also caused new challenges for uncertainty evaluation. First digital data processing made it possible to develop programmable CMM's. Then machine vision [5, 6] was developed and used for inspection and measuring tasks in industry.

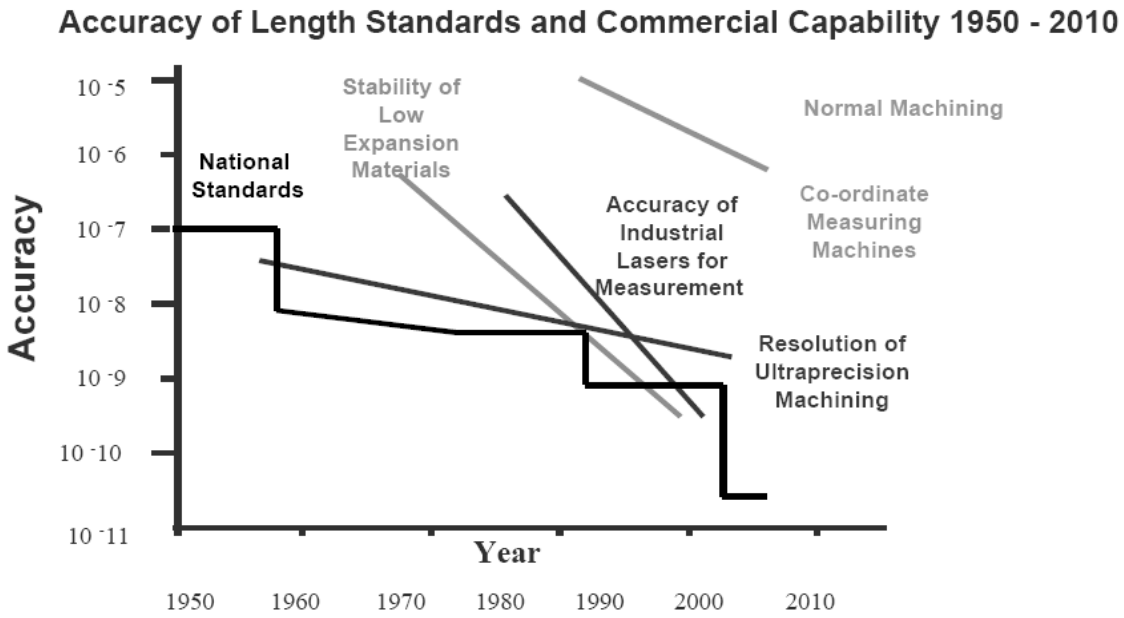

Figure 1. The demand for lower measurement uncertainty in dimensional measurements [7]

Finally, during the last ten years machine vision capabilities were installed to some CMM's and the Video Measuring Machine or optical CMM was developed. However, some new problems have emerged. According to Ref. [8] the uncertainty for CMM measurements is in many cases simply a guess from an experienced operator. Moreover, there are situations where intuition and experience may fail dramatically [9]. In machine vision, which is a younger technology than CMM, the situation is roughly the same or even worse. Machine vision has, during the recent years, gained from the cheaper computing costs. This means that more and more machine vision applications are developed all the time.

The amount of work and complexity in a measurement uncertainty calculation corresponds to the complexity of the measurement. If a part was previously measured

using a mechanical vernier or micrometer calliper and is now measured by machine vision, a lot of work would be needed to find the error sources of the new system. It seems that the measurement uncertainty and traceability chain is no longer as well known as it was before. In this thesis it is shown how traceability and measurement uncertainty are achievable in machine vision applications using the GUM method [10].

2. Measurement Traceability and Uncertainty

In 1799 in Paris, the Metric System was established by the deposition of two platinum standards representing the metre and the kilogram. This was the first beginning of the present International System of Units, the SI system [11]. From year 1983 the definition of the metre is given as the length of the path traveled by light in vacuum during a time interval of 1/299 792 458 of a second. Some concepts in the practical realisation work of the SI-unit metre are described in the following.

2.1. Measurement Traceability

A traceability chain is an unbroken chain of comparisons, all having stated uncertainties. This ensures that a measurement result or the value of a standard is related to references at the higher levels, ending at the realisation of the definition of the unit.

The definition of calibration according to Ref. [12] is the following: “Set of operations that establish, under specified conditions, the relationship between values of quantities indicated by a measuring instrument or measuring system, or values represented by a material measure or a reference material and the corresponding values realised by standards.” The most important measuring instruments in length and dimensional metrology are the laser interferometers, line scales, gauge blocks, ring gauges and form standards. Important reference standards used in coordinate metrology are step gauges and ball plates. All instruments and reference standards have to be calibrated regularly [13]. The result of the calibration is a certificate usually containing a table where instrument readings can be compared to reference values. It is then up to the end user how he will use the certificate and its results.

Sometimes the procedure, when a scale factor between a transducer output and a physical unit is established, is also called calibration. In machine vision literature there are many articles about camera calibration. Usually the purpose is to define the relation between the captured image and world coordinates.

Every measurement intended to be reliable should have a traceability chain to the corresponding definition of the SI-unit (figure 2). At MIKES there are six iodine-stabilized lasers. Thanks to advances in laser technology the traceability for these secondary frequency standards was recently achieved from a femtosecond frequency comb [14, 15]. The traceability to the frequency comb comes from a primary frequency standard, a Cs atomic clock. The wavelengths of the lasers of the primary interferometers are calibrated against the wavelengths of the iodine-stabilized lasers. These primary interferometers are then used to calibrate other reference instruments, such as gauge blocks, step gauges, line-scales and other laser interferometers [16]. Interferometrically calibrated gauge blocks are used to calibrate other gauge blocks using a gauge block comparator [17].

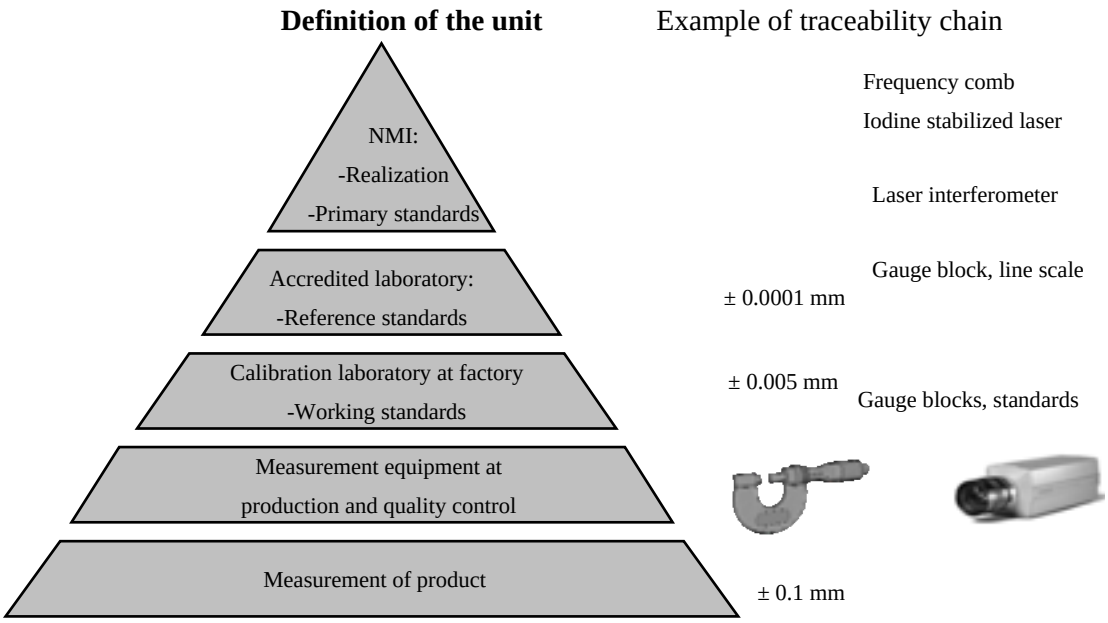

Figure 2. Traceability chain from national standard to product.

For example, a micrometer calliper may be used at factory floor to measure a product. The calibration of a micrometer calliper using calibrated gauge blocks [18] is simple and straightforward and the user has an understanding of both the calibration and the measuring process. It is also an advantage that the calibration using gauge blocks is quite similar to the measurement of the products. If the manual measurement of products is replaced by a machine vision based inspection system the benefits, such as speed, are obvious but the measuring process, and error sources too, get more complex.

In trade comparability and reliability of measurements are important, between buyer and seller. This gives a requirement of reliability and traceability, which cannot be neglected, when mechanical measurement is replaced by machine vision in industry.

2.2. Measurement Uncertainty

In a measuring process, there are several factors that influence the measuring results and measuring uncertainty. The most important factors are properties of the used measuring instrument and calibration and how well they are suited for measuring the object (figure 3).

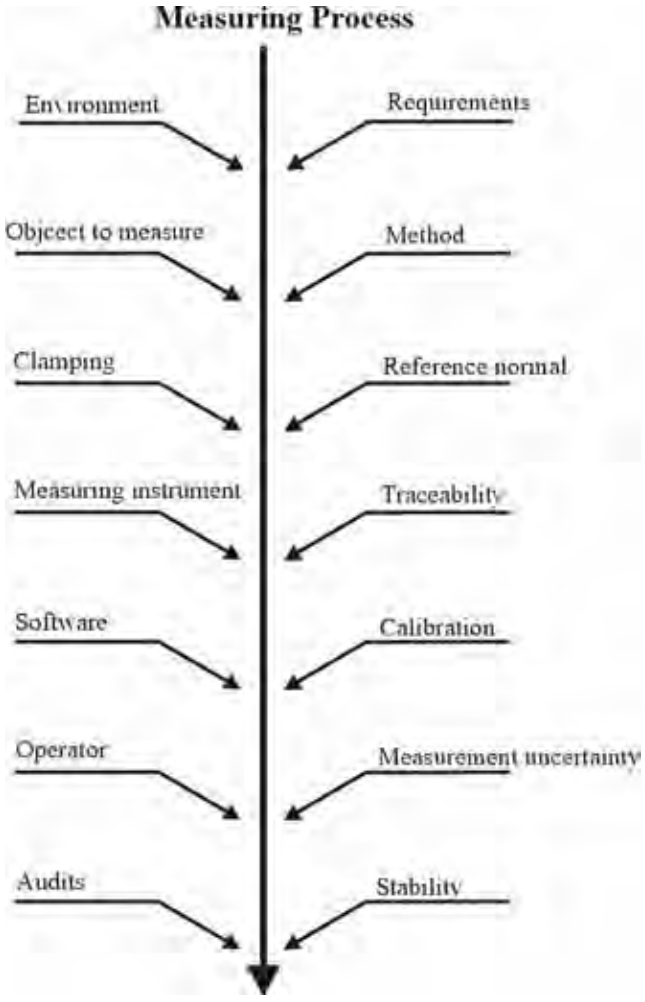

Figure 3. Factors affecting a measuring process (after [19]).

In the documentation of GUM [10] general rules for evaluating and expressing measurement uncertainty are described. In the GUM the estimate of the measurand *Y*, denoted by *y*, is obtained from input quantities x_1, x_2, ... , x_n representing *N* quantities X_1, X_2, ... , X_N. The output estimate *y*, which is the result of the measurement, is given by:

$$y = f(x_1, x_2, ..., x_n) \qquad (1)$$

The standard uncertainties for the input estimates are noted as $u(x_i)$. If the input quantities are independent, the combined standard uncertainty $u_c(y)$ is obtained from:

$$u_c^2(y) = \sum_{i=1}^{N} \left(\frac{\delta f}{\delta x_i} \right)^2 u^2(x_i) \quad . \qquad (2)$$

Usually the combined standard uncertainty is multiplied by the coverage factor k=2, to express the expanded uncertainty at a 95% confidence level.

Equation 1 represents the measurement model. In a simple measurement using a handheld instrument like a vernier calliper, the measurement model is trivial with only three or four input estimates. However, in a machine vision system containing hundreds of program lines in its software, the measurement model is quite complex. An example of this is seen in Publ. IV.

A lot of work has been done on accuracy problems in photogrammetry and accuracy questions in camera calibration in machine vision. However, measurement uncertainty for a whole system and the concepts of GUM are rare in these fields. There are some exceptions, which should be mentioned. In metrology institutes, machine vision has for some time been used for interferometric gauge block calibration [20], flatness measurements with Fizeau interferometers [21], line scale measurements [22] and photomask measurements [23]. For these applications a detailed analysis of measurement uncertainty is normally found.

2.3. Research Question

The area of interest in this thesis is measurement traceability and uncertainty in dimensional machine vision applications. This thesis is limited to two-dimensional applications where one gray-scale camera is used. It might be argued that the principles of GUM are well known and that also accuracy has been studied in the vast literature of machine vision. However, the principles of GUM have been applied only in very few machine vision applications, and there are gaps which should be filled. In this thesis the research question is:

what is the role and benefit of an uncertainty evaluation during the development of a measurement application where machine vision is used for a dimensional measurement?

On one hand, the development of a measurement application might be design, building and testing of new measurement equipment. On the other hand, in industry, where machine vision is used for quality control, there is a need for reliable measurements. Therefore the research question is divided into two subquestions:

how can uncertainty sources be evaluated during design of a measurement instrument based on machine vision ?

how is it possible to achieve traceability and reliability in a measurement based on machine vision ?

In this thesis applications using four different measurement systems are described; optical CMM, measurement of two-dimensional (2D) standards and two calibrations systems for micrometers and dial indicators. The original motivation for these applications was not only to answer the abovementioned research questions. Still the second subquestion is addressed in Publ. II and section 4 where the use of a commercial optical CMM is analysed. The other publications describe uncertainty budgeting during design of instruments.

The applications look quite different but on the other hand the 2D standard measuring instrument is in principle an optical CMM. Also, it should be noted that the border between optical CMM and machine vision will fade away in the future [24]. The requirement of traceability for production measurements where machine vision is used, causes a need of calibration standards such as line scales or 2D standards. These standards are in turn also calibrated using machine vision. Examples of traceability chains are also presented and discussed in this thesis. The hypothesis of this thesis is that a thorough uncertainty evaluation is crucial during the development of a measurement application where machine vision is used.

2.4. Progress in this work

Publ. I.

In dimensional metrology the traceability comes from lasers with stable and well-known wavelengths. An example is the calibration of line-scales using laser-interferometers. Using line-scales, measurement machines can be calibrated one axis at a time. One quick method to check and calibrate optical coordinate measuring machines is to use 2D standards.

A design and development project aiming at a new calibration service for two-dimensional length standards was started in 2000 at MIKES. In the developed measurement equipment the expanded (k=2) measurement uncertainty is Q[0.094; 0.142 L][1] µm, where L is the position in metres. This result is obtained by applying error compensation methods to the pitch error of the movements and to flatness errors of the mirror block. The achievable measurement uncertainty of 0.1 µm (k=2) for a position at 150 mm is sufficient for most calibrations.

---

[1] Expression for combination of non-length dependent and length (L) dependent uncertainty components: $Q[A; B\,L] = (A^2 + (B\,L)^2)^{1/2}$

Publ. II

Apertures are used in photometry and radiometry to limit a precisely known area of the incoming radiation field in front of a detector. The known area is needed to determine such quantities as illuminance or irradiance.

An optical CMM or video measurement machine is used for the measurement of mean diameters of apertures. It is obvious that the measurement uncertainty, even of a high accuracy optical CMM, cannot be as good as that of a dedicated aperture measurement facility in a National Measurement Institute. However, if the required standard uncertainty for the mean diameter is not less than 1 µm, the optical CMM is both useful and easy to use for aperture area measurements. In a comparison with probing CMM excellent agreement was found. This report presents the first full uncertainty analysis of the aperture area measurement by optical CMM, including confirmation of the results by Monte-Carlo method.

Publ. III

With machine vision it is possible to check hundreds of points on the scale of a dial indicator, giving new insight into error sources of the dial indicator. The article describes a machine vision based system for the calibration of dial indicators developed at MIKES. With the developed machine vision system the uncertainty of the reading and interpretation of the pointer is of the same order as when a dial indicator is calibrated manually. In the article the calculation of the measurement uncertainty is described in detail. Uncertainty evaluation according to GUM has not previously been published for an automatic measurement system for dial indicators.

Publ. IV

The manual calibration of a micrometer calliper according to IS0 3611 is done by using ten gauge blocks. This gives only a rough figure for the accuracy of the instrument and is not a complete check of the scale. Using automatic machine vision based systems; the calibration of measurement instruments can be extended.

Equipment for the automatic calibration of micrometers is presented. The purpose of the study is to show the feasibility of traceable calibration of micrometers using machine vision. Another similar system is not known to the author and therefore it is probably the first of its kind. Detailed uncertainty analysis following the recommendations of GUM is given.

3. Calibration of Reference Standards for Machine vision

3.1. Calibration of 2D standards

One important reference standard in high accuracy machine vision applications is a line-scale. In Finland line scales of length less than 1160 mm can be calibrated using a line-scale interferometer at MIKES [22, 25]. The uncertainty of the calibration of line-scales is Q[62; 82L] nm (k=2), where L is the length of the scale in metres. Longer line-scales and measurement tapes up to 30 m can be calibrated interferometrically at the 30 m measurement rail in MIKES.

Although traceability for a machine vision measurement can be achieved by a line-scale, a two dimensional standard or calibration grid is a very useful tool in camera calibration. The advantage is that a large measurement area and orthogonality error is covered in a single measurement. A practical disadvantage is that the correction of the misalignment of the two-dimensional standard depends on the selected alignment criteria or selected reference points. This makes it difficult to compare different calibration certificates for a two-dimensional standard. For a line scale it is much easier to compare the results and to document the stability.

Several instruments for measurements of 2D standards and photomasks with high accuracy have been developed during the recent ten years [26, 27, 28, 29, 30]. Error separation is also used in many applications [31, 32, 33]. In the manufacturing of integrated circuits, lithographic processes are used where accurate 2D positioning is needed. Therefore, the needs of these applications has led to a field called mask metrology. State of the art systems used in this industry achieve positional repeatabilities of the order of 10 nm [34].

The most accurate measurements systems for 2D measurements are equipped with interferometers and orthogonal two-plane mirror reflectors. The optical detection of the features and structures on the mask or 2D standard is done using a microscope, usually equipped with a camera. Such instruments are nowadays found in large national measurement institutes such as NPL in Britain, Physikalisch Technische Bundesanstalt (PTB) in Germany, Bundesamt für Metrologie (METAS) in Switzerland and National Institute of Standards and Technology (NIST) in the United States. Usually the 2D standard is measured in four different positions, each turned by 90°. The measurement uncertainty for the instrument at NPL is 0.06 µm (k=2) [26]. In another paper the instrument is verified to achieve the uncertainty of 0.08 µm (k=2), for an 80 mm x 80 mm grid [34].

The measurement range of the instrument developed in METAS is 300 mm x 400 mm. The equipment in METAS is especially developed for photomask measurements, but it can also be used for various calibration tasks for line scales and 2D standards. An important property of the instrument in METAS is that the Abbe error of the measurement beams is neglible [27]. In calibration measurements for the equipment using a 400 mm quartz line scale mirror, corrections of 40 nm and 140 nm were derived [27]. The final measurement uncertainty is not reported in Ref. [27] but according to the CMC database of BIPM it is about 0.04 µm (k=2) for a 100 mm x 100 mm grid. In a comparison between NPL and PTB for a 120 mm x 120 mm 2D standard the agreement between the results was within ±0.1 µm [23]. The dominating uncertainty source of the instrument in NPL is Abbe error [23]. Other uncertainty sources; discussed in the literature, are the flatness and orthogonality deviations of the two-plane mirrors and temperature effects, such as thermal expansion and refractive index of air.

3.2. Development of equipment for calibration of 2D standards

A design and development project aiming at a new calibration service for two-dimensional length standards was started in 2000 at MIKES. The technical requirement for the new calibration machine was an expanded uncertainty in calibrations of 0.1 µm (k=2) over the measuring range of 150 mm x 150 mm.

The operating principle of the device is based on use of a moveable xy-stage on air bearings. The mechanics of the equipment consist of two linear granite rails, two linear stepping motor actuators, and ten air bearings (figure 4). The two-dimensional standard under calibration is fastened to the Zerodur mirror block using three suction pads. A three-axis plane-mirror heterodyne interferometer system measures the position of the mirror block. The optical components of an old lithography machine were used. Unfortunately the use of this old hardware lead to an Abbe offset of 15 mm between the laser beams and the two-dimensional standard under calibration. Using online compensation, based on measured data on pitch angle, the Abbe error can be reduced but not completely eliminated.

The position of the feature in the standard is detected with a ½" CCD camera, equipped with a telecentric lens. The scale factor is from 0.3 µm/pixel to 6 µm/pixel, depending on the selected lens. The achieved expanded (k=2) uncertainty for a position measurement is Q[0.094; 0.142 L] µm, where L is the position in metres. For a length of 100 mm this equals 0.095 µm.

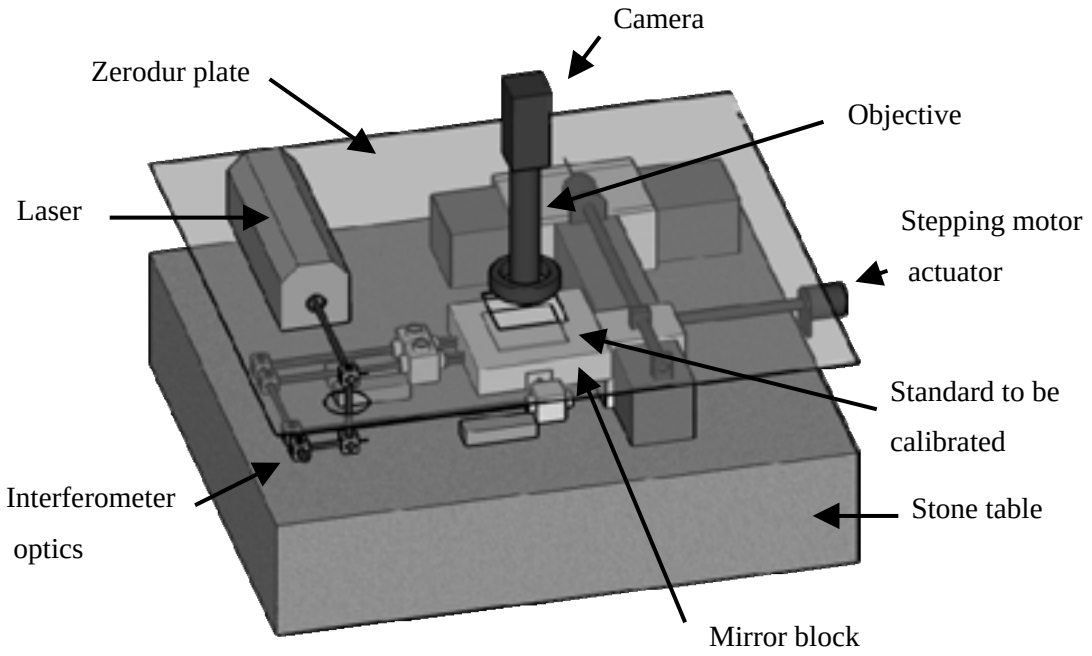

Figure 4. Calibration instrument for two-dimensional standards.

The graduation marks of the standard are positioned in turn at the centre of the image. The position of the graduation mark is measured using template matching or gray-scale correlation [35]. An alternative method to measure the position of the feature would be to use subpixel detector and minimization [36], or fitting of lines on the grid mark edges [37]. In some cases the Hough transform is a robust method to find lines in an image [38, 39, 40]. In this application gray-scale correlation was selected because it gives a good combination of accuracy and speed [41].

In order to test performance of the device, a 50 mm glass line scale was measured using the equipment. A line was used as a template and results were averaged from five measurements (figure 5). The differences of the results compared to measurements of MIKES' line scale interferometer were typically below 60 nm. The expanded uncertainty of the reference results for the particular scale were 90 nm (k=2). The line scale was too short to reveal errors due to temperature and mechanics, but the good result is a verification of the chosen image processing and machine vision parts of the developed system.

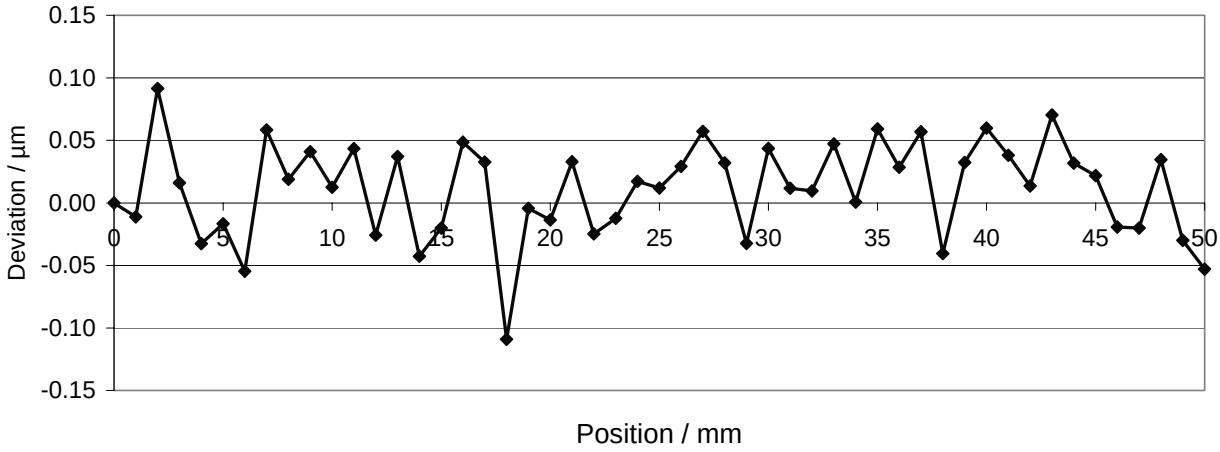

Figure 5. Deviation between results from the developed instrument and MIKES line-scale interferometer for a 50 mm line-scale [41].

Shown in figure 6 is an example of a standard of the size 100 mm x 100 mm calibrated with the instrument. In figure 7, the result of the calibration is shown. The user of a small optical CMM may use this kind of standard to measure the scale and orthogonality errors of the CMM. In Publ. I the uncertainty budget is presented, and it was found that the largest uncertainty source in the equipment is the uncompensated part of the previously mentioned Abbe error.

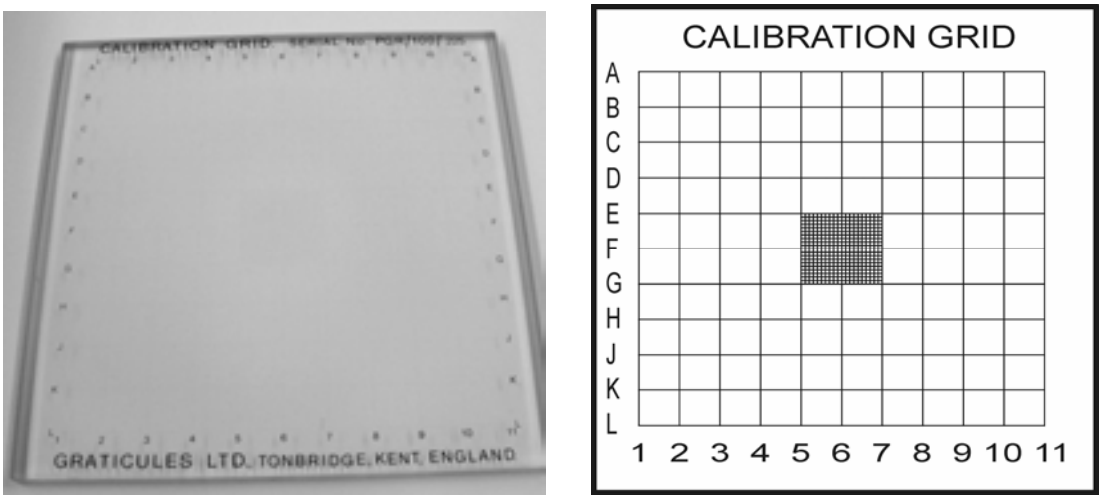

Figure 6. A photograph of the standard (left) and a drawing of the same standard (right). The larger grid has 10 mm intervals and in the middle there is a denser grid with 1 mm intervals.

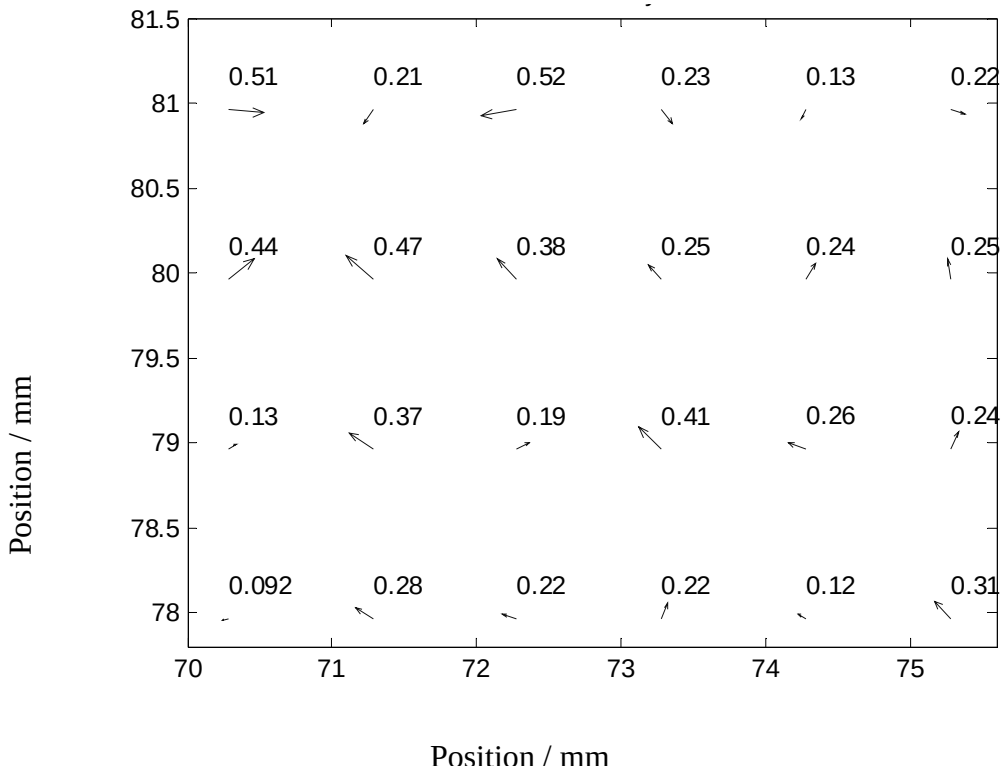

Figure 7. Detail of the results of the error vectors of a grid (unit of axes in mm, unit of error vectors in μm).

3.3. Discussion

The developed equipment is in many aspects similar to those developed in leading national measurement institutes. The accuracy is of the same order as the accuracies in these laboratories. The motivation for building the instrument was the estimated demand for more accurate 2D measurements (see figure 1), and now the demand from Finnish industry can be met. The traceability chain to the definition of metre is evident, as the lasers of the instrument are directly traceable to the frequency comb at MIKES. The equipment is verified to fulfil the required accuracy. However, due to the use of components from another instrument, there exists an Abbe error which is unfortunate. However, it should be noted that instruments of submicrometre precision cannot always be built at any cost, and that the technical compromise to achieve the budget is satisfying. The benefit of the uncertainty evaluation was ensuring that

traceable measurements of the required accuracy can be made. This conclusion is a partial, although not a complete answer to the research question.

As for any new measurement instrument in a NMI (National Measurement Institute), the participation in an interlaboratory comparison would be desirable, to finally prove the measurement capability and to give ideas for improvements to the instrument.

4. The Use of Optical Coordinate Measuring Machines

4.1. Introduction to CMM

The coordinate measuring machine is a universal measurement machine in dimensional metrology [42]. With these machines complex structures, for example, parts of engines and pumps, can be measured. The size or measurement volume of a CMM does vary a lot. A big CMM in the car industry may have axes of a length of several metres and a CMM for the measurement of microsystem components has an axis length of some centimetres [43, 44]. A complete description of the CMM and the measurement uncertainty of CMM is beyond the scope of this dissertation [45, 46, 47,48]. In some studies laser interferometers are used to get traceability and achieve a small measurement uncertainty [49]. Also error compensation methods are applied [50]. In one specific work error compensation is applied for a cylinder [51]. Measurement comparisons between laboratories using error separation methods have also been done [52].

The measurement uncertainty depends not only on the errors of the CMM but also on fitting algorithms of the measured feature and sampling. There are only few guidelines for the calibration of a CMM. One example can be found in Ref. [53].

One type of CMM is an optical CMM, which is a CMM equipped with a camera instead of a contacting probe. Typical lens magnifications provide a resolution of 0.5 µm/pixel to 2 µm/pixel [4]. The optical CMM is ideal for non contact 3D measurements of small elastic parts and features. Typical claimed measurement uncertainties for commercial optical CMM's range from 0.8 µm to 6 µm [54, 55].

A third type of CMM is equipped with an opto tactile sensor. Here an optical fibre is used for probing and the position of the fibre is measured by a camera [56].

The measurement uncertainty of a specific CMM measurement task is a widely studied subject and in figure 8 one approach is shown. A similarity between optical CMM's and machine vision is the importance of the illumination. Different operators may perform different illumination selections and the results of the dimensional measurements may therefore be different. Also the selected measurement strategy may affect the results [57]. Therefore it can be said that the skill of the user is critical for successful CMM measurements and figure 8 is a somewhat idealized presentation because it hides the human factor.

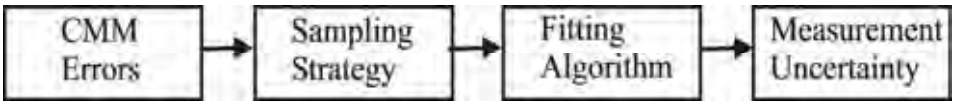

Figure 8. Factors affecting a CMM measurement [9].

In table 1, the relative distribution of uncertainty components for measurements using a CMM and an optical CMM are presented. The effect of the operator is very high for instruments operated in the industry. Especially for the case of the optical CMM the operator is responsible for the selection of illumination, measurement strategy and alignment compensation.

Table 1. Fractional distribution of uncertainty components for measurements using a CMM and an optical CMM [58].

	Operator	Instrument	Environment	Object
Probing CMM	30-50 %	5-20 %	5-20 %	10-30 %
Optical CMM	50-70 %	5-20 %	2-5 %	20-40 %

In metrology it is customary to test the claimed measurement capabilities by arranging comparisons where the same artifact is circulated and measured by different participants. As pointed out by a national comparison in Finnish industry [59], many

users do not know the real measurement uncertainties. In an other comparison for 11 optical and 12 mechanical CMM's, the results showed agreement with the reference values within the reference uncertainty, and also showed that optical CMM measurements can be as good as mechanical CMM measurements [60].

4.2. Task specified uncertainty for CMM

Although the question of measurement uncertainty for a specific measurement made with a CMM, has been intensively studied, there is still no single clear solution to this problem. In a survey [61] published in 2001 the following possibilities are classified as:

- Sensitivity analysis
- Expert judgement
- Experimental method using calibrated objects (Substitution method)
- Computer simulation (Virtual CMM)
- Simulation by constraints
- The expert CMM
- Statistical estimations from measurement history
- Hybrid methods

In [24] the possibilities are classified and presented as:

- Expert judgement
- Uncertainty evaluation based on step gauge results
- Simplified substitution without corrections
- Substitution according to ISO15330-3
- Uncertainty evaluation based on geometric errors together with simulation (PTB software Kalkom Megakal and VCMMtool)
- Virtual CMM (OVCMM)

In the following, three of the above approaches are discussed: sensitivity analysis, substitution method and virtual CMM. One conclusion of the survey was that there are large classes of coordinate measuring systems that have only been partially addressed in the literature such as photogrammetry systems and vision based CMM's [61]. Another conclusion was that none of the methods for task specific uncertainty appear to successfully address the interaction between sampling strategy and possible part form error. During the preparation of this thesis the new ISO 15530 series of standards "GPS- Coordinate measuring machines – Techniques for determining the uncertainty of measurements" was not yet completely published with the exception of ISO 15530:3 describing the substitution method. In the future, the remaining parts describing expert judgement, virtual CMM and methods using statistics from measurement history and methods using uncalibrated workpieces are expected to be published.

Sensitivity analysis

For simple measurements where a well defined mathematical model of the measurements can be formulated, the GUM method is easy to use and this is called sensitivity analysis in [61]. For example, when a CMM is used for a simple length measurement, the measurement model is also relatively simple and the sensitivity coefficients can be determined. For a 2D measurement task the measurement model is already of considerable complexity.

Experimental method using calibrated objects

This method, also called the substitution method, is based on the comparator principle. If a reference work piece, almost identical to the object to be measured is available, repeated measurements on both are performed. This means that it would be good to have quite a large number of different calibrated references avalable. One advantage with this straightforward method is that it is simple and can be brought and communicated to the user. On the other hand, any differences (for example thermal expansion coefficient) between the reference part and the object to be measured can lead to unwanted uncertainties [61].

Although the substitution method is valuable, it is not the complete solution to the task specific uncertainty problem [61]. Because the full substitution method is regarded as tedious a simplified substitution method is suggested in [24].

Computer simulation and virtual CMM

A straightforward application of GUM becomes very difficult or perhaps impossible in complex measurement processes such as form measurement and 2D or 3D coordinate measurements. In these measurements, digital filtering of measurement points is used, and at the points geometric elements are fitted. The question is how to formulate a measurement model with sensitivity coefficients. If for example a hole is measured by fitting a circle on say 100 measured (x, y) points, what is the contribution to diameter from the uncertainty of x-ordinate of one specific point ? And what if 4 points are used for the measurement, instead of 100 ? Here is a problem of interaction between sampling strategy, form error of the object to be measured and the geometric fit algorithm.

The concept of virtual CMM or VCMM, based on Monte Carlo simulations, has been presented by researchers at PTB during the last decade. Examples of Monte-Carlo simulations for uncertainty evaluation for CMM's are given in Refs. [62, 63, 64] and for other fields in metrology they are given in Refs. [65, 66]. There is also an ISO document [67] where this technique is documented. The amount of work needed for the Monte-Carlo analysis is a problem, but software packages have been developed at PTB [68]. The first commercial software packages aimed at non-academic users, was launched by the corporations Zeiss and Leitz in 2003 [24, 69]. One challenge when using virtual CMM is how to estimate the effect of form and roughness of the object to be measured.

4.3. Measurement of apertures using an optical CMM

Since 2002 an optical CMM [70] of high precision has been used in MIKES for several measurements tasks especially for the electronics industry and customers in the field of medicine (figure 9).

Figure 9. The optical CMM at MIKES.

The optical CMM is well suited for repeated measurement tasks and in 2005 a measurement series of apertures was initiated (Publ. II). Apertures are used in photometry and radiometry to limit a precisely known area of the incoming radiation field in front of a detector with calibrated power responsivity. The known area then gives access to quantities such as illuminance or irradiance which describe suitably weighted optical power density. Several contact [71] and non-contact [72, 73, 74, 75, 76, 77, 78] methods have been used for measurement of aperture areas. Non-contact methods are of special interest in radiometric applications because they do not damage the sharp edge of apertures which is essential to produce a well-defined area. The reported relative standard uncertainties are typically 10^{-4} or less. However, for many practical applications in photometry and radiometry an aperture area uncertainty

of 10^{-3} would be sufficient, provided that it can be achieved in a straightforward way. Apertures and diameters of apertures are also of interest in other applications than photometry and radiometry [79].

The purpose of the measurements was to study the stability of newly machined apertures. Ten conventionally machined aluminium apertures were measured eight times. The effects of illumination and amount of measured points along the circumference were found to be quite large. The effect of deviation from roundness (figures 10-11) can be decreased by increasing the number of measured points. In this work most measurements were made using 120 points, and this number can be considered as an acceptable minimum.

As pointed out in Ref. [55], the selection of the illumination is very critical. In Publ. II the effect of different illumination selections was studied. The resulting variation in diameter was taken to the uncertainty budget as an error source. The result of the uncertainty evaluation was an uncertainty of 2.3 µm (k=2) for diameter.

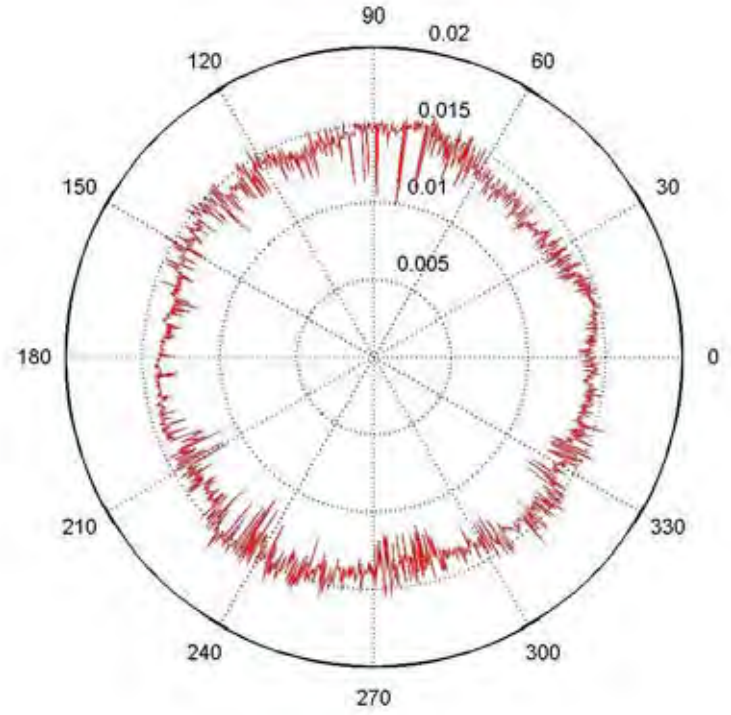

Figure 10. Roundness polar plot of aperture HUT-9 with 2000 points. Dashed circles indicate 5 µm scale grid in the polar plot (Publ. II).

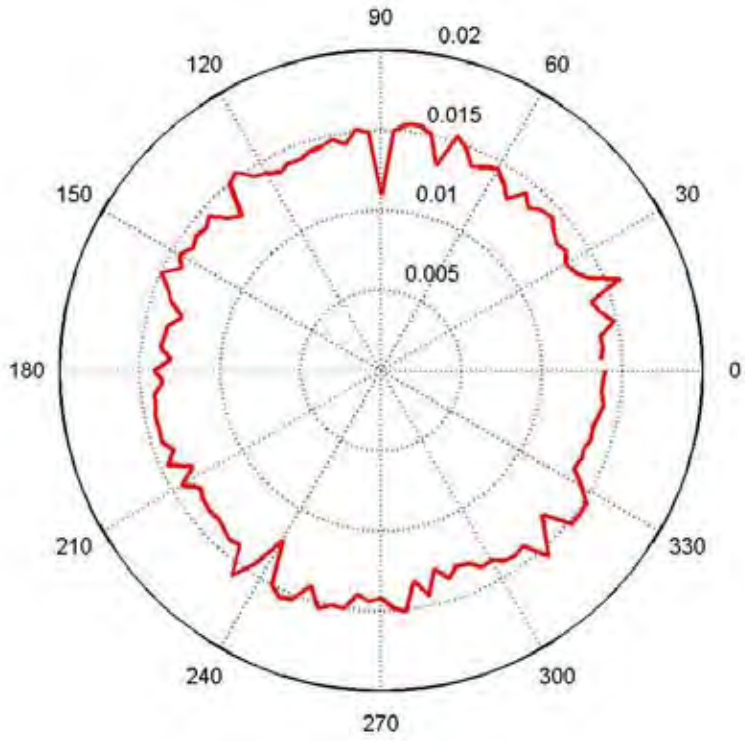

Figure 11. Roundness plot of HUT-9 with 120 points. (Publ. II).

Verification measurements

Verification measurements for one aperture were made on a high-accuracy CMM using a contact probe. Because the probe is large compared to the roughness of the aperture, the measured diameter is decreased by a contact error (figure 12). The contact between probe and aperture was simulated and this effect was corrected from the diameter result, together with the effect of measuring force [80]. The result of this simulation was an estimate of the contact error of 1.1 µm and a force correction of 0.06 µm. The difference in diameter between the contact probe CMM and the optical CMM, after these corrections were applied, was only 0.1 µm.

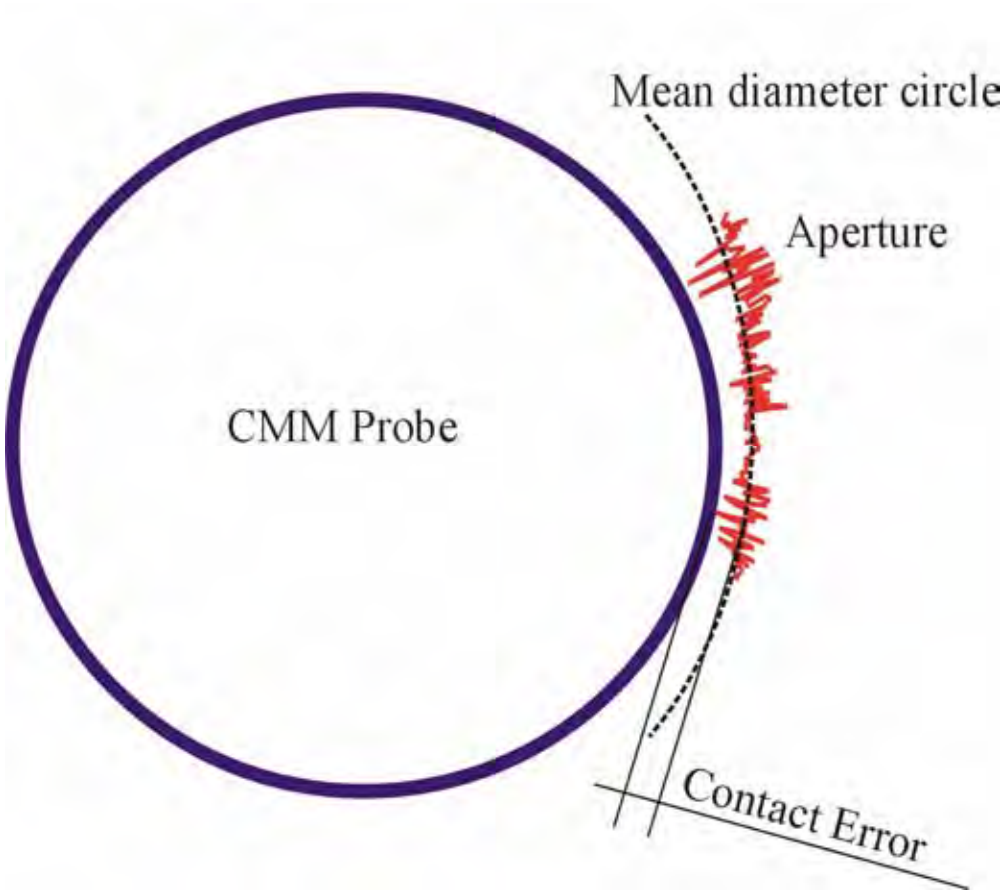

Figure 12. The roughness of the aperture results in an apparent diameter smaller than the mean diameter of the aperture.

4.4. Discussion

It is clear that the accuracies of dedicated aperture measurement instruments are better than the accuracy of a general purpose optical CMM. As pointed out by [56] one of the difficulties in using an optical CMM is edge detection which depends on illumination and algorithms (see also figure 13 in following section) and also, among others, distinct detection of edges distorted by material faults [56]. These problems were experienced in this study where an optical CMM was used for aperture measurements. Fortunately the errors sources can be quantified and estimated in an uncertainty budget. This is the first time an uncertainty budget for optical CMM has been presented for aperture diameter measurements. This uncertainty evaluation may serve as an example of how to achieve traceability and reliability in a measurement based on machine vision, giving an answer to the second research subquestion.

Although the roundness effects are believed to be reduced by averaging, it would be desirable to put more effort to the quality of drilling of the apertures. In the future diamond drilling could be considered. In future work the effects of illumination on the diameter measured by an optical CMM should be examined also analytically and not only empirically. The excellent agreement between contact probe CMM and optical CMM is regarded as a coincidence and not as an indication of an excessively pessimistic uncertainty evaluation.

The conclusion of Publ. II is that if the required uncertainty is not very low, the optical CMM used in this study is useful for aperture diameter measurements. A line-scale was used to evaluate the errors of the optical CMM.

A new type of CMM equipped with an opto tactile sensor appears to be an attractive alternative to an optical CMM, provided that the measurement force is very low. Similarly the probing CMM seemed to give an accurate diameter result. However, non-contact measurements are demanded or at least preferred by the end-users of the apertures in the photometric and radiometric laboratories.

5. Machine Vision Based Calibration Equipment

5.1. Introduction to Machine Vision

Machine vision is a vast field of science and engineering, where the image can be anything from a continent to a nanoparticle. However, in the industry many machine vision applications are inspection tasks where the position, orientation or dimension of a feature is measured [81, 82].

Sometimes the systems consist of two or more cameras as in the Finnish product Mapvision [83]. A more recent example of the use of two cameras in patient radiotherapy is given in [84]. Although there is a profound understanding of machine vision in universities and research institutes [85, 86] and the competence of machine vision vendors is high, measurement uncertainty statements are seldom seen.

The situation is that for most machine vision systems intended for dimensional measurements only results from performance test are given. Typically only repeatability tests are performed. If the performance tests are sufficiently extensive, the collected data may be enough for an adequate uncertainty evaluation. An example of this can be found in [87]. Sometimes accuracy statements according to procedures of VDI/VDE 2363 guidelines are given [88], which of course gives confidence in the reliability of the instrument. Hence the situation is similar to that of many CMM's. A verification is made but the measurement uncertainty is still unknown.

In figure 13 the error sources in a simple machine vision system intended for dimensional measurements are presented. Similarly to the presentation in figure 3, there might be errors from the setup and errors coming from environment such as temperature.

Illumination together with roughness and edge effects may affect the appearance of the object to be measured. Errors in the instrument, such as camera and lens error, may distort the image. Moreover, the selected measurement method, measurement strategy and simplifying assumptions affect the result. For example; how should the angle between two lines be measured when the lines are not straight ? Errors in edge finding may be the result of errors in software, but more probably due to non optimal parameter selection or just mistakes done by the operator. If the calibration of the scale factor is not properly done using a good reference standard, scale errors may occur, also.

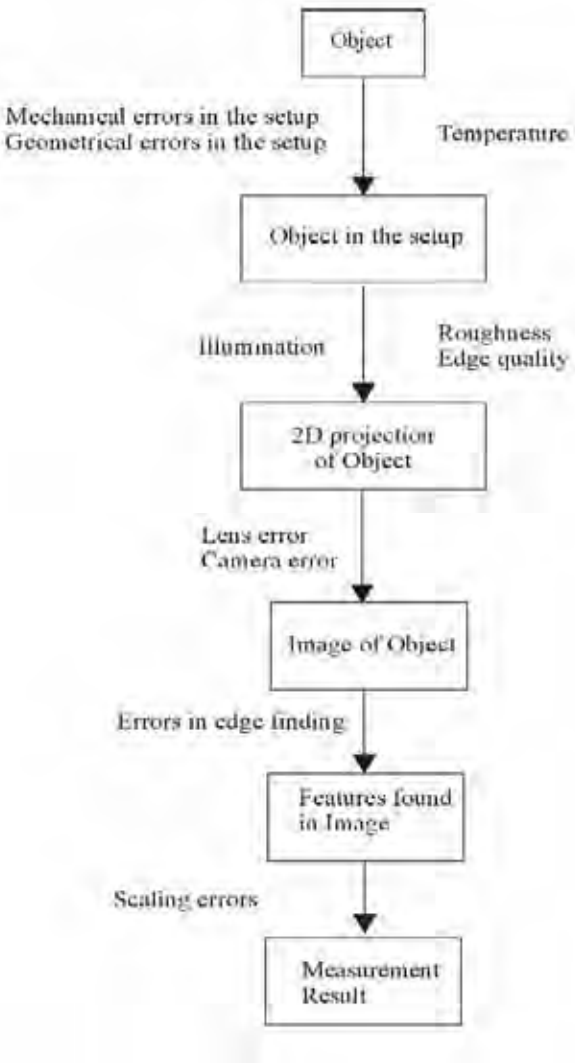

Figure 13. The dimensional error sources in a machine vision system

One important detail which is depending on the measurement task is shown in figure 14. Difficulties in edge detection are not critical, when the centre position of symmetrical features is measured. Therefore, the measurement of diameters of holes is very difficult, but the measurement of distances between holes is not so critical to the edge detection.

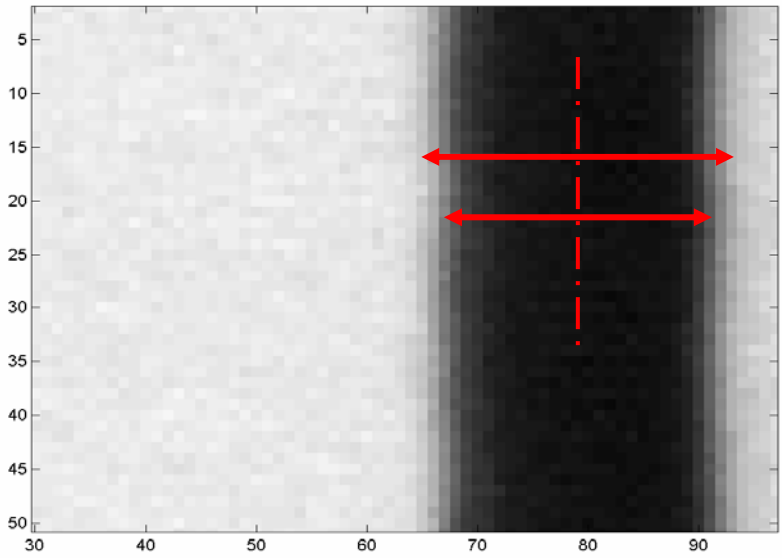

Figure 14. Illustration of the difference between measurement of the size of a feature and measurement of the centre position of a feature

It should be noted that any of the error sources shown in figure 3 may be a dominating error source. Stability is not included in the presentation of figure 3, but it might be the most important feature in many machine vision systems. When machine vision is used in the processing industry, the measurement result may be used as an input for the process control. Although traceability to the SI units is not crucial in process control, a drift in the measurement device can result in problems.

One way to address these problems has been the definition of acceptance tests, such as the VDI/VDE 2634 guidelines. The purpose of an acceptance test is to verify that the measurement errors lie within the limits specified by the manufacturer or the user. In the acceptance test, calibrated artefacts are measured. Acceptance tests for optical 3D

measuring systems are defined in Refs. [89] and [90]. The methods are similar to the methods of acceptance tests for coordinate measuring machines. Performance tests are very useful, but the measurement uncertainty for real measurements of real parts or products is probably not as good as the outcome or result of an acceptance test, where well defined artefacts of good quality are used.

5.2. Camera Calibration in Machine Vision

Camera calibration usually means setting the relation between world coordinates and camera coordinates at the captured image [91, 92, 93]. Camera calibration in machine vision is a widely studied subject [94, 95, 96, 97, 98, 99, 100] . The most well known camera calibration method presented by Tsai [101] and some basic ideas are briefly described. The camera model consists of extrinsic and intrinsic parameters. The extrinsic parameters are related to the position and angle of the camera in relation to the world coordinates. The intrinsic parameters may contain radial or tangential lens distortion. According to Tsai radial lens distortion should be evaluated and corrected (figure 15). The calculation of tangential lens distortion may result in numerical instabilities when the distortion parameters are searched [101].

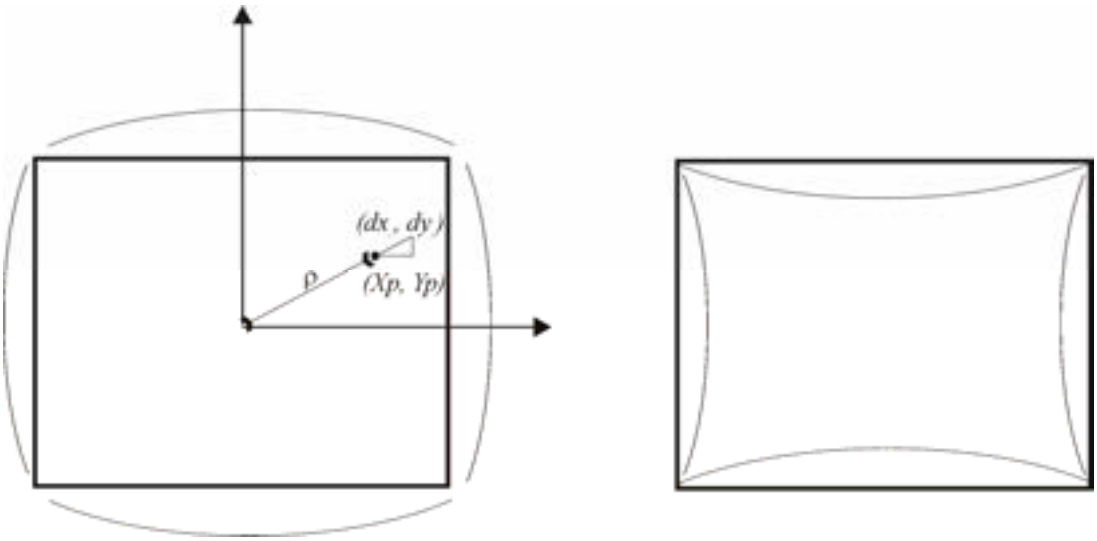

Figure 15. Barrel (left) and pin-cushion (right) types of radial distortion.

Radial distortion dx, dy in x- and y- direction is modelled by the polynoms:

$$dx = Xp\ (k_1\rho^2 + k_2\rho^4) \quad (3)$$

$$dy = Yp\ (k_1\rho^2 + k_2\rho^4) \quad (4)$$

where (Xp, Yp) is the undistorted position of a point in the image, k_1 and k_2 are cofficients for radial distortion and the distance from image centre (ρ) is:

$$\rho = \sqrt{Xp^2 + Yp^2} \quad . \quad (5)$$

According to Tsai the polynom of second order gives acceptable accuracy and the parameter k_2 can usually be neglected.

An example of camera calibration

The equipment used for the automatic calibration of micrometers (Publ. IV) was checked for lens errors using the afore-mentioned two-dimensional standard. In the equipment, the field of view is roughly 4 mm x 6 mm. Using gray-scale correlation the positions of the cross feature of the grid is retrieved. The coefficients of the camera models are solved using Matlab and Nelder-Mead minimization of the residuals which represent camera errors with respect to the standard.

Some results of camera calibration are presented in table 2. The average error found in the calibration is about 1 µm and equals 1/7 pixel. The average error becomes smaller when radial distortion is included in the camera calibration model. From table 2 it is seen that the horizontal scale factor S_x is in the range 7.22 µm/pixel - 7.23 µm/pixel depending on the chosen camera model. In Publ. IV, the value 7.24 µm/pixel was used, based on calibration measurements using a line-scale. In the application where

machine vision was used for 1D measurements, the line scale provided satisfactory accuracy. For applications with 2D measurements the calibration grid is a better choice, especially because radial distortion may be modelled and compensated for.

Table 2. Results of camera calibration using three different camera calibration models for the equipment in Publ. IV. The found scale factors S_x and S_y depend on the chosen camera model.

	No distortion included	2^{nd} order distortion included	2^{nd} and 4^{th} order distortion included
S_x / (mm/pixel)	0.00722	0.00723	0.00723
S_y / (mm/pixel)	0.00725	0.00726	0.00726
k_1 / mm^{-2}		-0.00026	-0.0003
k_2 / mm^{-4}			6.48×10^{-6}
Average error / µm	**1.39**	**0.93**	**0.91**

5.3. Calibration of Dial Indicators with Machine Vision

In Publ. III an automatic calibration system for the calibration of dial indicators is described. Dial indicators are widely used in industry for various measurement tasks [102]. In the industry and accredited calibration laboratories dial indicators are calibrated manually at an uncertainty level varying from 1µm to 3µm (k=2), mostly by comparing to either length transducers or mechanical micrometers.

The automatic system for the calibration of dial indicators is not unique. Two previous machine vision based systems for the calibration of dial indicators are known to the author. The Institute of Nuclear Energy in Bucharest has developed a laser interferometer based instrument [103]. In this instrument the linear displacement of the dial indicator rod is measured by a Michelson interferometer. Over the dial indicator face a specially designed angular transducer with phototransistors is placed.

A commercially available instrument is also offered by the Steinmeyer Feinmess corporation [104]. The measurement uncertainties of these systems are unknown or not given.

The system described in Publ. III consists of a motorised stage, a holder for the dial indicator and two length transducers, and a red LED ring light source together with a CCD camera [105]. The position of the stage was measured by the two length transducers and their average used as a position reference to eliminate the Abbe error (figure 16).

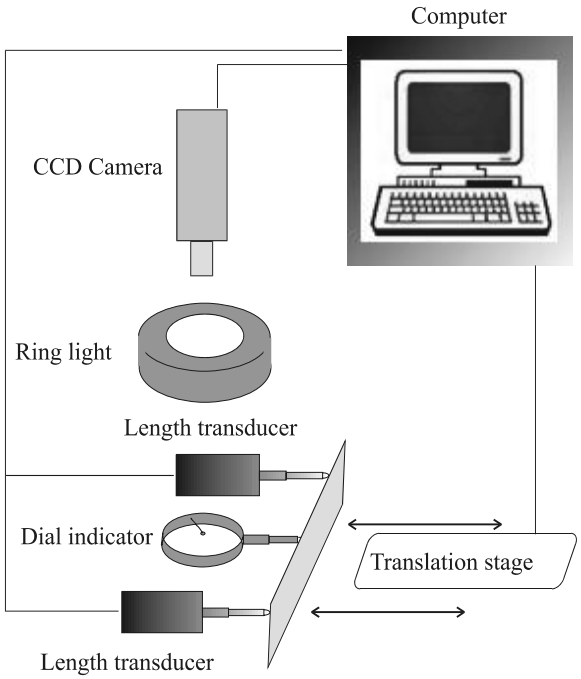

Figure 16. Operating principle of the equipment for calibration of dial indicators (Publ. III).

The image area is large and covers the whole face of the dial indicator to be calibrated. In order to exclude unwanted features from the image a simple method also used in Ref. [81] was implemented. Removal of the static background comprising the dial is done by subtracting the two images of the dial. Since the pointers are the only moving part of the dial, subtraction results in the removal of everything in the images except the pointers. It is assumed that the large pointer is on its right lap,

precluding the need to measure the position of the small pointer. The error in the camera and lens is about ±0.3 pixel in the *x* and *y* directions measured with a two dimensional grid. The measurement uncertainty for the developed instrument is 1.57 µm (*k*=2.01). When a dial indicator is calibrated manually, the uncertainty of the reading and interpretation of the pointer is of the same order as with the developed machine vision system. Using machine vision in normal routine calibration makes it possible to check hundreds of points on the scale of a dial indicator (figure 17).

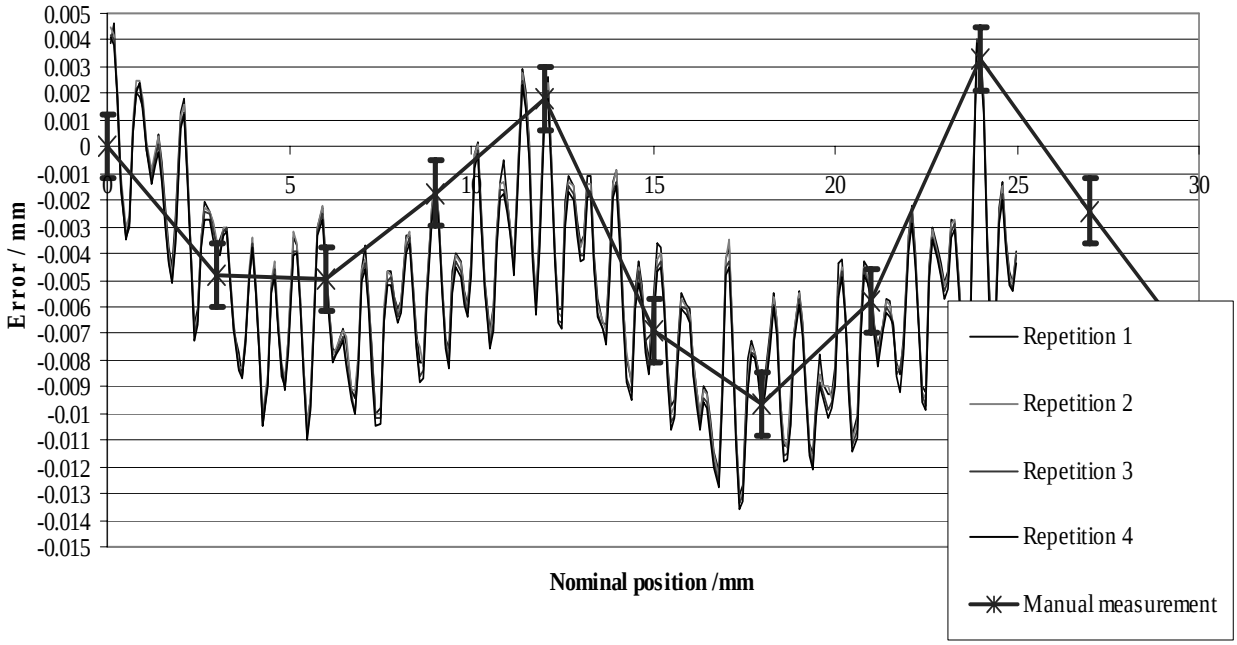

Figure 17. Error curve of a dial indicator measured manually (with uncertainty bars) and using the developed machine vision system with four repetitions (Publ. III).

5.4. Calibration of Micrometers with Machine Vision

The micrometer calliper is a simple but still accurate handheld mechanical instrument for measuring outside dimensions. For the measurement of inside dimensions there are also two-point micrometers and three-point micrometers. The scale of a micrometer is made from a screw usually with a pitch of 0.5 mm per revolution. According to requirements in ISO3611 the error of measurement to a typical micrometer calliper with a measurement range of 0 … 25 mm, should be below 4µm [18].

The cost of calibration of a hand-held measurement device such as a micrometer calliper or dial indicator is roughly equivalent to the price of a new instrument. Manual calibration therefore usually involves checking a mere 10 to 20 points. In some calibration laboratories a CCD camera together with a monitor are used as a magnification glass. Therefore, why not connect the camera to a computer and automate the reading of the micrometer or dial indicator? With automatic machine vision-based systems the calibration can be extended to several hundred points, giving a more complete picture of the errors.

The manual calibration of a micrometer according to IS0 3611 is done by using ten gauge blocks [18]. This gives only a rough figure of the accuracy of the instrument and is not a complete check of the scale. To reveal the error sources of a typical micrometer, many more points should be checked. Possible error sources are zero setting error, form error on the measuring faces, pitch error and nonlinearities in the screw, location errors or bad quality of graduation lines on the thimble and variations in the measuring force.

In Publ. IV an automatic calibration system developed for the calibration of micrometers is described. The instrument consists of two motorised stages, a length transducer, and a LED ring light together with a CCD camera. The rotation of the micrometer drum is motorised through a flexible coupling. A plate is fastened to a translation stage and the micrometer is run against this plate (figure 18). To keep the measuring force stable throughout a measurement, the motorized thimble of the micrometer is turned making two clicks at the ratchet drive of the thimble. A force transducer can also be placed between this plate and the measurement surface of the micrometer. A CCIR (Comité International des Radiocommunications) standard camera was installed to read the micrometer. The position of the stage was measured by a length transducer.

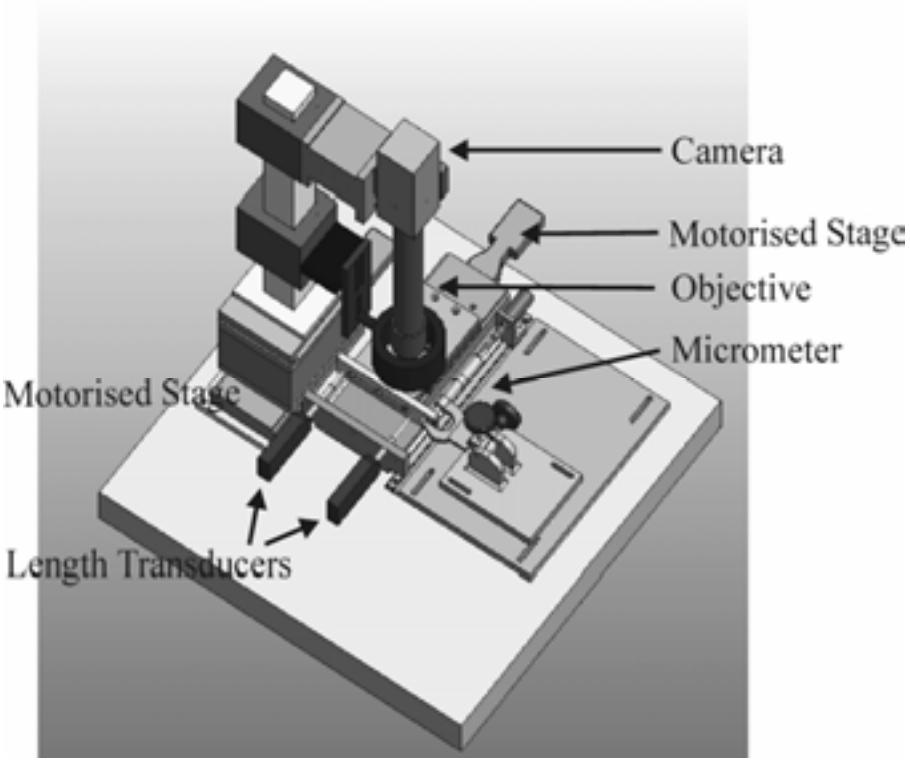

Figure 18. Instrument for automatic calibration of a micrometer.

The position of the division lines on the micrometer drum is found using the pattern-matching function in the Matrox Mil library. The pattern-matching algorithm is based on cross-correlation and the accuracy of about 1/8 pixel is verified by using Matlab. The field of view is only 4 mm x 6 mm. As indicated in figure 19, this field of view covers only the thimble. Before the measurement the angle and position of the fiducial line is separately and automatically measured.

Although both machine vision methods and mechanical design of the equipment could be improved, the main conclusion is that the presented new approach has the potential to produce more than ten times more calibration results at an uncertainty which is less than 10 % compared to the uncertainty of a manual calibration (figure 20). The large number of measurement points makes it possible to analyse the frequency spectrum of the error curve. The calibration result gives pitch error and nonlinearities in the screw at an uncertainty of 0.8 µm (k=2).

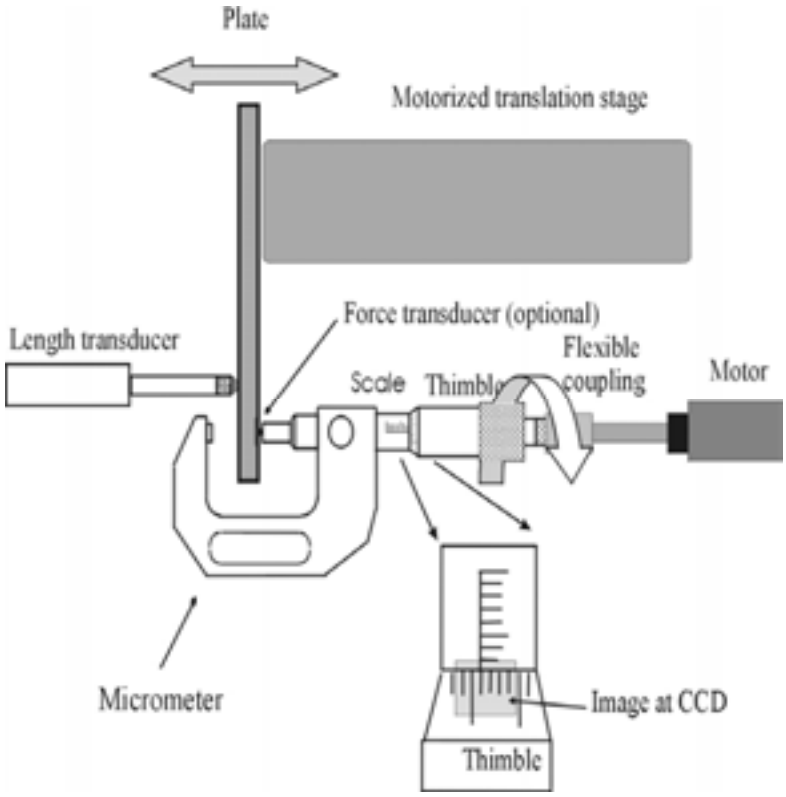

Figure 19. Setup for automatic calibration of a micrometer (Publ. IV).

The time needed for a detailed calibration with 0.05 mm intervals and 400 points is about two hours and, therefore; speed optimization should be made in the future. Limitations of the equipment are that flatness measurement of the measuring faces is not included and that force measurements require some extra setup. The deflection of a tested force transducer was large and therefore force cannot be measured during the dimensional calibration of the screw. Another limitation is that for a typical 25 mm micrometer only the range 5 mm – 25 mm can be calibrated. For larger micrometers such as 25 mm – 50 mm and 50 mm -75 mm, the whole 25 mm range can be calibrated. The instrument can also be operated in a semi-automatic mode, where gauge blocks are manually inserted between the measuring faces of the micrometer [106].

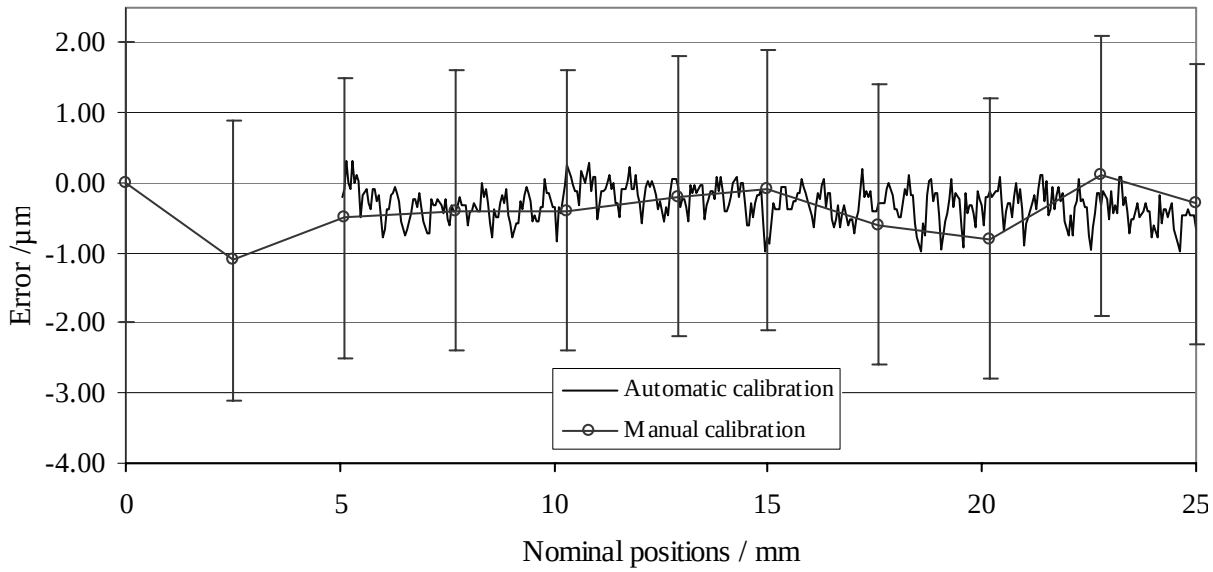

Figure 20. Calibration results using ten gauge blocks (with uncertainty bars for manual result) and using the automatic system (Publ. IV).

5.5. Discussion

The hardware of the equipment of Publ. III and Publ. IV are partly similar. The length transducers used as a reference are calibrated using a laser interferometer and the cameras and lenses are calibrated by traceable calibrated line scales. In both applications only centres of lines and features are measured, reducing the effects of illumination and problems in edge detection. A similar feature and benefit in both micrometer and dial indicator applications is that many points can easily be automatically measured. The large number of measurement points makes it possible to analyse the frequency contents of the error curve by Fourier transform. Another automatic system for the calibration of micrometers is not known to the author. The calibration of dial indicators by machine vision is not unique, still an uncertainty evaluation for such a system has not previously been published.

Some technical difficulties and marketing challenges were also noted. The equipment for calibration of micrometers in its first preliminary implementation requires too much time and effort for operation to be commercially profitable to its owner. Therefore a mechanical re-design should be considered in the future.

As both dial indicators and micrometers are cheap a meticulous calibration might sound as an exaggeration or bad cost-benefit. However, there are two things worth to note. If a micrometer is used for quality checking at a production line in a factory, measuring the same dimension thousands of times each year might cause wear, and errors at that single point of the scale of the micrometer. In a manual routine calibration, this wear would probably not be revealed. It can be concluded that the benefit of automation is an extensive calibration. And to be reliable, a detailed uncertainty budget is needed. The second thing worth to note is the nature of the error curve of the dial indicator in figure 16. The limited number of points in a manual calibration cannot give the complete picture of the errors.

For the equipment for calibration of dial indicators the largest uncertainty source comes from the machine vision sub-system (errors in camera and lens and edge finding algorithm for the pointer). On the other hand for the equipment for calibration of micrometers the uncertainty contribution from machine vision was very small compared to the contributions from mechanical errors and Abbe error. Hence, the dominating uncertainty source was quite different in each application. In one stage of the design process of the micrometer application cosine error of the micrometer appeared to be a dominating error source. The conclusion was that extra care is needed to align the micrometer.

These examples show that it is difficult to base uncertainty estimation on intuition, and that all mechanical, geometrical and optical uncertainty components should be separately estimated.

The hypothesis of this thesis was that a thorough uncertainty evaluation is crucial during the development of a measurement application where machine vision is used. The first subquestion of the research question was about uncertainty sources and design of a measurement instrument based on machine vision. The Publ. III and Publ. IV are considered to serve as two examples of how to evaluate the error sources, and a technically detailed answer to the subquestion is given in these publications.

6. Conclusions

Accurate dimensional measurements are needed in many fields, especially in the manufacturing industry. During the past decades the electronic industry, with the miniaturizing trend, has demanded precision measurements.

The benefits and dangers of machine vision in measurement are similar to the impact of computers in measurement. Many benefits are achieved through automation but the understanding and physical contact to the measurement is easily lost. One way to approach these problems has been the definition of acceptance tests such as the VDI/VDE 2363 guidelines. However, experiences with CMM's have shown that the operator is the largest uncertainty source. Therefore an acceptance test of a CMM performed by the supplier or a third party, does not completely give the accuracy of the production measurements of the CMM. The situation for optical CMM's and machine vision systems is the same or even worse, due to illumination effects. The best way to regain the understanding of the measurement is to make an uncertainty budget. In this budget the illumination contributions, selectable by the operator, are included.

The publications describe four different measurements or measurements systems, where the camera axis is perpendicular to a plane where the measured object is located. Another common feature is that the size of the objects is in the millimetre range and that the illumination is controlled.

There exist also more complex applications which are used in the industry, such as applications with two or more cameras and 3D measurement applications. The measurement uncertainty and traceability of these should be future research topics.

In this thesis, traceability and measurement uncertainty in machine vision applications are described. The most important reference standards are line-scales and two-

dimensional standards. The calibration and use of 2D standards is described. Together line-scales and 2D standards give traceability to the other applications described in this thesis. The largest uncertainty source in the presented equipment is the uncompensated part of the Abbe error, due to the offset between the laser beams and the calibrated standard.

The use of an optical CMM and its measurement uncertainty for the measurement of apertures is described. Here the largest uncertainty source is the selection of the illumination. Due to the complexity of the CMM measurement, a complete and strict uncertainty budget according to GUM was not made. However, a rough model of the measurement has been given together with a Monte-Carlo evaluation of uncertainty.

Measurement uncertainty and traceability for CMM's is widely studied in the literature. Still there is no easy single answer for how to obtain measurement uncertainty for a complex CMM measurement and especially not for a measurement performed with an optical CMM. In Publ. I the sensitivity analysis method is applied for the measurement of 2D standards. In Publ. II, the virtual CMM method is applied.

The use of machine vision in high accuracy measurements is described in one example concerning the calibration of dial indicators and in one example concerning the calibration of micrometers. In the equipment for calibration of dial indicators, the largest uncertainty source came from the machine vision, but in the equipment for calibration of micrometers, the uncertainty contribution from machine vision was very small compared to the contributions from mechanical errors and Abbe error. Hence, the dominating uncertainty source was quite different in each application. These examples show that it is difficult to base uncertainty estimation on intuition, and confirms the hypothesis of the importance of uncertainty budgeting already in the design process. The systems, especially the equipment for calibration of dial indicators, are quite simple but have no value in a metrological sense without an uncertainty budget. It is the view of the author that the uncertainty budget is part of the design of a measurement instrument, just like the drawings. The emphasis of both

Publ. III and IV is on the description on the uncertainty budget and the use of the GUM method.

A new scientific contribution of this work is the development of uncertainty analysis according to GUM method to machine vision applications. The obtained results clearly verify the hypothesis that a thorough uncertainty evaluation is crucial during the development of a measurement application where machine vision is used for a dimensional measurement. The author suggests that the GUM method should be more widely applied for machine vision based calibration and measurement equipment. In a situation where machine vision is used for calibration or measurements of products the measurement uncertainty and traceability should be understandable and believably documented. This is also an economical issue, because failure in measurement, at the end, means economic loss. For a manufacturer it is costly to reject a large production batch which is actually within the specifications. It is also bad practice to send products, which perhaps are within the specifications, to the customer to be rejected. If the measurement process is understood and measurement uncertainty is in correct proportion to the geometric tolerances, we get lower quality costs. Therefore potential economical benefits can be included to the answers to the research question.

Real confidence of a machine vision based measurement instrument is achieved only by systematic documentation and calculation of the uncertainties. When these uncertainties are studied during the design process of a measuring instrument or measuring application, the bottlenecks of metrological performance, can be corrected.

References

1 K. J. Hume, A History of Engineering Metrology, Mechanical Engineering Pub Ltd. 219p. (1980), ISBN 0 85298 448 0.

2 C.G. Thomas, Engineering Metrology, Butterworths (1974), ISBN-10: 0408705108.

3 P. Howarth, Metrology in short, first edition (1999), ISBN 87-988154-0-7.

4 H. Schwenke, U. Neuschaefer-Rube, T. Pfeifer, et al., Optical methods for dimensional metrology in production engineering, CIRP ANN-MANUF TECHN 51 (2): 685-699 (2002).

5 M. Sonka, V. Hlavac and R. Boyle Image Processing, Analysis and Machine Vision. Pacific Grove: Brooks/Cole Publishing Company, 770p, (1998).

6 H. R. Myler, Fundamentals of Machine Vision. Bellingham: Spie Optical Engineering Press, 133p (1999).

7 DTI, National Measurement System Orientation Meeting for the National Measurement System Programme for Time, Frequency and the Metre, 1 October 2006 to 30 September 2009 http://www.npl.co.uk/formulation/time/downloads/nms_overview.pdf. Accessed 11th October 2007.

8 C. J. Feng, A. L. Saal, J. G. Salsbury, A. R. Ness and G. C.S. Lin, Design and analysis of experiments in CMM measurement uncertainty study, *Precision Engineering*, **31**, 94-101, (2007).

9 S.D. Phillips, B. Borchardt, W.T. Estler and J. Buttress, The estimation of measurement uncertainty of small circular features measured by coordinate measuring machines, *Precision Engineering* **22**, 87–97 (1998).

10 Guide to the Expression of Uncertainty in Measurement, ISO (International Organization for Standardization, Geneva, Switzerland, 1993).

11 BIPM: The International System of Units, 8th edition (2006).

12 International Vocabulary of Basic and General Terms in Metrology, second edition, 1993, International Organization for Standardization (Geneva, Switzerland).

13 ISO/IEC 17025, General requirements for the competence of testing and calibration laboratories, (1999).

14 M. Vainio, M. Merimaa and K. Nyholm, Optical amplifier for femtosecond frequency comb measurements near 633 nm, *Appl. Phys.* **81,** 1053-7 (2005)

15 M. Merimaa, K. Nyholm, M. Vainio and A. Lassila Traceability of Laser Frequency Calibrations at MIKES, Instrumentation and Measurement, *IEEE Transactions*, **56**, 500-504 (2007).

16 V.-P. Esala, B. Hemming, K. Nyholm, and A. Lassila, MIKES' facility for calibration of commercial laser interferometers, in Proc. of Euspen 2005 Conference, 4 p (2005).

17 J. E. Decker, A. Ulrich and J. R. Pekelsky, Uncertainty of Gauge Block Calibration by Mechanical Comparison: A Worked Example for Gauge Blocks Of Dissimilar

Materials. Recent Developments in Optical Gauge Block Metrology, In Proc. SPIE, Volume 3477, San Diego, California, pp. 225-246 (1998).

18 ISO 3611:1978(E): Micrometer callipers for external measurements; 6 p, (1978).

19 H. Tikka, H. Lehto, and V-P Esala, Konepajatekniset mittaukset ja kalibroinnit: Metalliteollisuuden kustannus Oy, Tekninen tiedotus/Teknologiateollisuus 3, Tampere: 79 p. In Finnish. (2003)

20 E. Ikonen and K. Riski, Gauge-block interferometer based on one stabilized laser and a white-light source, *Metrologia* **30**, 95-104 (1993)

21 R E. Parks, L. Shao, and C. J. Evans, Pixel-based absolute topography test for three flats, *Applied Optics*, **37**, 5951-5956 (1998).

22 A. Lassila, E. Ikonen and K. Riski, Interferometer for calibration of graduated line scales with a moving CCD camera as a line detector, *Applied Optics* **33**, 3600-3603 (1994).

23 M. McCarthy, A rectilinear and area position calibration facility of sub-micrometre accuracy in the range 100-200 mm. Ph.D. Thesis, Cranfield University, School of industrial manufacturing science, 260 p .

24 H. Tikka, Koordinaattimittaus, Tampereen yliopistopaino OY, Juvenes Print, 473p. In Finnish (2007).

25 A. Lassila, Updated performance and uncertainty budjet of MIKES' line scale interferometer, In Proc. 4th EUSPEN International Conference, pp. 258-259 (2004) .

26 M. B. McCarthy, J. W. Nunn and G. N. Rodger, “NPL optical length scales in the range 300 nm to 400 mm”, LAMDAMAP 97, 3rd International Conference on Laser Metrology and Machine Performance III. Computational Mechanics Publications, pp. 195-204 (1997).

27 F. Meli, N. Jeanmonod, Ch. Thiess and R. Thalmann, “Calibration of a 2D reference mirror system of a photomask measuring instrument”, in Proc. SPIE , Vol 4401, pp. 227-233 (2001).

28 W. Häβler-Grohne and H.-H. Paul, “Two dimensional photomask standards calibration”, 11th Annual Symposium on Photomask Technology, BACUS,in Proc. SPIE, Vol 1604, pp. 212-223.

29 H. Bosse and W. Häβler-Grohne, “A New Instrument for Pattern Placement Calibration Using an Electron Beam Probe”, In Proc. 9th International Precision Engineering Seminar, Braunschweig, Germany, pp. 148-152 (1997).

30 G. Schubert, H. Bosse and W. Häβler-Grohne, “Large X-Y-Stage for Nanometer Positioning in Electron Beam System”, In Proc. 9th International Precision Engineering Seminar, Braunschweig, Germany, pp. 452-455 (1997).

31 M. R. Raugh, “Absolute two-dimensional sub-micron metrology for electron beam lithography, A theory of calibration with applications”, *Precision Engineering*, **7**, 3-13 (1985).

32 M. T. Takac, J. Ye, M. R. Raugh, R. F. Pease, C. N. Berglund and G. Owen, “Self-calibration in two-dimensions: the experiment”, In Proc. SPIE, Vol 2725, 130-146 (1996).

33 J. Ye, M. Takac, C. N. Berglund, G. Owen and R. F. Pease, “An exact algorithm for self-calibration of two-dimensional precision metrology stages”, *Precision Engineering,* , nr 1, 16-32 (1997).

34 M. J. Downs et al. The verification of a high-precision two-dimensional position measurement system. *Meas. Sci. Technol*. **9,** 1111-1114 (1998)

35 A. Wade and F. Fitzke, A fast, robust pattern recognition asystem for low light level image registration and its application to retinal imaging, *Optics Express*, **3**, 190-197 (1998).

36 B. Peuchot, Camera virtual equivalent model 0.01 pixel detectors. *Computerized Medical Imaging and Graphics*, **17**, 289-294 (1993).

37 M. Schroech and T. Doiron, Probing of two-dimensional grid patterns by means of camera based image processing. in Proc. SPIE, vol. 3966, 9-17 (2000).

38 R.O. Duda, and P.E. Hart, Use of the Hough Transformation to Detect Lines and Curves in Pictures. *ACM* **15**(1), 11-15 (1972).

39 K. Ehrenfried, Prosessing calibration-grid images using the Hough transformation. *Meas. Sci. Technol.* **13**, 975-983 (2002).

40 Q. Ji and R. Haralick, Error propagation for the Hough transform, *Pattern Recognition Letters*, **22**, 813-823 (2001).

41 I. Palosuo, B. Hemming and A. Lassila, Design of a Calibration Machine of Optical Two-Dimensional Length Standards, In Proc. 4th EUSPEN International Conference and 6th Annual General Meeting, 236-237 (2004) .

42 H. Tikka, Method for determining uncertainty of specified coordinate measurement. Diss. : Tampere University of Technology : TTKK, 1992. 110 p.

43 A. Kueng, F. Meli and R. Thalmann, Ultraprecision micro-CMM using a low force 3D touch probe *Meas. Sci. Technol.* **18**, 319-327 (2007).

44 U. Brand and J. Kirchhoff, A micro-CMM with metrology frame for low uncertainty measurements, *Meas. Sci. Technol.* **16,** 2489–2497 (2005).

45 B.W.J.J.A. van Dorp, F.L.M. Delbressine, H. Haitjema and P.H.J. Schellekens, Traceability of CMM Measurements, In Proc. ASPE 1999 Annual Meeting, Monterey ,(1999)

46 P. Cauchick-Miguel, T. King and J. Davis, CMM verification: a survey *Measurement*, **17**, 1-16 (1996).

47 S. Sartori and G.X. Zhang, Geometric Error Measurement and Compensation of Machines, *CIRP Annals - Manufacturing Technology* **44**(2), 599-609 (1995).

48 M. Abbe, K. Takamasu and S. Ozonoc, Reliability on calibration of CMM , *Measurement* **33**(4), 359-368 (2003).

49 H. Schwenke, M. Franke, J. Hannaford and H. Kunzmann, Error mapping of CMMs and machine tools by a single tracking interferometer, *CIRP Annals - Manufacturing Technology*, **54**, 475-478 (2005).

50 E. Trapet, E. Savio, and L. De Chiffre, New advances in traceability of CMMs for almost the entire range of industrial dimensional metrology needs *CIRP Annals - Manufacturing Technology* **53** (1): 433-438 (2004).

51 S. Osawa, K. Busch, M. Franke and H. Schwenke, Multiple orientation technique for the calibration of cylindrical workpieces on CMMs, *Precision Engineering*, **29**(1), 56-64 (2005).

52 A. Balsamo, G. Colonnetti, M. Franke, E. Trapet, F. Waldele, L. De Jonge and P. Vanherck, Results of the CIRP-Euromet Intercomparison of Ball Plate-Based Techniques for Determining CMM Parametric Errors, *CIRP Annals - Manufacturing Technology*, **46**(1), 463-466 (1997).

53 EAL-G17, Coordinate Measuring Machine Calibration, European cooperation for Accreditation og Laboratories, 28 p (1995).

54 A. Lazzari and G. Iuculano, Evaluation of the uncertainty of an optical machine with a vision system for contact-less three-dimensional measurement, *Measurement* **36,** 215–231 (2004).

55 H. Kivio, T. Ristonen, J. Salmi, and H. Tikka, Comparison of optical CMMs. VDI/VDE-GMA, In Proc. 8th International Symposium on Measurement and quality control in production , Erlangen, Germany, 145-156 (2004).

56 H. Schwenke, F. Wäldele, C. Weiskirch and H. Kunzmann, Opto-tactile sensor for 2D and 3D measurement of small structures on coordinate measuring machines, *Annals of the CIRP* **50**, 361–364 (2001).

57 F. M. Chan, T. King and K. Stout, The influence of sampling strategy on a circular feature in coordinate measurements. *Measurement*, **19**, 73-81 (1996).

58 H. Kiviö, J. Salmi, T. Tauren and H. Tikka, KOORDINAATTIMITTAUSKYVYN TESTAUS JA MITTAUSOHJEITA, Tampereen teknillinen

korkeakoulu,Tuotantotekniikan laitos,TTKK Raportti 57/01, TEKES Pro-Muovi – teknologiaohjelman julkaisu n:o 52, In Finnish. (2002).

59 H. Kivio, T. Ristonen, J. Salmi, and H. Tikka, Comparison of optical CMMs. VDI/VDE-GMA, In Proc. 8th International Symposium on Measurement and quality control in production, 12.-15. October, 2004, Erlangen, Germany, pp. 145-156 (2004).

60 L. De Chiffre, H.N. Hansen and R.E. Morace, Comparison of Coordinate Measuring Machines using an Optomechanical Hole Plate, *CIRP Annals - Manufacturing Technology*, **54**(1), 479-482 (2005).

61 R.G. Wilhelm, R. Hocken and H. Schwenke, Task Specific Uncertainty in Coordinate Measurement, *CIRP Annals - Manufacturing Technology*, **50**(2), 553-563 (2001).

62 P.B. Dhanish and J. Mathew, Effect of CMM point coordinate uncertainty on uncertainties in determination of circular features, *Measurement*, **39**, 522-531 (2006).

63 B.W.J.J.A. van Dorp, H. Haitjema and F.L.M. Delbressine, A virtual CMM using Monte Carlo Methods based on Frequency Content of the Error Signal, In Proc. SPIE vol 4401, (2001).

64 H J Pahk, M Burdekin and G N Peggs. Development of virtual coordinate measuring machines incorporating probe errors, *Proceedings of the Institution of Mechanical Engineers, Part B: Journal of Engineering Manufacture*, **212**(7) (1998).

65 M. Brizard et. al. Absolute falling-ball viscometer: evaluation of measurement uncertainty, *Metrologia*, **42**, 298–303 (2005).

66 V. Mudronja et. al. Examples of applying Monte Carlo simulations in the field of measurement uncertainties of the standard of length. XVII IMEKO Worl Congress June 22-27, Dubrovnik Croatia, pp 1130-1134 (2003).

67 Guide to the expression of uncertainty in measurement (GUM) — Supplement 1: Numerical methods for the propagation of distributions using a Monte Carlo Method (ISO), Draft.

68 H. Schwenke, B.R.L. Siebert, F. Wäldele and H. Kunzmann Assessment of Uncertainties in Dimensional Metrology by Monte Carlo Simulation: Proposal of a Modular and Visual Software *CIRP Annals - Manufacturing Technology*, **49**(1), 395-398, (2000),

69 Zeiss: B. Blom and J. Wanne, OVCMM Enables Efficient Determination of Measuring Uncertainty, www.zeiss.com referred 11.4.2007

70 Mitutoyo America Corporation , Hyper Quick Vision Brochure, Bulletin No 1510. New Jersey Paramus: Mitutoyo America Corporation (2001).

71 J. Martin et. al. Determination and comparisons of aperture areas using geometric and radiometric techniques *Metrologia* **35**, 461-464 (1998) .

72 J. Fowler et. al. Summary of high-accuracy aperture-area measurement capabilities at the NIST *Metrologia* **37,** 621-623 (2000).

73 J. Fowler, R. Durvasula and A. Parr, High-accuracy aperture-area measurement facilities at the National Institute of Standards and Technology, *Metrologia* **35**, 497-500 (1998).

74 A. Lassila, P. Toivanen and E. Ikonen, An optical method for direct determination of the radiometric aperture area at high accuracy, *Meas. Sci. Technol.*, **8**, 973-977 (1997).

75 E. Ikonen, P. Toivanen and A. Lassila, A new optical method for high-accuracy determination of aperture area, *Metrologia* **35,** 369-372, (1998) .

76 A. Razet and J. Bastie, Uncertainty evaluation in non-contact aperture area measurements, *Metrologia* **43** 361-366 (2006).

77 J. Hartmann, J. Fischer and J. Seidel, A non-contact technique providing improved accuracy in area measurements of radiometric apertures *Metrologia* **37**, 637-640 (2000).

78 J. Fowler and M. Litorja, Geometric area measurements of circular apertures for radiometry at NIST *Metrologia* **40**, 9-12 (2003).

79 H. Caoa, X. Chena, K. T. V. Grattan and Y. Suna Automatic micro dimension measurement using image processing methods. *Measurement* **31**, 71-76 (2002).

80 M. Puttock and E. Thwaite, Elastic Compression of Spheres and Cylinders at Point and Line Contact, National Standards Laboratory Technical Paper No. 25, Division of Appled Phyics, National Standards Laboratory, Commonwealth Scientific and Industrial Research Organization (CSIRO), University Grounds, Chippendale, New South Wales, Australia 2008, 1969.

81 N. Aggarwal, T. Doiron and P. S. Sanghera Vision system for dial gage torque wrench calibration. in Proc. SPIE, Vol. 2063. pp. 77-85 (1993).

82 M. Robinson et al. The accuracy of image analysis methods in spur gear metrology, *Meas. Sci. Technol.* **6**, 860-871 (1995).

83 I. Niini, On the calibration of Mapvision 4D systems, in Proc. ISPRS Technical Commission III Symposium, 3p (2002)

84 S. Tao, A. Wu, Y. Wu, Y. Chen and J. Zhangy, Patient Set-up in Radiotherapy with Video-based Positioning System, Clinical Oncology **18**, pp 363-366 (2006) .

85 S. Yi, Haralick R and Shapiro L. Error propagation in machine vision, *Machine Vision and Applications*. **7,** pp 93-114 (1993).

86 C. Yisong and H. S Horace, Single view metrology of wide-angle lens images, *Visual Computing* **22,** 445–455 (2006).

87 G. Xu et. al, Calibration tool for a CCD-camera-based vision system, In Proc. SPIE Vol. 4099, p. 154-165 (2000).

88 Solutionix: Photogrammetry System
http://www.solutionix.com/product/pro_02_a.asp, referred 12.4.2007

89 VDI-Richtlinie: VDI/VDE 2634 Part 1, Optical 3D measuring systems - Imaging systems with point-by-point probing , 2002-05 , VDI/VDE-Gesellschaft Mess- und Automatisierungstechnik 10p.

90 VDI-Richtlinie: VDI/VDE 2634 Part 2, Optical 3D measuring systems –Optical systems based on area scanning , 2002-05 , VDI/VDE-Gesellschaft Mess- und Automatisierungstechnik 11p, (2002).

91 C. C. Slama (ed.) Manual of Photogrammetry, 4th ed., American Society of Photogrammetry, Falls Church, Virginia, 1050 p. (1980).

92 Z. Zhang. A flexible new technique for camera calibration. Technical Report MSR-TR-98-71. Microsoft Research, Microsoft Corp., Redmond, WA 98052. 21 p.

93 J. Weng, Camera calibration with distortion models and accuracy evaluation, *IEEE Transactions on pattern analysis and machine intelligence* **14** ,965-980, (1992).

94 L. Wang and G.C.I. Lin A new effective calibration method for machine vision system. in Proc. The 12th International Conference on CAD/CAM Robotics and Factories of the Future, Middlesex, UK pp. 1090- 1095 (1996).

95 E. Grano, Fundamentals of Photogrammetry in Automatic Object Recognition, College of William and Mary in Virginia, Bachelor Thesis. Williamsburg, 28 p. (2001).

96 R. G. Wilson, Modeling and calibration of automated zoom lenses, In Proc SPIE Vol. 2350 Videometrics III, pp. 170-186 (1994).

97 T. Echigo, A camera calibration technique using three sets of parallel lines. *Machine Vision and Applications* **3**, 159-167 (1990).

98 T. Echigo, A camera calibration technique using sets of parallel lines. International Workshop on Industrial Applications of Machine Intelligence and Vision (MIV-89), Tokyo, April 10-12, pp. 151-156 (1989).

99 J. Heikkilä and O. Silvén, Calibration procedure for short focal length off-the-shelf CCD cameras, In Proc. 13th International Conference on Pattern Recognition, Vienna, Austria, pp. 166-170 (1996) .

100 M. Li and J-M. Lavest, Some Aspects of Zoom-Lens Camera Calibration. CVAP172, Kungl Tekniska Högskolan. 30 p.

101 R. Y. Tsai, A versatile camera calibration technique for high-accuracy 3d machine vision metrology using off-the-shelf tv cameras and lenses. *IEEE Journal of Robotics and Automation*, RA-**3**(4), 323-344 (1987).

102 M. Kobayoshi and Q. S. H. Chui, The positioning influence of dial gauges on their calibration results, *Measurement* **38**, 67-76 (2005).

103 D.G. Sporea and N. Miron, Dial indicators checking-up by laser interferometry, *Rev. Sci. Instrum.* **67,** 612-614 (1996).

104 Feinmess Suhl. Präzisionsmessrechnik. Suhl: Feinmess Suhl GmbH, 86p, (1999).

105 B. Hemming and H. Lehto, Calculation of uncertainty of measurement in machine vision. Case: a system for the calibration of dial indicators, In Proc. 18th IEEE Instrumentation and Measurement Technology Conference, Vol. 1, pp. 665-670 (2001).

106 B. Hemming and A. Tanninen, High-Precision Automatic Machine Vision-Based Calibration of Micrometers , In Proc. 4th EUSPEN International Conference and 6th Annual General Meeting, Glasgow, pp 240-241 (2004).

Errata:

Publ I

In both Section 3 and Section 4 instead of

The combined uncertainty at 95% confidence level is Q[0.047; 0.071 *L*] µm....

There should be

The combined standard uncertainty is Q[0.047; 0.071 *L*] µm....

I

Publication I

B. Hemming, I. Palosuo, and A. Lassila, “Design of Calibration Machine for Optical Two-Dimensional Length Standards”, in Proc. SPIE, Optomechatronical Systems III, Vol. 4902, pp. 670-678 (2002).

© 2002 SPIE

Reprinted with permission.

Design of a calibration machine for optical two-dimensional length standards

Björn Hemming, Ilkka Palosuo, Antti Lassila
Centre for Metrology and Accreditation (MIKES)
Metallimiehenkj. 6 Espoo, FIN-02150, Finland
Phone: +358 9 616 761, Fax: +358 9 616 7467
E-mail Ilkka.Palosuo@mikes.fi, Bjorn.Hemming@mikes.fi, Antti.Lassila@mikes.fi

ABSTRACT

Optical measurements with coordinate measurement machines equipped with optical sensors, and video measurement machines, are clearly increasing in industry. Accurately manufactured two-dimensional standards, with a precision typically between 0.05 µm and 5 µm, are used to check and calibrate these measuring machines. In order to start a calibration service for two-dimensional standards, a new calibration machine is currently under development at the Centre for Metrology and Accreditation (MIKES). In this paper we describe the mechanical design, properties and present a detailed uncertainty analysis of position measurement. By modeling and compensating mechanical error sources the required standard uncertainty level of 50 nm is achievable.

Keywords: Calibration, 2D coordinate measurements, two-dimensional standard

1. INTRODUCTION

The last few years have seen a rapid growth in the use of machine vision in measurement equipment in length metrology. Optical coordinate measurement machines and video measurement machines are widely used, for example, in plastic industry. These measurement machines are very versatile, but on the other hand have several subjects fo calibration. One straightforward method to check and calibrate optical coordinate measuring machines is to use two-dimensional standards (figure 1). These reference standards have a precision typically between 0.05 µm and 5 µm. In order to achieve traceability, also these two-dimensional standards should be calibrated.

A design and development project aiming at a new calibration service for two-dimensional length standards was started in 2000 at MIKES. The technical requirements for the new calibration machine are an expanded uncertainty in calibrations 0.1 µm (at 95% confidence level) over the measuring range of 150 mm x 150 mm. The principle of operation of the device is similar to instruments used to measure photolithographic masks

In recent years calibration machines have also been developed at several National Measurement Institutes [1, 2, 3, 4, 5, 6]. The measurement principle is usually to measure movements of standard with laser interferometers and then to measure the position of the dot or grid on the standard with CCD camera and machine vision methods. In NPL a photomask comparator is also used to measure the relative displacement of commonly placed features between a pair of photomasks. Typical expanded uncertainties for the x-y coordinate measurement are 50 - 120 nm (k=2). Error separation or self-calibration methods have been presented especially by authors affiliated with the microlithographic industry [7, 8, 9]. In these methods it is assumed that the artifact is rigid and is measured in three or four different orientations. Much of the mathematical research in this field is concerned with how to deal with fourfold rotational symmetric errors [8].

In this paper we describe the mechanical and optical design of the developed instrument. Systematic error sources ar measured and modeled for on-line compensation. Also a detailed uncertainty analysis of position measurement is

Optomechatronic Systems III, Toru Yoshizawa, Editor, Proceedings of SPIE Vol. 4902 (2002)
© 2002 SPIE · 0277-786X/02/$15.00

presented. Although the equipment is under development and the presented numerical results are preliminary, the uncertainty analysis is useful for future improvement of the instrument.

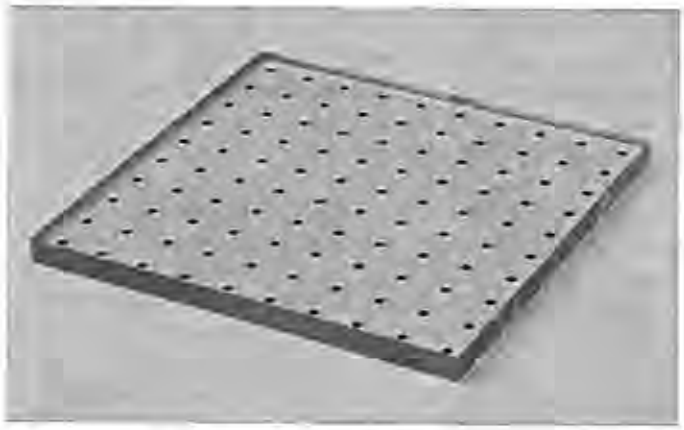

Figure 1. Example of a two-dimensional standard with dots (Photo: R. Rajala).

2. CURRENT DESIGN

The mechanics of the equipment consists of two linear granite rails, two linear stepping motor actuators and ten air bearings (figure 2 and figure 3). The type of air bearings used is vacuum preloaded. Vacuum preloaded bearings hold themselves down and lift themselves off a guide surface at the same time. The benefit of this bearing type is that only one guide surface is needed and the air gap is very stable. With these parts the mirror block can be moved on the granite block via two perpendicular movement axes. Together with linear actuators, piezo actuators are also installed to facilitate movements smaller than the resolution of the stepping motor-type actuators.

The two-dimensional standard under calibration is fastened to the zerodur mirror block using three suction pads. A three-axis plane-mirror interferometer system measures the position of the mirror block. The optical components are fixed to a large zerodur plate. The laser, which is of heterodyne type, measures axes denoted X, Y1 and Y2. Using the difference between Y1- and Y2-axis measurement results, angular yaw movement along the x-axis can be calculated. The optical components of an old lithography machine were used. Due to its original design Abbe's principle cannot be followed.

The position of the feature in the standard is detected with a ½ " CCD- camera, equipped with a high-magnification telecentric lens. In this project a 1024 x 768 square pixel camera with digital output according to the new IEEE 1394 standard was chosen. A far more critical decision is the type of lighting. Currently a fiber ring light is being tested, but coaxial light is also considered. The illumination will of course be dependent on the type of standard being calibrated.

The air temperature is measured with two Pt-100 sensors. Atmospheric air pressure and humidity are measured with capacitive sensors. The environmental measurement data is used to calculate the refractive index of air [10, 11].

The calibration of a two-dimensional standard is briefly a series of movements from one measurement mark to another using stepping motors and piezo actuators. The position of each mark within the camera field of view is measured using pattern matching correlation techniques. Using the two piezo actuators the measurement mark (i.e. two-dimensional standard) is positioned at the center of the field of view. Next the position given by the lasers is read and appropriate corrections are applied.

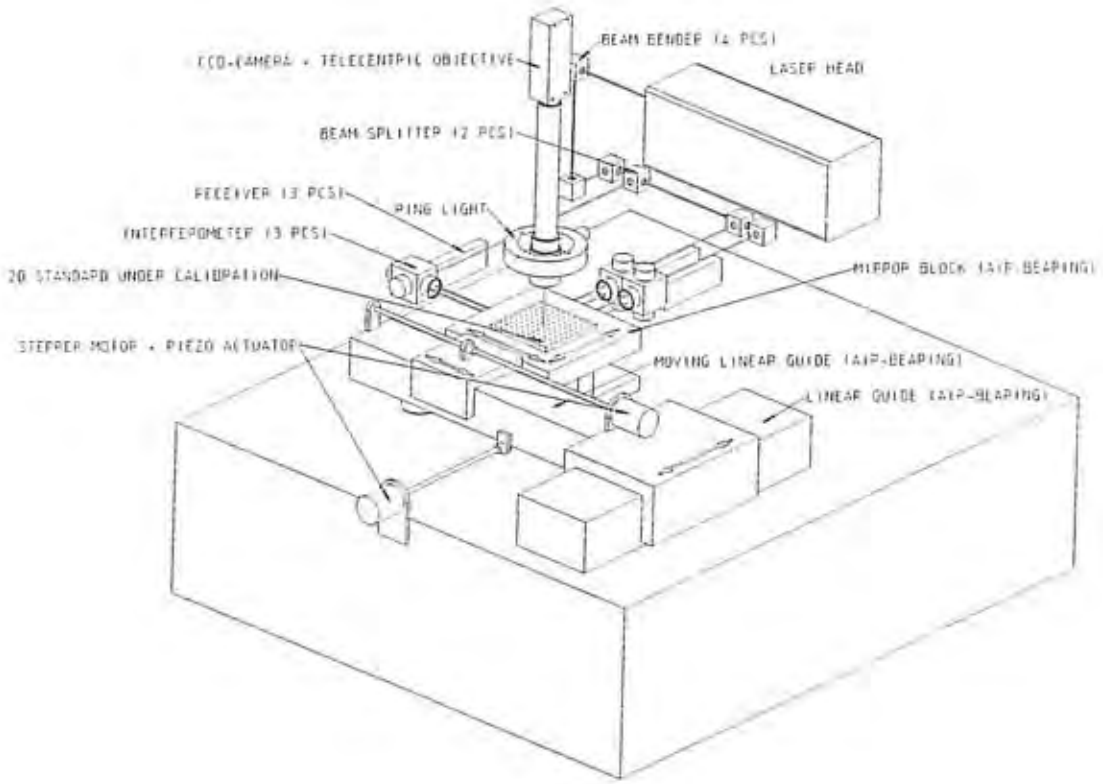

Figure 2. Schematics of the developed calibration machine.

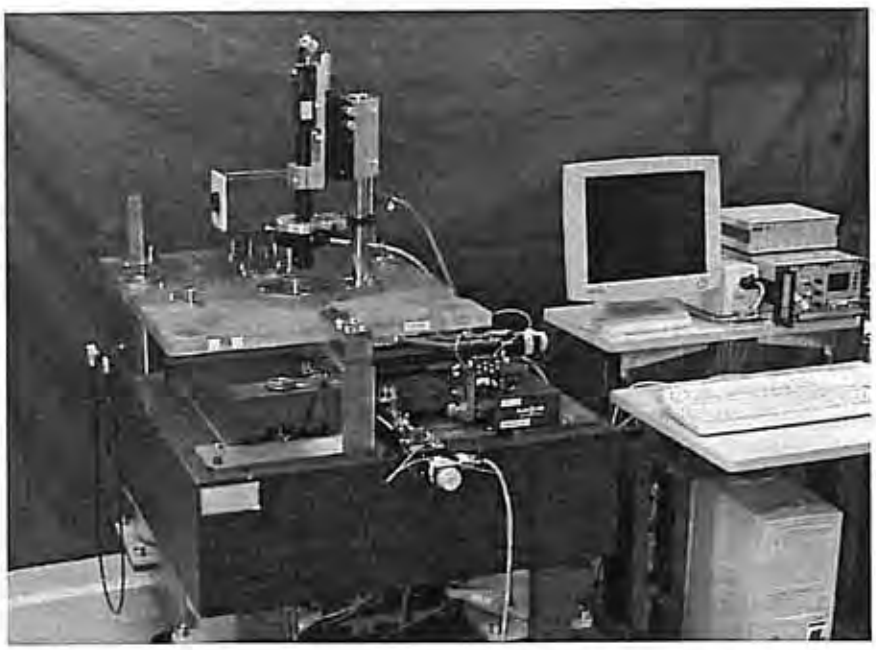

Figure 3. The developed calibration machine.

3. UNCERTAINTY ANALYSIS

To evaluate the achievable precision an approach described in the ISO Guide to the Expression of Uncertainty in Measurement is used [12]. A simple mathematical model for the measurement is derived. Each variable in the model is associated with a standard uncertainty, which should be evaluated from measurements, experiments, data sheets or experience. Numerical values for correction of systematic errors are used when available. The uncertainty budget in this paper is made only for the position measurement of the two-dimensional standard.

Factors affecting accuracy of the movements are straightness of the movement axis, roll, pitch, yaw and perpendicularity of the movement axis. The accuracy of the XY stage was evaluated by measuring the straightness of both axis and roll, pitch, yaw and perpendicularity of the axis. These measurements together with the measured flatness and squareness of the mirror block (see figure 4) and alignment errors of the lasers give input data for the error compensation and uncertainty analysis. Although operating in a temperature stabilized room, also temperature effects should be considered as correction for laser wavelength, thermal expansion of the calibration machine and thermal expansion of the two-dimensional standard. Due to limitations in the calibration machine the measurements cannot be done fully according to Abbe's principle, with a vertical Abbe offset of about 15 mm. This forms the largest error source. However, the Abbe error is measured and modeled, and it is described how this estimate is used to correct the measurement results (figure 5).

The model for the position measurement of x- and y-coordinates is:

$$x_0 = \frac{f_x \lambda_0}{4n(t,p,h)} + h_x \tan(\beta_x(L_x, L_y)) + L_y \tan(\varepsilon) + \delta x_{yaw} + F_x(L_y) + \delta x_{cos} \qquad (1)$$

$$y_0 = \frac{f_y \lambda_0}{4n(t,p,h)} + h_y \tan(\beta_y(L_x, L_y)) + \delta y_{yaw} + F_y(L_x) + \delta y_{cos} \qquad (2)$$

where:

f_x	fringe count for x-axis interferomete
f_y	fringe count for y-axis interferomete
λ_o	vacuum wavelength for laser
$n(t, p, h)$	refractive index of air as function of air temperature, pressure and humidit
h_x	effective distance for Abbe correction for x-axis due to pitch
h_y	effective distance for Abbe correction for y-axis due to pitch
$\beta_x(L_x, L_y)$	pitch angle of x-axis movement as function of position (L_x, L_y)
$\beta_y(L_x, L_y)$	pitch angle of y-axis movement as function of position (L_x, L_y)
ε	orthogonality deviation between plane mirrors
δx_{yaw}	correction for Abbe error in x-axis due to ya
δy_{yaw}	correction for Abbe error in y-axis due to ya
$F_x(L_y)$	flatness correction as function of position L_y
$F_y(L_x)$	flatness correction as function of position L_x
δx_{cos}	correction for cosine error of laser alignment
δy_{cos}	correction for cosine error of laser alignment

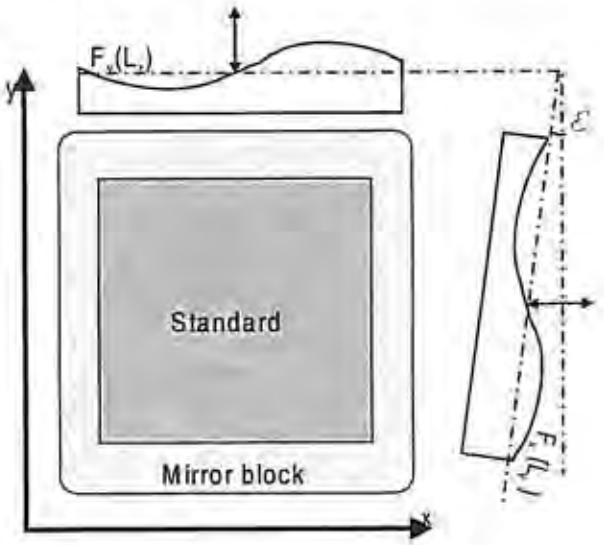

Figure 4. Effects of flatness error of mirror faces and orthogonality error on position measurement.

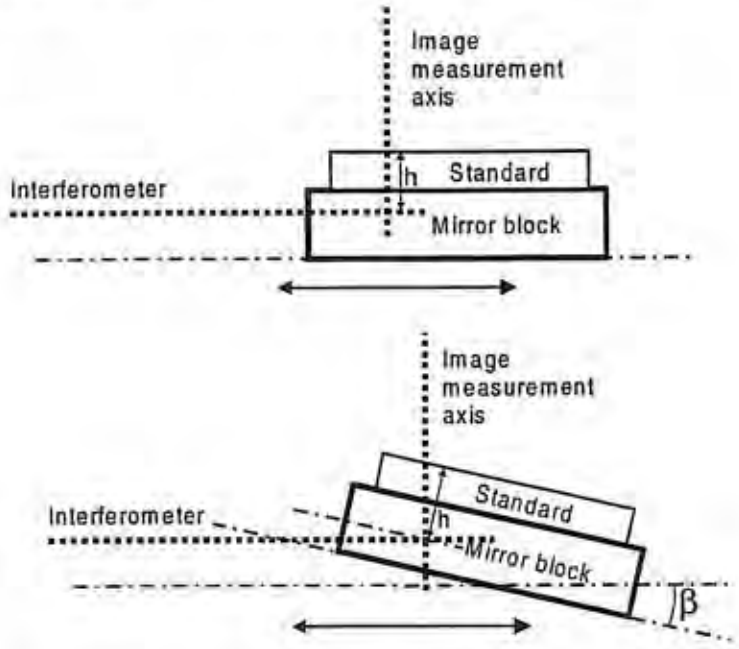

Figure 5. Effect of pitch angle and Abbe error.

In the following the components are described together with estimated standard uncertainties. In many cases a rectangular distribution is assumed and the standard uncertainty (k=1) is simply the limits divided b $\sqrt{3}$ [12]. The emphasis is on the description of mechanical errors and uncertainties.

Fringe count, f_x, f_y

The uncertainty of the fringe count consists of optical and electronic non-linearity and resolution of the laser interferometer. When the resolution is 5 nm and the non-linearity of similar devices is approximately 10 nm (peak to peak) the total uncertainty is 3.2 nm.

Vacuum wavelength of laser, λ_0

Based on experience for similar Zeeman stabilized lasers, the relative uncertainty for laser vacuum wavelength is estimated to be 5×10^{-9}.

Refractive index of air, $n(t, p, h)$

The refractive index of air is related to the determination of the laser wavelength in air. The uncertainty of the refractive index is caused mainly by inaccuracy in the measurement of the environmental parameters and the updated Edlen's formula itself [11]. Relying on experience the estimated standard uncertainties are 0.05 K for air temperature, 8 Pa fo air pressure, 2.9% for humidity and 10^{-8} for the formula.

Orthogonality deviation between plane mirrors, ε

The orthogonality of the plane mirrors was measured with an autocollimator and a rotary table. The measured angle was 89°59' 59.82" equaling an orthogonality deviation of 0.87 μrad. The uncertainty of this measurement was 0.73 μrad. The uncertainty of the orthogonality would result as a large uncertainty contribution for the x- and y-coordinates if measured by an autocollimator only. In the future, orthogonality deviation will be measured using diagonal measurements of glass scales [3]. The standard uncertainty of the orthogonality correction is estimated to be 0.02 μrad.

Abbe error due to yaw, δx_{yaw}, δy_{yaw}

The yaw angle of the movements was measured with a laser interferometer. For both axes the yaw angle was below 14.5 μrad, equaling the standard uncertainty of 8.4 μrad. The CCD camera is aligned close to the crossing of the laser beams; however, an Abbe offset distance of approximately 0.5 mm is difficult to avoid. This corresponds to a standard uncertainty of 0.004 μm. There is no need to compensate for the yaw angle, but the magnitude 8.4 μrad is used as a uncertainty for yaw Abbe error on both axis.

Flatness correction for mirror block, $F_x(L_y)$, $F_y(L_x)$

Flatness deviations of the mirror surfaces are 0.048 μm for the x-face and 0.041 μm for the y-face, measured with a Zygo GPI Fizeau interferometer (figure 6). The uncertainty of these measurements is 0.018 μm (k=1). The data is used for correction of the flatness error. The uncertainty of correction is estimated to be 0.010 μm. The combined uncertaint of the flatness correction is 0.021 μm.

Figure 6. Flatness deviations of the mirror surfaces (left x-axis mirror surface, right y-axis mirror surface).

Correction for cosine error for laser alignment, δx_{cos}, δy_{cos}

The standard uncertainty for the uncompensated cosine error is estimated to be 200 μrad.

Abbe error due to pitch angle, $h_x \tan \beta_x(L_x, L_y)$, $h_y \beta_y(L_x, L_y)$

The position of the normal to be calibrated is situated 15 mm above the measurement plane formed by the laser beams (figure 5). The pitches of the x- and y-axis axes are measured with a laser interferometer (figure 7). The uncertainty of these measurements is about 2 μrad (k=1). Polynoms are fitted to the pitch measurement data for x- and y- axes and used for calculation of correction. For both axes the standard uncertainty for the fit is estimated to be 2 μrad. The combined uncertainty for the measurement and the fit is 2.8 μrad (k=1).

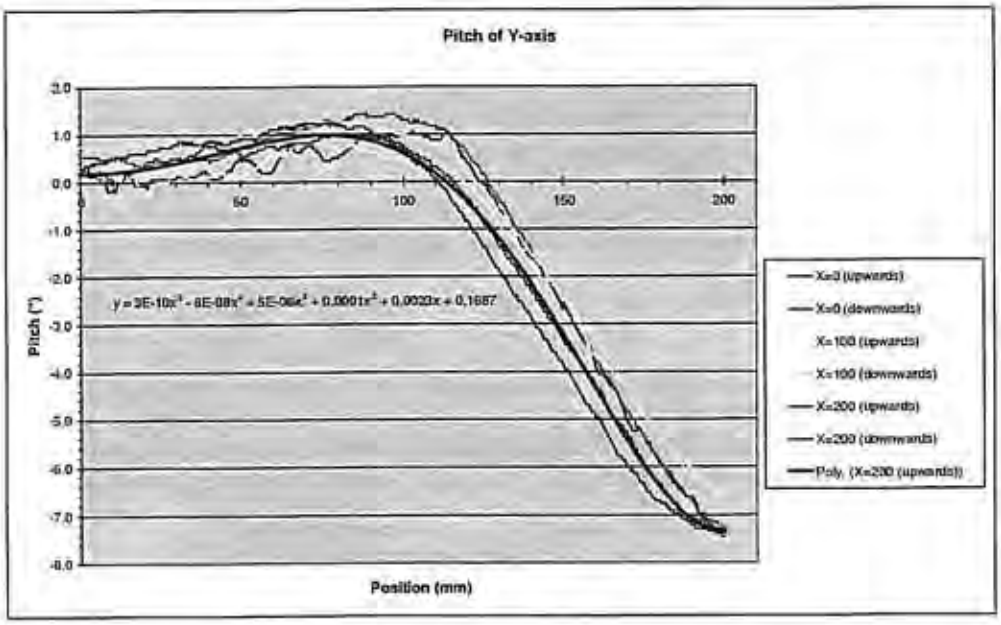

Figure 7. Pitch error of the y-axis modeled by a polynom as a function of the x-position.

None of the input quantities are considered to be correlated to any significant extent. The uncertainty sources for a measured and calculated x-axis coordinate are collected together in an uncertainty budget shown in table 1. The combined uncertainty at 95% confidence level is Q[0.047; 0.071 L][1] μm where $L = L_x$ is the position in m. For a position at 100 mm this equals the uncertainty of 0.048 μm (k=1) or 0.096 μm (k=2). The uncertainty budget for the y axis coordinate is similar to the x-axis coordinate; however, the orthogonality error is excluded.

[1] $Q[A; B\,L] = (A^2 + (B\,L)^2)^{1/2}$

Table 1. Uncertainty budget for measurement of the x-coordinate. L is equal to measured x-coordinate, y is 150 mm.

Quantit		Estimate		Distri-bution	Standard uncertaint		Sensitivity factor		Uncertainty contribution	
Fringe count	f_x	≡ 0.1m		normal	0.0032	µm	1		0.0032	µm
Abbe correction due to pitch	$\beta(L_x, L_y)$	0	µrad	rectang.	2.800	µrad	1.5×10^{-8}	m/µrad	0.0420	µm
Orthogonality	ε	0.873	µrad	normal	0.02	µrad	1×10^{-7}	m/µrad	0.0020	µm
Flatness of mirror block	$F_x(L_y)$	0		rectang.	0.021	µm	1		0.0210	µm
Abbe correction due to yaw	δs_{yaw}	0		rectang.	0.004	µm	1		0.0041	
Vacuum wavelength	λ_{vt}	0.633	µm	normal	5×10^{-9}		1	L	0.005 L	µm
Air temperature	t	20	°C	normal	0.05	K	9.6×10^{-7}	1/K L	0.048 L	µm
Air pressure	p	1013	Pa	normal	8.0	Pa	2.7×10^{-9}	1/Pa L	0.022 L	µm
Air humidity	h	50	%	normal	2.9	%	8.5×10^{-9}	L	0.025 L	µm
Edlen formula		1.000267		normal	1×10^{-8}		1	L	0.010 L	µm
Cosine correction	$\delta s_{\cos}$	0	µrad	rectang.	200.000	µrad	2×10^{-10}	1/µrad L	0.040 L	µm

Components independent of length	0.047	µm
Components dependent on length	0.071	µm
Standard uncertainty for L_x = 100 mm	0.048	µm

The complete uncertainty budget for the calibration of a two-dimensional normal will be reported in a future paper when data from repetitive tests and different measurement strategies are available. It is clear that thermal drift of both the equipment and typical error sources of machine vision such as pixel resolution, lens distortion, noise, and pattern-matching algorithms will be included.

4. CONCLUSIONS

The developed device and calculation of the error budget or uncertainty of measurement is presented. The combined uncertainty at 95% confidence level is Q[0.047; 0.071 L] µm where L is the position in m. This result is obtained b applying error compensation methods to pitch error of the movements and to flatness errors of the mirror block. The effect of pitch error could be reduced by a re-design of the mirror block to fulfill Abbe's principle. The measurement and correction of the orthogonality error can be done using a self-calibration method. The achievable accuracy of 0.1 µm (at 95 % confidence level) for a position at 150 mm is sufficient for many calibrations, but can be further reduced by error separation methods where the artifact is measured in several orientations.

5. REFERENCES

1 M. B. McCarthy, J. W. Nunn and G. N. Rodger, "NPL optical length scales in the range 300 nm to 400 mm", LAMDAMAP 97, 3rd International Conference on Laser Metrology and Machine Performance III. Computational Mechanics Publications, pp. 195-204.

2 M. McCarthy, *A rectilinear and area position calibration facility of sub- micrometre accuracy in the range 100-200 mm.* Ph.D. Thesis, Cranfield University, School of industrial manufacturing science, 260 p.

3 F. Meli, N. Jeanmonod, Ch. Thiess and R. Thalmann, "Calibration of a 2D reference mirror system of a photomask measuring instrument", Proceeding of the SPIE – The International Society for Optical Engineering (2001), Vol **4401**, pp. 227-233.

4 W. Häβler-Grohne and H.-H. Paul, "Two dimensional photomask standards calibration", 11th Annual Symposium on Photomask Technology, BACUS, SPIE, Vol **1604**, pp. 212-223.

5 H. Bosse and W. Häβler-Grohne, "A New Instrument for Pattern Placement Calibration Using an Electron Beam Probe", Proceedings of the 9th International Precision Engineering Seminar, Braunschweig, Germany, 1997, pp. 148-152.

6 G. Schubert, H. Bosse and W. Häβler-Grohne, "Large X-Y-Stage for Nanometer Positioning in Electron Beam System", Proceedings of the 9th International Precision Engineering Seminar, Braunschweig, Germany, 1997, pp. 452-455.

7 M. R. Raugh, "Absolute two-dimensional sub-micron metrology for electron beam lithography. A theory of calibration with applications", *Precision Engineering*, **7**(1) Jan 1985, pp. 3-13.

8 M. T. Takac, J. Ye, M. R. Raugh, R. F. Pease, C. N. Berglund and G. Owen, "Self-calibration in two-dimensions: the experiment", Proceeding of the SPIE – The International Society for Optical Engineering (1996), Vol **2725**, pp. 130-146.

9 J. Ye, M. Takac, C. N. Berglund, G. Owen and R. F. Pease, "An exact algorithm for self-calibration of two-dimensional precision metrology stages", *Precision Engineering*, , nr 1, 1997, pp..

10 K. P. Birch , M. J. Downs , "An Updated Edlén Equation for the Refractive Index of Air" *Metrologia*, 1993, 30, n°3, 155-162

11 K.P. Birch and M. J. Downs, "Letter to the Editor: Correction to the Updated Edlén Equation for the Refractive Index of Air",*Metrologia*, 1994, 31, n°4, 315-316

II

Publication II

B. Hemming, E. Ikonen, and M. Noorma, “Measurement of Aperture Diameters using an Optical Coordinate Measuring Machine”, *International Journal of Optomechatronics*, **1**, 297 – 311 (2007).
.

© 2007 Taylor & Francis, www.informaworld.com

Reprinted with permission.

International Journal of Optomechatronics, 1: 297–311, 2007
Copyright © Taylor & Francis Group, LLC
ISSN: 1559-9612 print/1559-9620 online
DOI: 10.1080/15599610701548803

Downloaded By: [Hemming, Björn] At: 07:05 11 September 2007

MEASUREMENT OF APERTURE AREAS USING AN OPTICAL COORDINATE MEASURING MACHINE

Björn Hemming,[1] Erkki Ikonen,[1,2] and Mart Noorma[2,3]
[1]*Centre for Metrology and Accreditation (MIKES), Espoo, Finland*
[2]*Metrology Research Institute, Helsinki University of Technology (TKK), Finland*
[3]*University of Tartu, Tartu, Estonia*

The use of an optical coordinate measuring machine (CMM) for the diameter measurement of optical apertures is described. The traceability and mechanical stability of the aperture areas are of importance for accurate photometric and radiometric measurements. Detailed evaluation of the measurement uncertainty for the aperture diameter is presented. High-accuracy mechanical CMM was used to confirm the validity of the optical CMM results. The difference between the contact and non-contact measurement was 0.1 μm for the mean diameter result. If the required standard uncertainty for the mean diameter is of the order of 1 μm, the optical CMM provides an efficient method for aperture area measurements.

1. INTRODUCTION

Apertures are used in optical radiometry* to define a precisely known area of an incoming radiation field in front of a detector. When the detector has a calibrated optical power responsivity, the known aperture area allows to determine such quantities as illuminance or irradiance which describe optical power divided by area. An ideal aperture would have zero thickness in order to avoid shadowing of light rays entering in other than exactly perpendicular direction to the aperture plane. Reliable area measurements of apertures with thin edges are especially important to primary scale realizations, as otherwise it is not possible to get access to many essential radiometric quantities.

The area of a nominally round aperture can be measured via determination of its effective diameter. A straightforward method for diameter measurement is to determine in different directions the largest distance between the edges of the aperture. The edges can be observed either by a microscope in an optical coordinate measuring machine (CMM) or by a physical contact in a mechanical CMM. The main advantage of the non-contact optical CMM method is that it does not damage the thin aperture edge. Furthermore, the measurement setup and alignment can be made

*Optical radiometry is the field of science which studies the measurement of electromagnetic radiation, including visible light. Light is also measured using the techniques of photometry that deal with brightness as perceived by the human eye.

Address correspondence to Björn Hemming, Centre for Metrology and Accreditation (MIKES), Tekniikantie 1, FIN-02150 Espoo, Finland. E-mail: bjorn.hemming@mikes.fi

Downloaded By: [Hemming, Björn] At: 07:05 11 September 2007

NOMENCLATURE

D	diameter	δe	error for measurement of D due to optical parameters and edge sharpness
$\overline{D}$	mean diameter		
k	coverage factor	δr	error for measurement of r due to edge roundness of aperture
i, j, m	index variables		
n	number of measured points	δx	repeatability error for measurement of x-coordinate
R, r	Radius		
x, y	Cartesian coordinate	δy	repeatability error for measurement of y-coordinate

relatively simple and it is easy to get a large number of diameter values in different directions. For mechanical contact measurements, utmost care is needed to protect the thin aperture edge and to achieve correct alignment of the aperture plane relative to the probe and probe motion. As a whole the contact measurement, per aperture diameter value, takes considerably longer time than the non-contact measurement. However, the measurement uncertainty of the contact method can be lower than that of the non-contact method since in the latter case uncertainty is limited by the difficulty in reliable determination of the aperture edge position in the microscope image.

Several contact (Martin et al. 1998) and non-contact (Fowler et al. 2000; Fowler et al. 1998; Lassila et al. 1997; Ikonen et al. 1998; Stock and Goebel 2000; Razet and Bastie 2006; Hartmann et al. 2000; Fowler and Litorja 2003) methods have been used for measurement of aperture areas. Some non-contact methods (Lassila et al. 1997; Ikonen et al. 1998; Stock and Goebel 2000) can measure the area directly and are thus not sensitive to the shape of the apertures, but still require long measurement time. The reported relative standard measurement uncertainties are typically 10^{-4} or less. However, even the best measurements of illuminance responsivity (Köhler et al. 2004) and spectral irradiance (Woolliams et al. 2006) have relative standard uncertainties larger than 10^{-3}. Therefore, in some cases an increase in measurement uncertainty for area is acceptable to improve the speed and efficiency of the aperture area measurements. Such an efficiency improvement is especially important for a method (Kubarsepp et al. 2000) where more than ten separate detectors (filter radiometers) are used to realize the spectral irradiance scale, as each of these filter radiometers would need a dedicated 3-mm-diameter aperture with known area. Another need for straightforward aperture area measurement comes from the study of mechanical stability of aperture diameter over time scales of several months after the drilling. The non-contact optical CMM method is a good candidate for an efficient aperture area measurement. However, if the aperture area uncertainty starts to approach other uncertainty components in the spectral irradiance uncertainty budget, the need for a reliable uncertainty evaluation of aperture diameter measurement with the optical CMM is emphasized.

During the last 10 years, coordinate measurement machines fitted with CCD cameras and machine vision software have been developed. These optical CMM's are nowadays used widely especially in the electronic industry, because of their ability for fast automated and accurate non-contact measurements. Typical claimed

Downloaded By: [Hemming, Björn] At: 07:05 11 September 2007

accuracies for optical CMM's range from 0.8 μm to 6 μm. (Lazzari et al. 2004; Kiviö et al. 2004). These accuracies apply for one length measurement only, but with these machines complicated measurements, for example flatness, roundness, cylindricity, coaxiality, etc., are often carried out without knowledge of the task specified uncertainty. Moreover, the uncertainties written on manufacturers brochures are quite seldom realistic and therefore the apparent estimated uncertainty of measurements may be far too small (Kiviö et al. 2004).

Calculation of the measurement uncertainty for a real measurement task with a CMM is considered to be demanding mainly because there is a large number of uncertainty sources and error components. Also several measurement strategies can be used for the same task. Finally, the measurement task itself may include complex geometries or fitting algorithms (Chan et al. 1996). Additional practical difficulty comes from the object to be measured with optical CMM: depending on the selected light source and magnification, on the edge detection parameters, and on the edge itself, different results may be the outcome of measurements.

In this work, the use of optical CMM is studied as a candidate for an efficient aperture area measurement method. A detailed uncertainty analysis of optical CMM measurements is presented for the first time with uncertainty budgets for diameter measurements to help for a better understanding of the measurement method. Especially, the measurement geometry and measurement strategy together with the effects of the quality of the edges are explained. A specific purpose of the measurements was to study the stability of diameters of aluminium apertures over a time scale of six months after the drilling. After drilling the diameter might change, for example due to oxidation or stresses in the material. The measured diameters showed only minor changes comparable with the uncertainties in the measurements. The standard deviation for the measured diameter for one aperture was 35% or less of the standard uncertainty of the measurement. Measurements with a high-accuracy mechanical CMM were used to confirm the validity of the optical CMM results. The optical method was found to provide a fast way for aperture area measurements at an uncertainty level which is sufficient for most practical applications in photometry and radiometry and satisfies the needs of even the most accurate spectral irradiance measurements.

This article is organized as follows. Section 2 describes the measurement setup and Section 3 the measurement results. To confirm these non-contact measurements, measurements with contacting probe are made and described in Section 4. Before any conclusions can be drawn on the stability of the apertures or the suitability of the measurement method, an uncertainty budget is needed as described in Section 5. In Section 6, conclusions on these two topics are presented.

2. OPTICAL APERTURE MEASUREMENTS

The optical diameter measurements were conducted using Mitutoyo Quickvision Hyper CMM at the Centre for Metrology and Accreditation (MIKES) shown in Figure 1. Quickvision CMM is equipped with crystallized glass scale with the resolution of 0.02 μm and thermal expansion coefficient of 0.08×10^{-6}/K. The best specified measurement uncertainty in one axis is 0.8 μm (Mitutoyo 2001). As shown in Figure 1, the object to be measured is placed on the motorized Y-table and the

Downloaded By: [Hemming, Björn] At: 07:05 11 September 2007

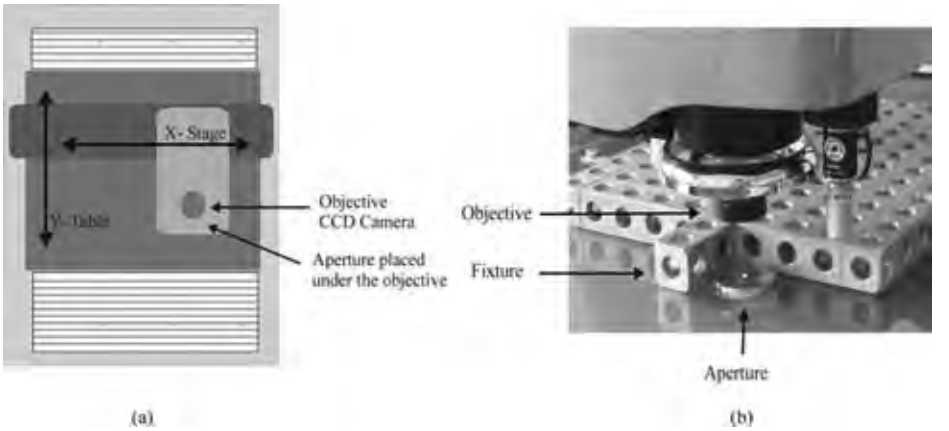

Figure 1. A CMM used for the measurement of optical apertures. *a*) Schematic diagram and *b*) measurement of apertures positioned using a fixture.

camera is moved using an X-stage and a vertical Z-stage. The instrument can be used with coaxial light and stage light. Stage light, also called contour illumination, uses a light source beneath the glass-made measuring table, and is useful when the object is too reflective for coaxial light. The apertures have been made of aluminium with a nominal diameter of 3 mm. Properties of the apertures are shown in Table 1. To avoid a situation where both the new apertures and the CMM would be unstable, old, presumably stable apertures were also measured. The new apertures were machined by conventional turning some days before the first measurement. If the aperture dimensions would be unstable immediately after turning, the difference in the behaviour of new and old apertures would reveal this phenomenon.

A measurement program was made, where 120 points at the circumference of the apertures were measured and combined to a circle using the least-squares criteria. During the measurement X-Y-movements are made and a small part of the edge of the aperture is seen by the camera. Using the point measurement tool in the

Table 1. Studied apertures and illumination used in the measurements. The percent values indicate the fraction of full light intensity of the Quickvision Hyper

Aperture	Age	Coating	Illumination (%)
HUT-1	new	anodized	Coaxial 80
HUT-2	old	anodized	Coaxial 80
HUT-3	new	anodized	Coaxial 80
HUT-4	new	none	Stage 30
HUT-5	new	anodized	Coaxial 80
HUT-6	old	none	Stage 30
HUT-7	old	anodized	Coaxial 80
HUT-8	new	none	Stage 30
HUT-9	new	none	Stage 30
HUT-10	old	none	Stage 30

Downloaded By: [Hemming, Björn] At: 07:05 11 September 2007

Table 2. Results for mean diameters (in mm) of ten apertures for the period of six months

Day	HUT-1	HUT-2	HUT-3	HUT-4	HUT-5	HUT-6	HUT-7	HUT-8	HUT-9	HUT-10
0	3.0082	3.0387	3.0063	3.0084	3.0025	3.0016	3.0336	3.0039	3.0076	2.9992
1	3.0085	3.0387	3.0057	3.0083	3.0034	3.0018	3.0333	3.0040	3.0070	2.9992
3								3.0039	3.0076	
7								3.0037	3.0080	
14	3.0079	3.0389	3.0054	3.0082	3.0033	3.0003	3.0332	3.0038	3.0081	2.9993
34	3.0083	3.0388	3.0056	3.0085	3.0034	3.0019	3.0330	3.0041	3.0074	2.9989
77	3.0085	3.0387	3.0056	3.0085	3.0032	3.0018	3.0334	3.0038	3.0083	2.9994
196	3.0080	3.0388	3.0052	3.0083	3.0036	3.0016	3.0332	3.0040	3.0083	2.9996

Quickvision software, one point on the edge is measured. This sequence is repeated at equal angle steps until a circle is completed. In addition to the calculated diameter, an out-of-roundness estimate was obtained from the circle-fitting function of the QVPak program of the CMM. Some raw measurement data of coordinates (x,y) were also saved for verification and plotting using Matlab (MathWorks, Inc.). During the measurements the temperature of the CMM varied from 19.3°C to 20.4°C due to the change of the ambient conditions. To ensure a good reproducibility and to minimize the influence of the systematic errors of the CMM, a fixture was used to position the apertures (Figure 1).

3. MEASUREMENT RESULTS

The apertures were named HUT-1, HUT-2 . . . HUT-9. Results of the measurements are shown in Table 2. The variations in diameter for nine apertures were within 1.3 μm and for one old aperture, HUT-6, the maximum variation was 1.6 μm. It is difficult to see any trend indicating a systematic change in any of the apertures. Figure 2 shows the results graphically for apertures HUT-8 and HUT-9, which were randomly selected to be measured also on day 3 and day 7.

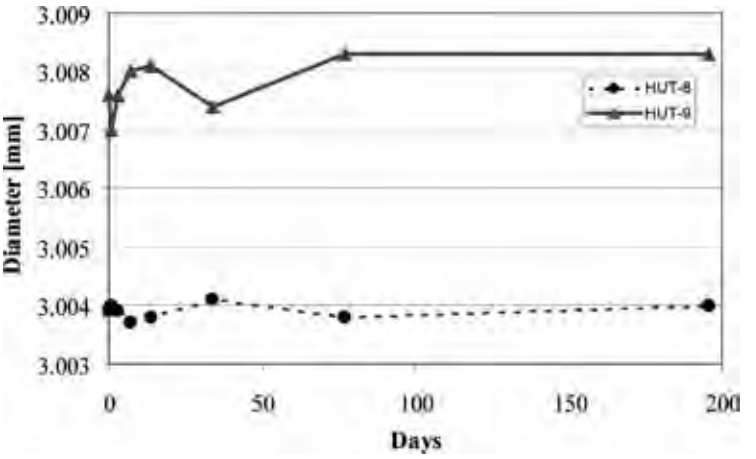

Figure 2. Measurement results of mean diameter for two apertures.

Downloaded By: [Hemming, Björn] At: 07:05 11 September 2007

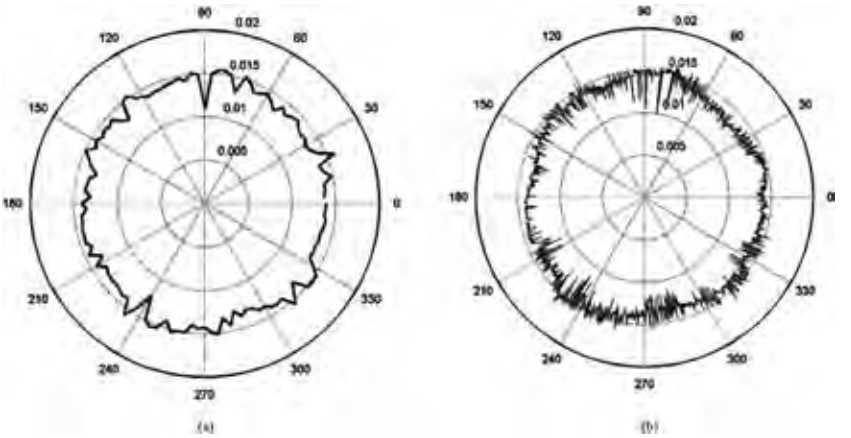

Figure 3. Roundness polar plot of aperture HUT-9 measured with 120 points: *a*) measured with 2000 points; *b*) dashed circles indicate 5 μm scale grid in the polar plot.

In diameter measurements, the roundness plots are helpful when judging the quality of the data. From Figure 3, it can be seen that there are rather large local out-of-roundness variations in the measurement results. In Razet and Bastie (2006), this variation is referred to as edge scatter. The reason is probably actual geometrical form and roughness of the apertures combined with the effects of illumination. These variations should be included in the uncertainty analysis as reproducibility errors because the position of the aperture cannot be exactly the same in every measurement.

4. COMPARISON TO THE RESULTS OBTAINED WITH MECHANICAL CMM

Verification measurements with a probing CMM Mitutoyo Legex were made for the aperture HUT-1. The nominal maximum permissible error (MPEe error) defined in ISO 10360–2 (for this high-accuracy CMM is $(0.35 + L/1000)$ μm) where L is the measured length in millimetres. The MPEe error is verified to be less than 0.2 μm for measurement distances shorter than 100 mm using zerodur gauge blocks. The diameter of the probe was 2 mm and the measuring force was 0.045 N (Figure 4). Although the measurement force is quite small, the thin edges of optical apertures may be damaged by the mechanical measurement, and therefore this verification using probing CMM was done for only one aperture. The average measured diameter from 120 points was 3.0061 mm, as determined with mechanical CMM.

Because the probe is large compared to the roughness of the aperture, the measured diameter is decreased by the contact error. During the measurement of each point, the probe approaches the aperture in a radial movement starting approximately from the aperture center. The first contact between the probe and the aperture is registered as a measurement point. Because there are roughness peaks on the aperture, most measurement points will be registered from these peaks. Thus, the mechanical contact between the probe and aperture edge was simulated using optical

Downloaded By: [Hemming, Björn] At: 07:05 11 September 2007

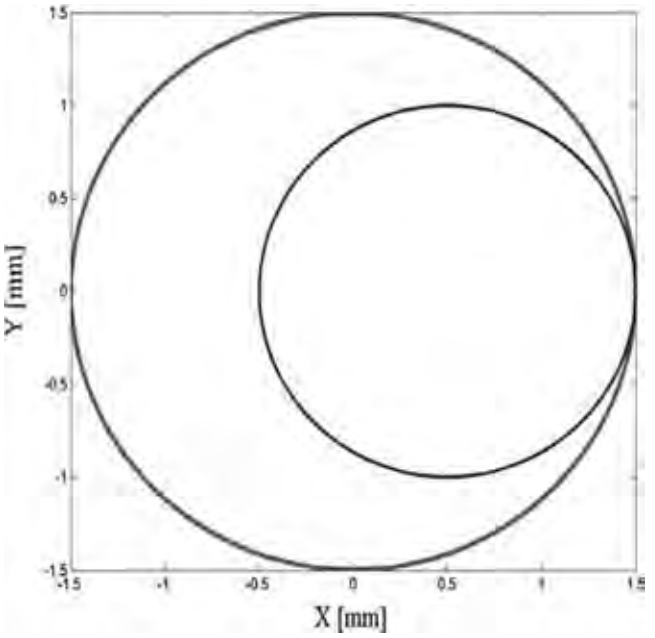

Figure 4. Basic geometry when measuring a 3-mm inner diameter using a 2-mm touch probe (scales in millimetres).

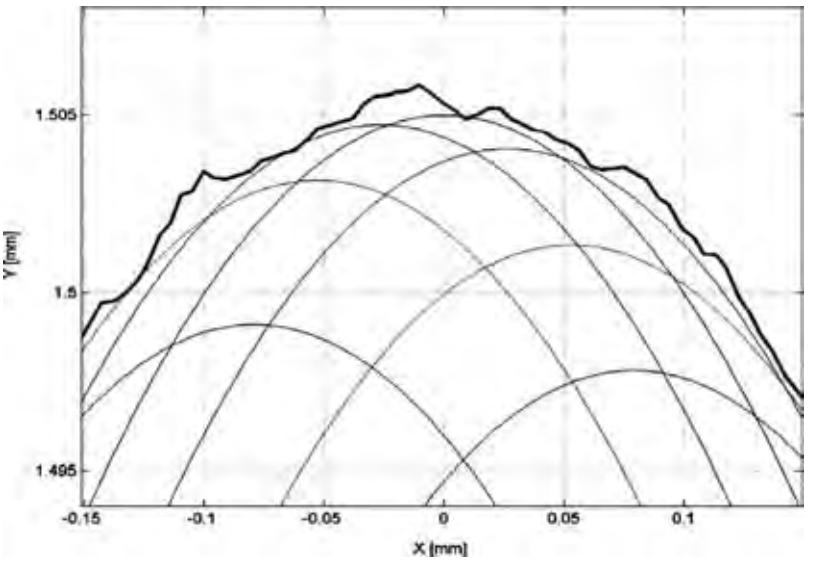

Figure 5. Simulation of the contact between the aperture and the probe at several positions. The center of the aperture is at (0, 0).

Downloaded By: [Hemming, Björn] At: 07:05 11 September 2007

CMM profile data. A Matlab script was written to adjust a radial offset to the theoretical probe to match roughness peaks in a 2000-point aperture profile (Figure 5). The result of this simulation was an estimate of the contact error of 1.1 μm in radius. The surface roughness of the probe was measured with a form and surface roughness measuring instrument. The roughness value Ra (arithmetical mean roughness) is less than 0.05 μm, and therefore errors due to roughness effects of the probe are negligible.

In addition, a force correction should be applied to the mechanical CMM result. The force correction of −0.05 μm (in radius) was calculated from formulas for elastic compression for the case of the sphere in contact with the internal cylinder (Puttock and Thwaite 1969). The depth of the cylindrical land in the aperture is about 150 μm. After applying the force correction and the contact error correction, the resulting diameter is 3.0081 mm. The mean value of the measurements, conducted with the optical CMM, was 3.0082 mm (Table 2), so there is good agreement between the results.

5. UNCERTAINTY ANALYSIS FOR MEASUREMENT OF MEAN DIAMETER

5.1. Auxiliary Measurement Results

The formal definition of uncertainty of a measurement is "parameter associated with the result of a measurement, that characterizes the dispersion of the values that could reasonably be attributed to the measurand" (GUM 2004). The compilation of the uncertainty budget requires additional studies of general stability of the instrument and repeatability and reproducibility of the measurements. In this article, especially where the stability of the apertures has been studied, the reproducibility of the measurements and the stability of the optical CMM are critical. As previously mentioned, a relative aperture area uncertainty of 10^{-3} would be sufficient for most needs in photometry and radiometry. An aperture with a nominal diameter of 3 mm corresponds to a standard uncertainty of 1 μm for the mean diameter. In the following, an uncertainty analysis is made to show that the accuracy of the measurements of the mean diameter is sufficient for these needs. Also, to make reliable conclusions on the stability of the apertures a similar accuracy is needed.

The best measurement capability for Quickvision Hyper optical CMM is 0.8 μm ($k = 2$, k is the coverage factor with which the standard uncertainty is multiplied to get an uncertainty at 95 % confidence level) in one axis for a short distance measurement. There is also an additional length-dependent component of uncertainty, but it is negligible in our case because the measured dimension is small. This measurement capability has during recent years been verified by several calibrations and verification measurements of glass scales. It is assumed that the uncertainty consists mainly of the uncompensated error of the scale (0.6 μm, $k = 2$) and of the repeatability error (0.5 μm, $k = 2$). To ensure the accuracy in current measurements, additional verification measurements were performed using a 50-mm glass scale positioned close to the area where the apertures were measured (Figure 6).

The position of each scale mark on the glass scale is taken as the middle between the two edges of a scale line. The reference values for the glass scale were

Downloaded By: [Hemming, Björn] At: 07:05 11 September 2007

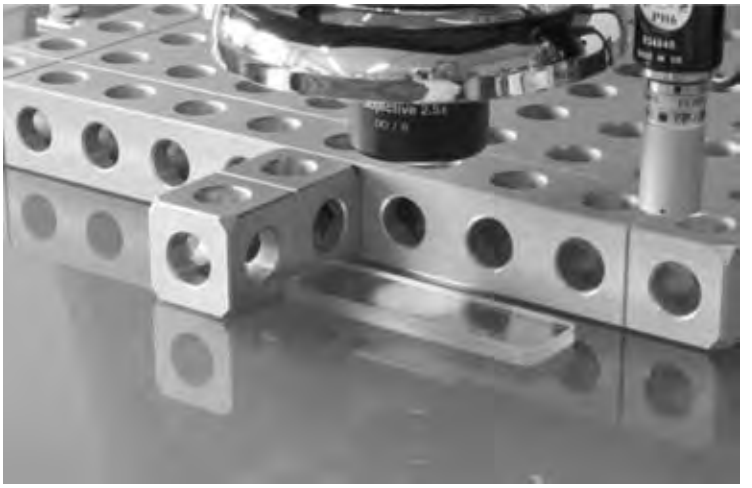

Figure 6. Verification measurements using a reference glass scale in the same position as the aperture.

measured using the MIKES line-scale interferometer (Lassila et al. 1994). The uncertainties of the reference values are almost negligible in this case (0.09 μm, $k = 2$) and by repeating the measurement of this glass scale at the optical CMM, the error of the CMM scale and repeatability error can be evaluated. Averaging a large number of measurements (point by point) shows a systematic contribution below $\pm 0.6\,\mu m$ (Figure 7), and from these measurements the standard deviation for each point was 0.2 μm. The systematic contribution is assumed to come from the error of the CMM scale. These results are in agreement with the above mentioned division of the measurement uncertainty into a component of 0.6 μm for the CMM scale and 0.5 μm for the CMM repeatability (at coverage factor $k = 2$).

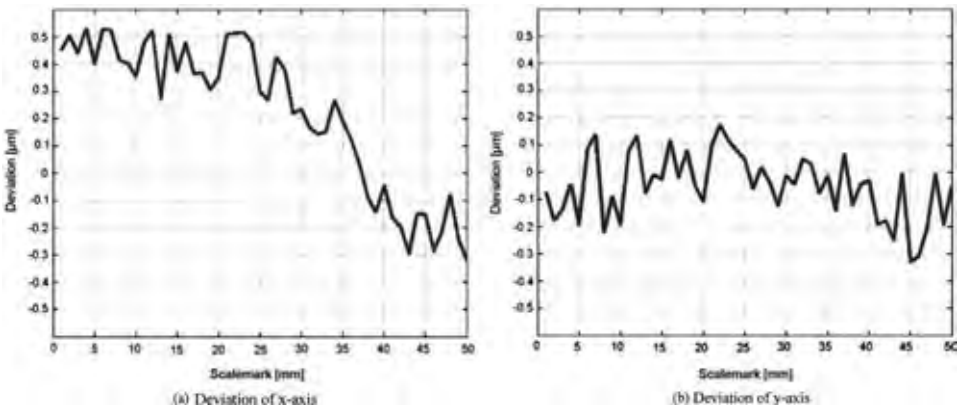

Figure 7. Difference between the values measured with MIKES line scale interferometer and Mitutoyo Quickvision in the direction of the *a*) *x*-axis and *b*) *y*-axis.

Downloaded By: [Hemming, Björn] At: 07:05 11 September 2007

5.2. The Simplified Measurement Model

When estimating measurement uncertainty according to the guidelines presented in GUM (1993), the first task is to write a formula for the measurement model. The basic measurement model for a simple two-point diameter (D) measurement in the direction of the x-axis is

$$D = x_2 - x_1 + \delta x_1 + \delta x_2 + \delta r_1 + \delta r_2 + \delta e, \tag{1}$$

where x_1 and x_2 are the first and second measured coordinates, δx_1 and δx_2 are the repeatability errors, δr_1 and δr_2 are the errors from edges of the measured object (roundness errors), and δe is the edge detection error for diameter. The errors δr_1 and δr_2 are due to roundness errors in the horizontal plane of the aperture, and the edge detection error δe depends on user selected illumination, focus and sharpness of the edge. In one measurement, parameter D is calculated only from the estimates x_1 and x_2 but the measurement model contains also contributions from errors. The principle of two-point measurement is shown in Figure 8.

The measurements were actually made of 120 points and the resulting diameter can be interpreted as the mean $\overline{D}$ of 60 diameter measurements. Therefore, the effect of the repeatability error (δx_1 and δx_2) and the roundness error, including roughness, (δr_1 and δr_2) should be decreased by the factor $1/\sqrt{60}$. The position of the found edge depends on user selected illumination, focus, and sharpness of the edge. The related error δe is of systematic type and cannot be reduced by averaging and thus the measurement model of repeated measurements is rewritten as

$$\overline{D} = \frac{1}{60}\sum_{m=1}^{60}[x_{2,m} - x_{1,m} + \delta x_{1,m} + \delta x_{2,m} + \delta r_{1,m} + \delta r_{2,m}] + \delta e. \tag{2}$$

The contribution of the uncertainty component δe was studied by changing illumination. It should be noted that this uncertainty component is much more complicated in the detection of the aperture edge than, for example, in the detection

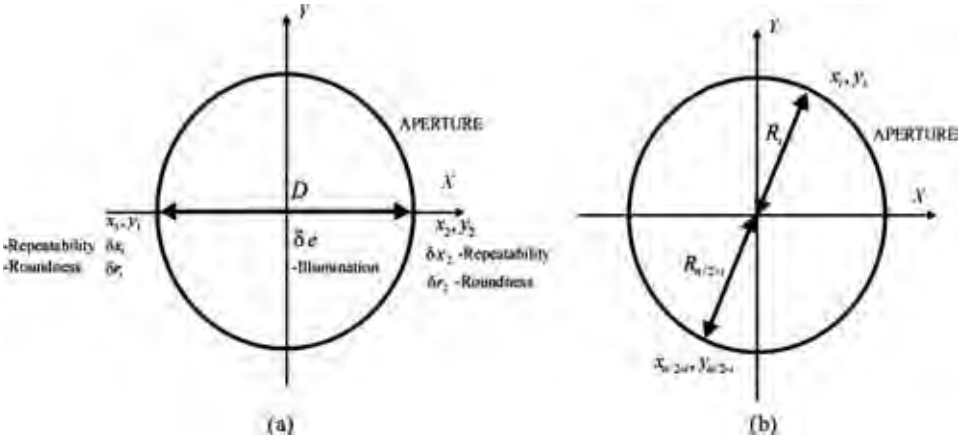

Figure 8. *a*) Two-point measurement of diameter and *b*) multi-point measurement of diameter.

Downloaded By: [Hemming, Björn] At: 07:05 11 September 2007

of the scale mark distances on the reference glass scale. When using stage light, the aperture is between the camera and the light source. The aperture appears as dark area and at the edge there is a transition of illuminance level. When illumination is increased, the amount of light coming to the CCD camera increases, and finally the whole image would be saturated to bright signal. Before this happens, it can be seen that the transition range between dark and bright seems to move away from the bright area. This phenomenon increases the diameter of bright holes, and decreases the width of dark lines on glass scales. However, the distance between the centers of the scale marks remains unaffected when the position of the scale marks is taken as the center of the dark lines.

One matte aperture (HUT-1) and one bright aperture (HUT-9) were measured with a large range of combinations of coaxial and stage light. The standard deviation of obtained diameters was 0.86 μm for the matte aperture and 0.61 μm for the bright aperture. The results for the illumination experiment for the matte aperture are given in Table 3. It is seen that strong illumination (50% column for stage light) leads to roughly 4 μm larger diameter than with moderate or zero stage light. However, the user also receives a ''saturation warning'' so these diameter results are excluded from the data when calculating the above mentioned standard deviations. The standard uncertainty related to δe is estimated to be 1 μm, from Table 3. The value is conservative and rounded upwards to include the contribution of effects which can not be addressed by varying illumination conditions.

Next, the error of roundness type is dealt with. When the diameter measurement was immediately repeated, the variation in results was typically only 0.1 μm. However, if the aperture was removed and measured again, with 120 points, in a slightly different position, the change in diameter was typically 0.1 μm–0.5 μm, indicating a considerable reproducibility error. The reason is seen in Figure 3; i.e., the edge appears to be rough and uneven. The roundness error was typically within ±4 μm. The related standard uncertainty, assuming a rectangular distribution, is $\delta r_1 = \delta r_2 = (4\,\mu\text{m})/\sqrt{3} = 2.31\,\mu\text{m}$ (GUM 1993).

Table 3. Effects of illumination on the diameter of a matte aperture (HUT-1), in millimetres. The illumination selected for measurements of matte apertures was 80% for coaxial light and 0% for stage light

Coaxial light illumination magnitude [%]	Stage light illumination magnitude [%]				
	0	20	30	40	50
0		3.0071	3.0074	3.0084	3.0115
10					
20		3.0073	3.0075	3.0084	3.0115
30					
40					
50	3.0064	3.0076	3.0076	3.0087	3.0116
60	3.008				
70	3.0081				
80	3.0079	3.0079	3.0076	3.0096	3.0121
90	3.008				
100	3.008	3.008	3.0084	3.0105	3.0128

Downloaded By: [Hemming, Björn] At: 07:05 11 September 2007

Table 4. Uncertainty budget for an averaged diameter measurement

	Uncertainty Component	Standard uncertainty [μm]
x_1	Uncompensated error of CMM scales	0.30
$\delta x_1/\sqrt{60}$	Repeatability for one point	0.03
$\delta r_1/\sqrt{60}$	Local error of edge of measured object	0.30
x_2	Uncompensated error of CMM scales	0.30
$\delta x_2/\sqrt{60}$	Repeatability for one point	0.03
$\delta r_2/\sqrt{60}$	Local error of edge of measured object	0.30
δe	Edge detection	1.00
	Combined standard uncertainty ($k = 1$)	1.17
D	Expanded uncertainty ($k = 2$)	2.33

The uncertainty budget for the simplified model is shown in Table 4. The expanded measurement uncertainty for the average diameter is 2.33 μm ($k = 2$) and the corresponding relative standard uncertainty is 8×10^{-4} for a 3-mm-diameter aperture.

For analysis of the stability of the apertures, the uncertainty component δe is zero assuming no changes in ambient illumination or ageing of light bulbs in the optical CMM. It may also be assumed that the effect of the uncompensated systematic error of the CMM scales can be neglected in a reproducibility analysis. With these assumptions, the expanded diameter uncertainty of Table 4 is reduced to 0.85 μm ($k = 2$) for analysis of temporal drift of the aperture diameters. From data in Table 2, it can be calculated that the standard deviation of one measured aperture was on the average 0.29 μm.

During the measurement series the variations of temperature were less than ±0.55 K. The thermal expansion of the glass scale of the optical CMM is very low (0.08×10^{-6}/K) and the dimension of the aperture is small. Therefore, variation in the average temperature of the measurement is not significant and is not included in the uncertainty analysis. Another temperature-related error source is the rapid change of temperature of the CMM body structure during one measurement. In an experiment using a 2000-W heat-fan warming at one side of the CMM, the sensitivity of 0.6 μm/K was found for the diameter measurement. During the measurements, the slow changes of temperature in the measurement laboratory can therefore be neglected.

5.3. Measurement Model for Actual Geometry and Monte-Carlo Simulations

The measurement model of Eq. (2) contains only x-axis components and is therefore not entirely correct. The next step is to rewrite the equation to match the actual measurement of n points giving $n/2$ diameters (Figure 8) along the circumference.

$$D_i = R_i + R_{n/2+i} + \delta e, \quad i = 1 \ldots n/2, \tag{3}$$

Downloaded By: [Hemming, Björn] At: 07:05 11 September 2007

where

$$R_j = \sqrt{(x_j + \delta x_j)^2 + (y_j + \delta y_j)^2} + \delta r_j, \quad j = 1..n \tag{4}$$

Equation (3) can be interpreted as the sum of 60 pairs of opposite 120 radii giving 60 diameters.

The Monte-Carlo method is clearly useful in uncertainty analysis in metrology (Brizzard et al. 2005; Mudronja et al. 2003). Briefly, the idea is to simulate the measurement model M times using random numbers. According to the law of large numbers the distribution of the M outputs of the model converge to the actual distribution if the input distributions are reasonably correct. The systematic part of the uncompensated error of the CMM is simulated by a sine function with an amplitude of 0.5 μm, and the repeatability of the CMM is simulated by a normal distribution. The edge detection and local error of the measured object were also simulated by normal distributions based on standard uncertainties described in the previous sections.

The measurement model was implemented in Matlab using random numbers from these distributions. The measurement software of the CMM uses least-squares circle fitting, and least-squares circle fitting was also included in the measurement model in Matlab. Finally, the standard deviation and the 95% confidence interval are calculated from the distribution.

The 95% coverage interval for diameter based on 100,000 simulations from the distribution of the simulated values is 2.1 μm (Figure 9). This is slightly less than the result in Table 4 (2.33 μm). A major advantage with the Monte-Carlo approach is the correct simulation of the measurement strategy, and now the number of measurement points n can be easily changed in the model. Table 5 shows that if the number of measurement points in the model is changed from 120 to 2 points, the expanded uncertainty from the simulation is 6.7 μm which is close to the value 6.6 μm obtained

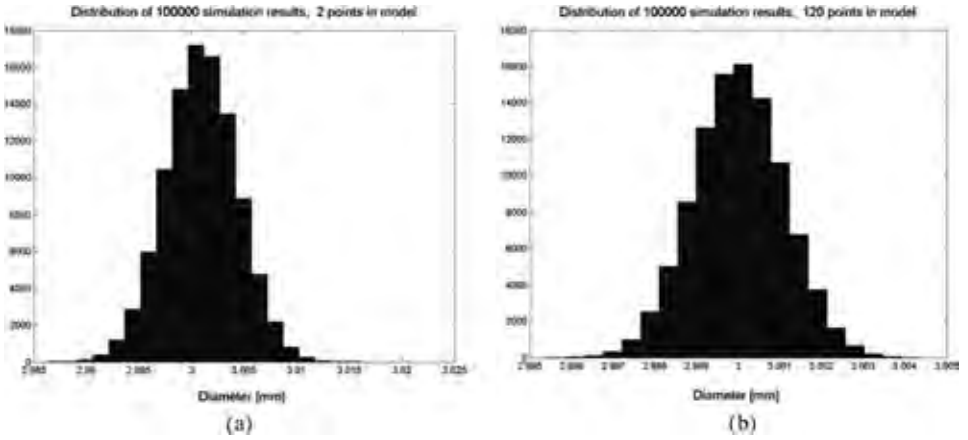

Figure 9. Distribution of the simulated diameter measurements using *a*) 2 points and *b*) 120 points.

Downloaded By: [Hemming, Björn] At: 07:05 11 September 2007

Table 5. Measurement uncertainty and reproducibility using Monte-Carlo simulation

n	Uncertainty at 95% confidence level, [μm]	Reproducibility at 95% confidence level [μm]
2	6.7	6.4
4	4.9	4.5
12	3.3	2.6
36	2.5	1.5
60	2.3	1.2
120	2.1	0.8
360	2.0	0.5

for 2-point measurement with the values in Table 4. The reproducibility according to the simulation with 120 points is 0.8 μm, slightly less than the result of 1.2 μm in the previous section.

6. CONCLUSION

The optical CMM was found to be a suitable device for the diameter measurement of optical apertures. The repeatability of the aperture measurement results is very good with a typical standard deviation of 0.2 μm for a point and 0.1 μm for the mean diameter (average from 120 points). The reproducibility, affected by roundness error of the specimen, temperature and ambient light, is much larger, about 1 μm ($k = 2$) for the diameter obtained as an average of 120 points.

Although some of the measured changes in the aperture diameter are close to the estimated reproducibility of the measurement, the nature of these variations suggests that there has not been any systematic growth or shrink, for example, from oxidation or stresses of the apertures. Therefore, it appears that the aperture diameters have been stable during the studied period.

Earlier experiences with the optical CMM and the comparisons with the probing CMM have shown a large operator-dependent factor which probably can be traced to illumination selections. The expanded measurement uncertainty for average diameter is 2.33 μm ($k = 2$). However, in this study the measurements with the probing CMM appear to confirm the optical CMM's result very well. The conclusion is that if the required relative uncertainty in the aperture area is of the order of 0.1% the optical CMM used in this study is useful for aperture diameter measurements.

REFERENCES

Brizard, M., M. Megharfi, and C. Verdier. 2005. Absolute falling-ball viscometer: Evaluation of measurement uncertainty. *Metrologia* 42(4):298–303.

Chan, F. M., T. King, and K. Stout. 1996. The influence of sampling strategy on a circular feature in coordinate measurements. *Measurement* 19(2):73–81.

Fowler, Joel, R. Saunders, and Albert Parr. 2000. Summary of high-accuracy aperture-area measurement capabilities at the NIST. *Metrologia* 37(5):621–623.

Downloaded By: [Hemming, Björn] At: 07:05 11 September 2007

Fowler, Joel, R. Durvasula, and Albert Parr. 1998. High-accuracy aperture-area measurement facilities at the National Institute of Standards and Technology. *Metrologia* 35(4):497–500.

Fowler, Joel and Maritoni Litorja. 2003. Geometric area measurements of circular apertures for radiometry at NIST 2003. *Metrologia* 40(1):S9–S12.

Guide to the expression of uncertainty in measurement (GUM). 2004. Supplement 1: Numerical methods for the propagation of distributions using a Monte Carlo Method (ISO), draft.

Hartmann, Juergen, Joachim Fischer, and Joachim Seidel. 2000. A non-contact technique providing improved accuracy in area measurements of radiometric apertures. *Metrologia* 37(5):637–640.

International Organization for Standardization (ISO). 1993. Guide to the expression on uncertainty in measurement (GUM); Geneva.

Kiviö, Heli, Tero Ristonen, Jaakko Salmi, and Heikki Tikka. 2004. Comparison of optical CMMs. VDI/VDE-GMA, Proceedings of the 8th International Symposium on measurement and quality control in production. 145–156.

Köhler, Rainer, Michael Stock, and C. Garreau. 2004. Final report on the international comparison of luminous responsivity CCPR-K3.b. *Metrologia* 41(1A) Tech Suppl.:1–30.

Kubarsepp, Toomas, Petri Kärhä, Manoocheri Farshid, Nevas Saulius, Ylianttila Lasse, and Ikonen Erkki. 2000. Spectral irradiance measurements of tungsten lamps with filter radiometers in the spectral range 290 nm to 900 nm. *Metrologia* 37(4):305–312.

Ikonen, Erkki, Pasi Toivanen, and Antti Lassila. 1998. A new optical method for high-accuracy determination of aperture area. *Metrologia* 35(4):369–372.

Lassila, Antti, Pasi Toivanen, and Erkki Ikonen. 1997. An optical method for direct determination of the radiometric aperture area at high accuracy. *Meas Sci Technol* 8(9):973–977.

Lassila, Antti, Erkki Ikonen, and Kari Riski. 1994. Interferometer for calibration of graduated line scales with a moving CCD camera as a line detector. *Applied Optics* 33(16): 3600–3603.

Lazzari, Annarita and Gaetano Iuculano. 2004. Evaluation of the uncertainty of an optical machine with a vision system for contact-less three-dimensional measurement. *Measurement* 36(3–4):215–231.

Martin, John, N. Fox, N. Harrison, B. Shipp, and M. Anklin. 1998. Determination and comparisons of aperture areas using geometric and radiometric techniques. *Metrologia* 35(4):461–464.

Mitutoyo America Corporation. 2001. *Hyper quick vision brochure, bulletin no 1510*. Paramus, NJ: Mitutoyo America Corporation.

Mudronja, Vedran, Biserka Runje, and Srdan Medic. 2003. Examples of applying Monte Carlo simulations in the field of measurement uncertainties of the standard of length. Proceedings of the XVII IMEKO World Congress, 1130–1134.

Puttock, M. and E. Thwaite. 1969. Elastic Compression of Spheres and Cylinders at Point and Line Contact, National Standards Laboratory Technical Paper No. 25, Division of Appled Phyics, National Standards Laboratory, Commonwealth Scientific and Industrial Research Organization (CSIRO), University Grounds, Chippendale, New South Wales, Australia.

Razet, Annick and Jean Bastie. 2006. Uncertainty evaluation in non-contact aperture area measurements. *Metrologia* 43(5):361–366.

Stock, Michael and Roland Goebel. 2000. Practical aspects of aperture-area measurements by superposition of Gaussian laser beams. *Metrologia* 37(5):633–636.

Woolliams, Emma R., Nigel P. Fox, Maurice G. Cox, Peter M. Harris, and Neil J. Harrison. 2006. Final report on CCPR K1-a: Spectral irradiance from 250 nm to 2500 nm. *Metrologia* 43(1A) Tech Suppl.:1–396.

III

Publication III

B. Hemming and H. Lehto, “Calibration of Dial Indicators using Machine Vision,” *Meas. Sci. Technol.* **13,** 45-49 (2002).

http://www.iop.org/EJ/abstract/0957-0233/13/1/306/

© 2002 IOP, http://www.iop.org/EJ/journal/MST

Reprinted with permission.

INSTITUTE OF PHYSICS PUBLISHING MEASUREMENT SCIENCE AND TECHNOLOGY
Meas. Sci. Technol. **13** (2002) 45–49 PII: S0957-0233(02)25083-3

Calibration of dial indicators using machine vision

Björn Hemming and Heikki Lehto

Centre for Metrology and Accreditation, Metallimiehenkj. 6 Espoo, FIN-02150, Finland

E-mail: Bjorn.Hemming@mikes.fi and Heikki.Lehto@mikes.fi

Received 22 May 2001, in final form 30 August 2001, accepted for publication 19 October 2001
Published 23 November 2001
Online at stacks.iop.org/MST/13/45

Abstract
Using automatic machine vision-based systems, the calibration of measuring instruments can be extended. With machine vision it is possible to check hundreds of points on the scale of a dial indicator, giving new insight into its sources of error.

This paper describes a machine vision-based system for the calibration of dial indicators developed at the Centre for Metrology and Accreditation in Finland, with emphasis on the calculation of measurement uncertainty.

Keywords: metrology, calibration, dial indicator, machine vision

(Some figures in this article are in colour only in the electronic version)

1. Introduction

The cost of calibration of a hand-held measuring device such as a micrometer, calliper or dial indicator is roughly equivalent to the price of a new instrument. Manual calibration therefore usually involves checking a mere 10 to 20 points. This only gives a rough figure of the precision of the instrument and is not a complete check of the scale. To reveal the sources of error for a typical dial indicator, many more points should be checked. If a dial indicator is used for quality checking on a factory production line measuring the same dimension thousands of times each year wear might occur and there would be errors at this single point on the scale of the dial indicator. If manual calibration was performed this wear would probably not be revealed and the result would be quality problems when the dial indicator gave incorrect dimensions to the part on the production line.

With automatic machine vision-based systems the calibration can be extended to several hundred points, giving a more complete picture of the errors. Developing a system of this kind is now both cheap and easy, and machine vision-based measurement systems of similar complexity have been developed in many laboratories and throughout industry. However, during development work the calculation of the uncertainty of measurement is often poorly reported. A calculation of uncertainty of measurement can be regarded as good if it complies with the guidelines given in the *Guide to the Expression of Uncertainty in Measurement* [1].

A commercially available instrument is offered by the Steinmeyer Feinmess corporation. This system is based on a video camera and a motorized length transducer. The Institute of Nuclear Energy in Bucharest has developed a laser interferometer-based instrument [2]. In this instrument the linear displacement of the dial indicator rod is measured by a Michelson interferometer. A specially designed angular transducer with phototransistors is placed over the face of the dial indicator. A vision system for calibration of a dial gauge torque wrench is also described in [3]. The problem of measuring the angle position of the pointer of a dial gauge torque wrench is similar to the measurement of the angle position of the pointer of a dial indicator.

In this particular field the authors have not found calculations of uncertainty of measurement. This paper describes a machine vision-based system, with emphasis on the calculation of measurement uncertainty. It is assumed that the reader knows the basics of the calculation of uncertainty according to [1] and is familiar with dial indicators.

2. The developed instrument

The operating principle is shown in figure 1. With future expansion of the instrument in mind, it was originally designed to be bigger than required for the calibration of dial indicators (figure 2). The instrument consists of a motorized stage (Physik Instrumente M 405.DG), a holder for the dial indicator

 © 2002 IOP Publishing Ltd Printed in the UK

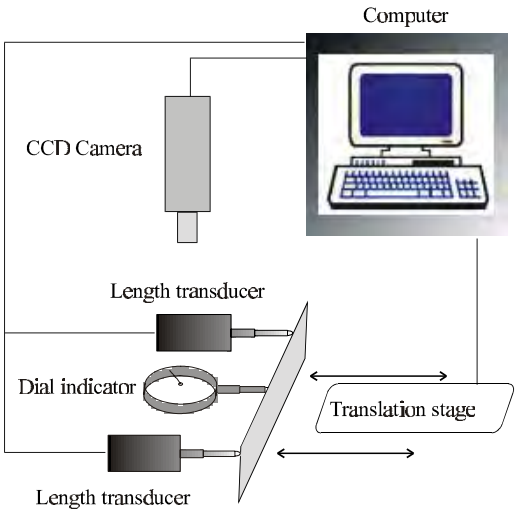

Figure 1. Operating principle of the instrument.

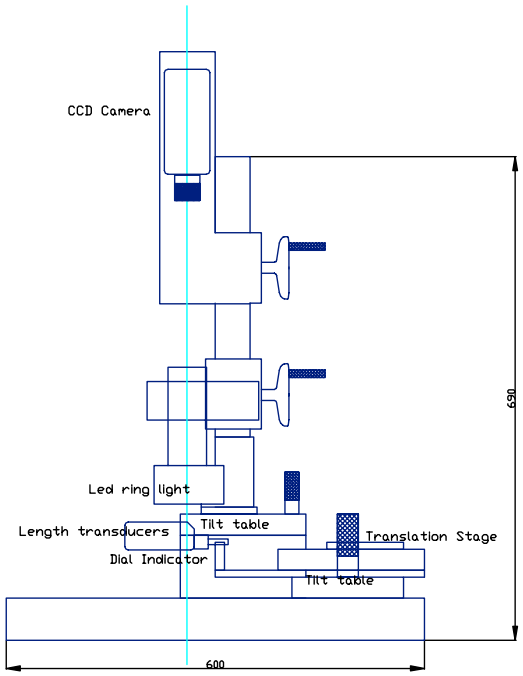

Figure 2. The developed instrument.

and two length transducers (Heidenhein MT25), and a height-adjustable red LED ring light (CSI FPR-100) together with a CCD camera (figure 3). A fibre ring light was also tested but reflections occurred on the glass of the dial indicator under test. The ring light has 65 LEDs, and by adjusting it to the appropriate height there are almost no shadows or glints on the dial indicator.

A CCIR standard camera (Cohu 4910) with resolution 752 × 582 was installed with a 50 mm Rainbow G50 lens. The position of the stage was measured by the two length transducers and their average used as a position reference to eliminate the Abbe error. The software was written with the Visual Basic 6 development tool in Windows NT 4 using the Matrox ActiveMIL library.

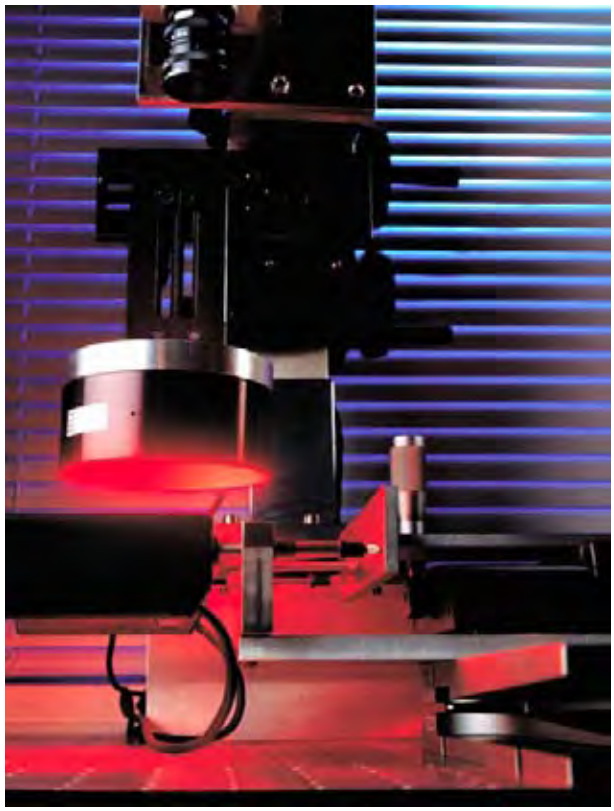

Figure 3. The ring light and length transducers (photo E Makkonen).

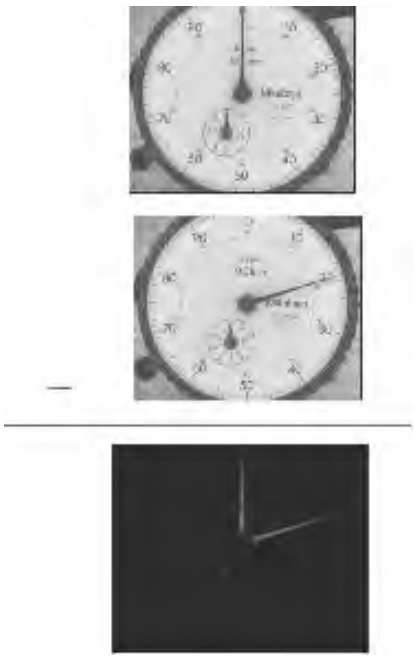

Figure 4. Subtraction gives a pixel by pixel difference between the images.

3. Image aqcuisition and segmentation

The image is digitized at the frame grabber (Matrox Meteor II) to a resolution of 768 × 576. In order to exclude unwanted features from the image a simple method also used in [3] was

Figure 5. Measurement of the scale marks on the dial.

implemented. Removal of the static background comprising the dial is done by the subtraction of two images of the dial (figure 4). Since the pointers are the only moving part of the dial, subtraction results in the removal of everything in the images except the pointers [3]. The resulting image is of good quality and it was felt that thresholding would not increase the edge-finding precision. It is assumed that the large pointer is on its right lap, making it unnecessary to measure the position of the small pointer. The position of the outer part of the large pointer is found using the edge-finding functions of the MIL library. The centre of the pointer is given by the user mouse-clicking on a pair of points on the image of the dial indicator assumed to be symmetrical to the centre. The angle of the large pointer is calculated from the line crossing the assumed static centre and the established position of the outer part of the pointer. Calibration of the scale marks on the dial is also implemented in the software as a separate task (figure 5).

4. Results

The first test on the system was performed with an almost new Compac dial indicator with scale marks at 0.01 mm division. The error curve of the dial indicator in figure 6 shows that to get a complete picture of the errors several hundred points need to be measured. Figure 6 shows an oscillating pattern in the error curve. This frequency information can be further studied by calculating the spectrum using a Fourier transform (figure 7). In signal analysis the spectra are usually plotted as a function of frequency, but in length metrology the wavelength is more informative. The spectrum reveals harmonics at wavelengths of 0.625, 1 and 12.5 mm which possibly correspond to respective sources of error in the mechanism of the dial indicator.

5. Uncertainty budget

The principle of the calculation of uncertainty of measurement is described in [1] and a complete worked example for gauge blocks is described in [5]. The error sources should be evaluated from measurements, experiment, data sheets or experience. The error ΔL of a 0.01 mm division dial indicator is obtained from the relationship

$$\Delta L = L_p - \Delta L_k - L_{\text{ref}} \tag{1}$$

where L_p is the measured pointer position of the dial indicator, ΔL_k is the measured error of the kth scale mark on the dial indicator and L_{ref} is the reference position.

The pointer position L_p of a 0.01 mm division dial indicator is obtained from the relationship

$$L_p = \frac{1}{2\pi} \tan^{-1}\left[\frac{x_c - x_m}{y_m - y_c}\right] + \delta L_\alpha \tag{2}$$

where x_m, y_m is the position of the indicator tip found by

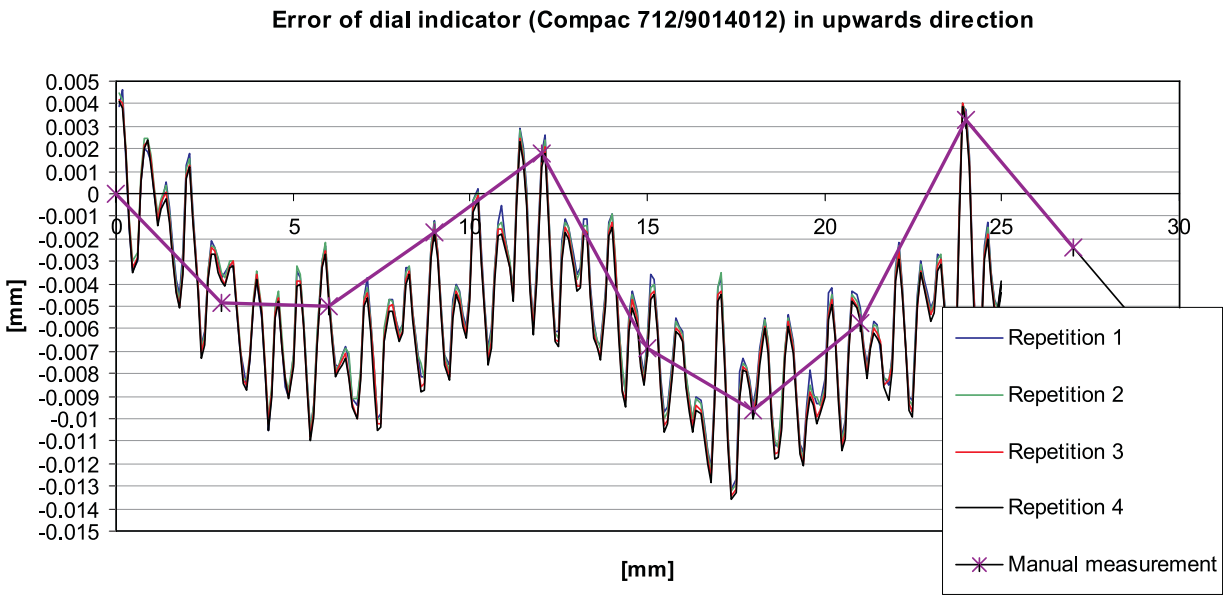

Figure 6. Error curve of a dial indicator measured manually and using the developed machine vision system with four repetitions.

Table 1. Uncertainty budget for the pointer of a 0.01 mm graduated dial indicator over a movement of 10 mm. Ideally the angle of the indicator should be 0°, but in this example the position of the indicator is found half a pixel away at 365.5, 166.

Uncertainty component	Estimate	Standard uncertainty	Distribution	Sensitivity coeff.	Uncertainty	Degrees of freedom
δL_α	0	1.0°	Normal	0.01 μm/°	0.01 μm	8
x_c	366 pixels	0.23 pixel	Rectang.	0.94 μm/pixel	0.22 μm	7
y_c	311 pixels	0.23 pixel	Rectang.	0.94 μm/pixel	0.22 μm	7
x_m	365.5 pixels	0.34 pixel	Rectang.	0.94 μm/pixel	0.32 μm	6
y_m	116 pixels	0.34 pixel	Rectang.	0.94 μm/pixel	0.32 μm	6
L_p	0.4 μm				0.55 μm	22

Table 2. Uncertainty budget for the scale mark 0.0 mm ($k = 1$) on the dial of a 0.01 mm graduated dial indicator. Ideally the mark should be 0°, but in this example the position of the indicator is found 0.2 pixel away at 365.8, 81.

Uncertainty component	Estimate	Standard uncertainty	Distribution	Sensitivity coeff.	Uncertainty	Degrees of freedom
k	1	— —	—	— —	—	—
δL_α	0	1.0°	Normal	0.01 μm/°	0.01 μm	8
x_c	366 pixels	0.23 pixel	Rectang.	0.66 μm/pixel	0.15 μm	7
y_c	311 pixels	0.23 pixel	Rectang.	0.66 μm/pixel	0.15 μm	7
x_k	365.8 pixels	0.34 pixel	Rectang.	0.66 μm/pixel	0.22 μm	7
y_k	81 pixels	0.34 pixel	Rectang.	0.66 μm/pixel	0.22 μm	7
ΔL_k	−0.1 μm				0.38 μm	25

Table 3. Uncertainty budget for the reference position together with the mechanical error sources.

Uncertainty component	Estimate	Standard uncertainty	Distribution	Sensitivity coeff.	Uncertainty	Degrees of freedom
$\delta\Delta L$	0 mm	0.3 μm	Normal	1	0.30 μm	5
L_i	10 mm	0.24 μm	Rectang.	1	0.24 μm	5
δL_β	0	0.5°	Normal	0.04 μm/°	0.02 μm	8
δL_T	0 K	1 K	Normal	0.12 μm/K	0.12 μm	5
L_{ref}	10 mm				0.40 μm	12

Table 4. Uncertainty budget for the measurement error of a 0.01 mm graduated dial indicator over a movement of 10 mm. The number of laps of the pointer are not counted and $L_{\text{ref}} = 0$ mm is used instead of 10 mm.

Uncertainty component	Estimate	Standard uncertainty	Distribution	Sensitivity coeff.	Uncertainty	Degrees of freedom
L_p	−0.4 μm	0.55 μm	Normal	1	0.55 μm	22
ΔL_k	0.1 μm	0.38 μm	Normal	1	0.38 μm	25
L_{ref}	0 μm	0.40 μm	Normal	1	0.40 μm	12
ΔL	−0.4 μm				0.78 μm	53

the edge finding algorithm, x_c, y_c is the estimated centre of the indicator and δL_α are the vertical plane alignment cosine errors.

The error ΔL_k of the scale marks noted as $k = 1, 2 \ldots 100$ is obtained from the relationship

$$\Delta L_k = \frac{1}{2\pi} \tan^{-1}\left[\frac{x_c - x_k}{y_k - y_c}\right] - 0.01k + \delta L_\alpha \qquad (3)$$

where x_k, y_k is the position of the kth scale mark found by the edge-finding algorithm, x_c, y_c is the estimated centre of indicator and δL_α are the vertical plane alignment cosine errors.

The errors in the camera and lens are about ±0.3 pixel in the x and y directions measured with the calibration grid [4]. The standard uncertainty, assuming a rectangular distribution, is

$$\frac{0.3 \text{ pixel}}{\sqrt{3}} = 0.18 \text{ pixel}.$$

The error for the edge-finding algorithm for the pointer is estimated to be ±0.5 pixel and the standard uncertainty is

$$\frac{0.5 \text{ pixel}}{\sqrt{3}} = 0.29 \text{ pixel}.$$

Adding the camera and lens errors gives

$$\delta x_m = \delta y_m = \sqrt{0.29^2 + 0.18^2} = 0.34 \text{ pixel}.$$

To estimate the centre of the indicator it is assumed that the user gives two pairs (divisor $\sqrt{4}$) of points, each having an uncertainty of ±0.5 pixel. The standard uncertainty is

$$\frac{0.5 \text{ pixel}}{\sqrt{4}\sqrt{3}} = 0.14 \text{ pixel}.$$

Adding the camera and lens errors gives

$$\delta x_c = \delta y_c = \sqrt{0.14^2 + 0.18^2} = 0.23 \text{ pixel}.$$

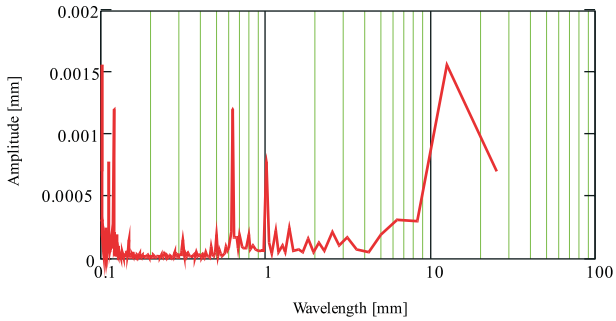

Figure 7. Spectrum of the error curve in figure 6 (repetition 1) as a function of wavelength.

The reference position L_{ref} together with the mechanical error sources is

$$L_{\text{ref}} = L_i + \delta L_T + \delta\Delta L + \delta L_\beta \tag{4}$$

where L_i is the average reading of the two length transducers used as reference, δL_β are the horizontal plane alignment cosine errors, $\delta\Delta L$ is the repeatability of the dial indicator and δL_T is the error due to thermal expansion caused by heating from the ring light.

The calibration result for the length transducers gives a ± 0.6 μm uncertainty for each length transducer for a 10 mm length. The distribution of the error is assumed to be rectangular (divisor $\sqrt{3}$) and the average reading of the two transducers (divisor $\sqrt{2}$) is used. The standard uncertainty is

$$\delta L_i = \frac{0.6\ \mu\text{m}}{\sqrt{2}\sqrt{3}} = 0.24\ \mu\text{m}.$$

The standard uncertainty for alignment cosine errors is estimated to be 0.5° for horizontal errors and 1° for vertical errors. The vertical is interpreted as squareness between the dial indicator and the optical axis of the camera and lens. The standard uncertainty for the repeatability of a good 0.01 mm graduated dial indicator is estimated to be 0.3 μm. The standard uncertainty for warming is estimated to be 1 K which corresponds to thermal expansion of 0.12 μm for a length of 10 mm.

An example of calculation of the uncertainty for the measured error of the dial indicator at one point for each group of error sources is shown in tables 1–3. The total combined uncertainty is shown in table 4. The tables also give values for the degrees of freedom. The degrees of freedom ν_i are estimated according to the relative uncertainty in the uncertainty $\Delta u/u$:

$$\nu_i = \frac{1}{2}\left[\frac{\Delta u(x_i)}{u(x_i)}\right]^{-2}. \tag{5}$$

The degrees of freedom are combined using the Welsh–Satterthwaite formula [1]:

$$\nu_{\text{eff}} = \frac{u_c^4(y)}{\sum_{i=1}^{N}\frac{u_i^4(y)}{\nu_i}}. \tag{6}$$

To express the expanded uncertainty at the 95% confidence level the combined standard deviation (table 4) is multiplied by 2.01 (t-distribution for $n = 53$ and 0.95) giving ± 1.57 μm.

When a dial indicator is calibrated manually, the uncertainty of the reading and interpretation of the pointer is of the same order as that obtained with the developed machine vision system.

6. Conclusion

Using machine vision in a normal routine calibration makes it possible to check hundreds of points on the scale of a dial indicator. This extension of the calibration gives new insight into the errors and error sources of the dial indicator. The frequency information of the error curve can also be studied by calculating the Fourier transform.

Questions of measurement error and uncertainty are often ignored. There are some natural reasons for this: if a new measurement system has been developed and it seems to work, why should anyone exceed the budget and timetable by making tests that might show that the instrument is not within the specification?

It is the view of the authors that the uncertainty budget is part of the design process for a of a measuring instrument, just like the drawings. Real confidence in a machine vision-based measuring instrument is only achieved by systematic documentation and calculation of the uncertainties as shown in this paper.

References

[1] ISO 1993 *Guide to the Expression of Uncertainty in Measurement* (Geneva: International Organization for Standardization)

[2] Sporea D G and Miron N 1996 Dial indicators checking-up by laser interferometry *Rev. Sci. Instrum.* **67** 612–14

[3] Aggarwal N, Doiron T and Sanghera P S Vision system for dial gage torque wrench calibration *Proc. SPIE* **2063** 77–85

[4] Tsai R Y 1987 A versatile camera calibration technique for high-accuracy 3D machine vision metrology using off-the-shelf TV cameras and lenses *IEEE J. Robot. Autom.* **3** 323–44

[5] Decker J E, Ulrich A and Pekelsky J R 1998 Uncertainty of gauge block calibration by mechanical comparison: a worked example for gauge blocks of dissimilar materials *Proc. SPIE* **3477** 225–46

IV

Publication IV

B. Hemming, A. Fagerholm, and A. Lassila, “High-accuracy Automatic Machine Vision Based Calibration of Micrometers”, *Meas. Sci. Technol.* **18**, 1655-1660 (2007).

http://www.iop.org/EJ/abstract/0957-0233/18/5/058/

©2007 IOP, http://www.iop.org/EJ/journal/MST

Reprinted with permission.

Meas. Sci. Technol. **18** (2007) 1655–1660 doi:10.1088/0957-0233/18/5/058

High-accuracy automatic machine vision based calibration of micrometers

B Hemming, A Fagerlund and A Lassila

Centre for Metrology and Accreditation, Tekniikantie 1, Espoo, FIN-02150, Finland

E-mail: Bjorn.Hemming@mikes.fi

Received 12 December 2006, in final form 7 March 2007
Published 13 April 2007
Online at stacks.iop.org/MST/18/1655

Abstract
The calibration of simple handheld instruments is often more expensive than the price of a new device. Therefore, the amount of manual labour is kept at a minimum in order to keep the price of calibration at a tolerable level. This also means that only a few points of e.g. a length scale can be checked. By using automatic machine vision based systems, the calibration of measurement instruments can be done faster and more thoroughly. In order to study the possibilities of machine vision automation for volume calibration tasks a set-up for micrometer calibration was constructed at Centre for Metrology and Accreditation (MIKES). With the developed automated machine vision system it is possible to check hundreds of points on the scale of a micrometer, giving new insight into error sources of the micrometer screw. The attained uncertainty is at the same level as calibration with gauge blocks according to ISO 3611.

Keywords: metrology, calibration, micrometer, machine vision

1. Introduction

The manual calibration of a micrometer calliper according to IS0 3611 is done by using ten gauge blocks [1]. This gives only a rough figure of the accuracy of the instrument and is not a complete check of the scale. To reveal the error sources of a typical micrometer, many more points should be checked. Possible error sources are zero setting error, form error on the measuring faces, pitch error and nonlinearities in the screw, location errors or bad quality of graduation lines on the thimble and variations in the measuring force.

During recent years many measurement tasks both in industry and in laboratories have been automated using machine vision. With automatic machine vision based systems the calibration can be extended to several hundred points, giving a more complete picture of the errors.

Two important matters in measurements and calibrations are traceability and measurement uncertainty. The complexity of measurement uncertainty increases along with the complexity of the measurement equipment. Accuracy and measurement uncertainty in machine vision were previously discussed thoroughly in papers [2–4], but the presentation differs from the approach in the *Guide to the Expression of Uncertainty in Measurement* (GUM) [5].

In a previous paper the author has presented equipment for automatic calibration of dial indictors [6]. In this paper the updating of that equipment into a calibration device for micrometers is described. Detailed uncertainty analysis following recommendations of GUM is also given.

2. The developed instrument

The calibration of a micrometer according to ISO 3611 includes flatness and parallellity inspection of the measurement surfaces, measurement of the measurement force of the micrometer, checking the zero adjustment and measurement of the micrometer scale. The measurement of micrometer screw errors and measurement of force can be done with the developed instrument.

The instrument consists of two motorized stages, a length transducer and a red LED ring light together with a CCD camera (figures 1 and 2). The rotation of the micrometer thimble is motorized through a flexible coupling. A plate is fastened to the measurement stage (motorized stage 1) and the micrometer is run against a ball attached to this plate. A force transducer can also be placed between this plate and the measurement surface of the micrometer. The position of the measurement stage is measured by a length

 © 2007 IOP Publishing Ltd Printed in the UK

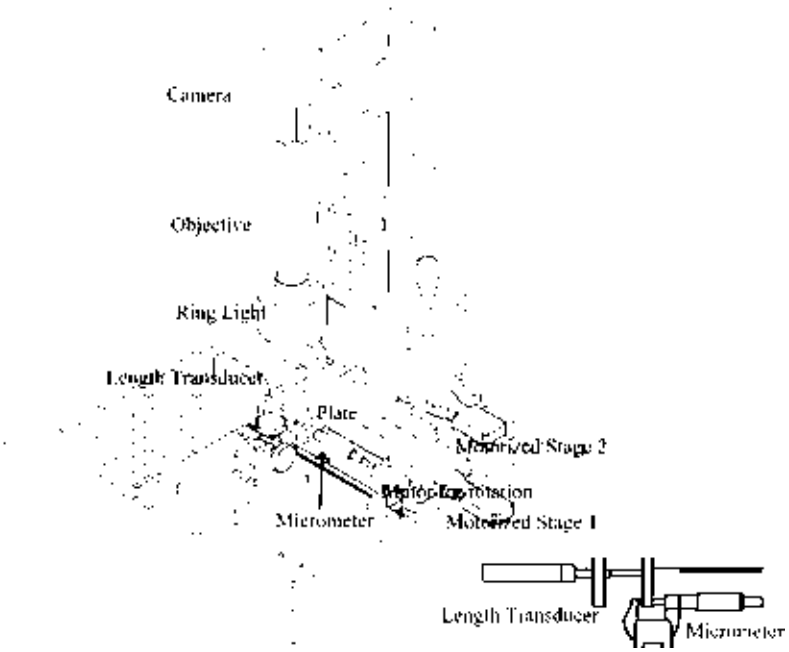

Figure 1. Drawing of the developed instrument.

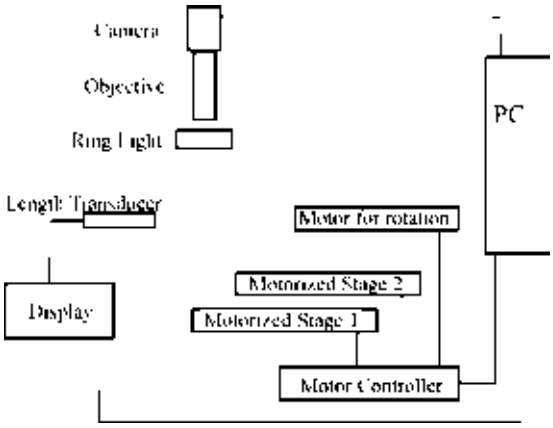

Figure 2. Schematic of the developed instrument.

transducer. A CCIR standard camera with resolution 752 × 582 is installed with a variable zoom objective. In order to achieve high accuracy, the field of view is small; therefore, another motorized stage (motorized stage 2) is needed to move the camera. The software was written using Visual Basic 6.

3. Image processing

At the frame grabber (Matrox Meteor II) the image is digitized to a resolution of 768 × 576. Although a zoom objective was used, the magnification is locked to a fixed magnification. The field of view is 4 mm × 6 mm and a typical image is shown in figure 3. The position of the division lines on the micrometer thimble is found using the pattern-matching function in the Matrox Mil library. The pattern matching in MIL is a speed optimized greyscale cross-correlation peak detection algorithm [7]. The accuracy of the algorithm is about 1/8 pixel, verified by using Matlab.

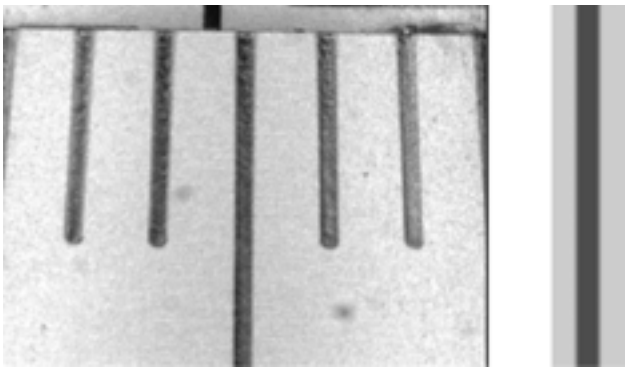

Figure 3. Typical image (left) and target (right).

On the thimble of a micrometer there are ten long division lines, and one revolution corresponds usually to 0.5 mm. The target for pattern matching is similar to the 0.05 mm division line of the thimble and it is generated by a Matlab script. Because the 0.05 mm division line of the thimble is longer than the 0.01 mm division line, only the 0.05 mm division line is found by the algorithm at the required score level. Typically the error of a small micrometer is below 5 μm. If there is a hypothetical error of 50 μm in the micrometer the software would give zero error as result. On most micrometers the thimble is bevelled and therefore the division line is parallel with the fiducial line only when the reading is zero, otherwise the division line will be tilted from vertical in the image. If the error of the micrometer exceeds 15 μm, the division line appears tilted, and the score of pattern matching is low and the user is notified.

4. Calibration procedure

First the zero setting of the micrometer is checked together with a manual measurement of a 5.1 mm gauge block. Then

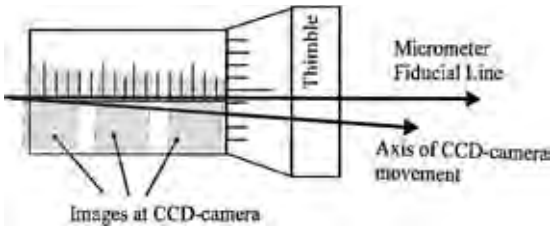

Figure 4. Measurement of the alignment error between the micrometer and the direction of movement of the camera.

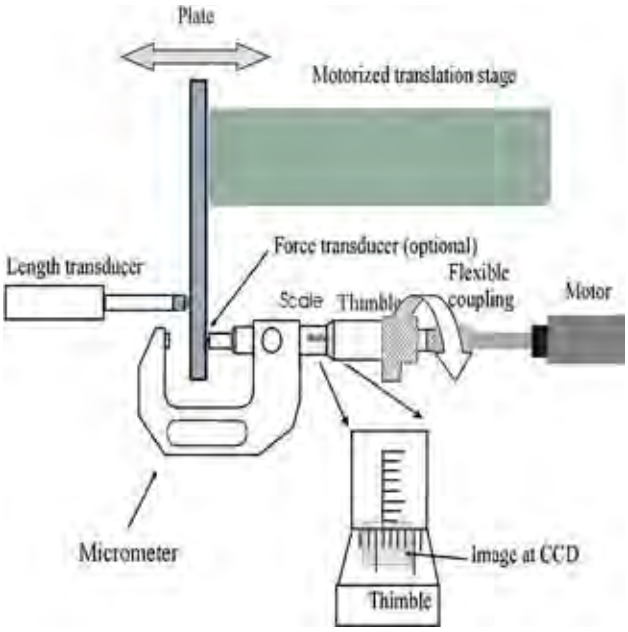

Figure 5. The operating principle of the instrument in an automatic calibration.

the micrometer is fastened to the clamp and aligned parallel to the length transducer using a dial indicator.

Then, the alignment error between the micrometer and the direction of the movement of the camera is measured (figure 4). This alignment error, which is smaller than 1°, is calculated from 15 images along the 5–25 mm range of the micrometer. The position of the fiducial line is found using the above-mentioned pattern-matching method. Using a least-squares line fit on the found positions of the micrometer fiducial line, an offset and a slope are obtained. This result is used to define the fiducial line in the camera coordinate system.

The next step is the automatic measurement of the micrometer screw errors where the length transducer is used as reference (figure 5). The calibration is done at 0.05 mm intervals but the operator can also specify a longer step length. The position of the division line in the image is measured (see figure 3) and the reading of the micrometer is the distance between the division line and the fiducial line, defined and measured earlier (see figure 4).

The time needed for setting up the micrometer is about 15 min and the duration of the automatic calibration of 400 points with 0.05 mm intervals is about 2 h. The time needed for the automatic measurement of one point is 18 s. The sequence for one point involves rotation of the thimble, movement of the measurement stage (motorized stage 1), movement of the camera (motorized stage 2), rotation of the thimble into contact, reading of the reference value and processing of the captured image. Each mechanical movement is allowed to take 3–4 s. A speed optimization and tuning of the written software would probably shorten the measurement time considerably. The manual ISO 3611 calibration of the micrometer screw using ten gauge blocks would take about 10 min, but the interval step is 2.1–2.6 mm. For a manual calibration the uncertainty is typically 2 μm ($k = 2$), and roughly half of this uncertainty comes from reading the thimble.

With the developed instrument it would be possible to measure also the measurement force during the automatic measurement of the micrometer scale. However, the deflections of the used force transducer were about ten times bigger (about 10 μm) than expected typical errors (about 1 μm) of the micrometer. Therefore, the measurement of force would influence the length measurements, which therefore have to be done with the force transducer removed.

To keep the measuring force stable throughout a measurement, the motorized thimble of the micrometer is turned making two clicks. This is a benefit compared to a manual calibration, because different human operators can cause large variations in force and measurement result, depending on the handling. With small changes the equipment is also ready to calibrate a dial indicator (see [6]).

5. Measurement uncertainty for an automatic calibration

A complete calculation of measurement uncertainty according to GUM includes a mathematical measurement model together with thorough description of each uncertainty component. The error sources were evaluated from measurements, experiment, data sheets or experience. The first step of an uncertainty analysis was formulating the model of the measurement. The measurement model is basically the expression used in the actual measurement software together with error sources named as corrections.

In the calibration of the micrometer only the position of the thimble is measured and the reading l_{ix} of the micrometer is

$$l_{ix} = c_x(x_i - x_0 - a \cdot L) + L \qquad (1)$$

where c_x is the magnification factor, x_i is the found position of the 0.05 mm division line of the thimble, x_0 is the position of the fiducial line at $L = 0$, a is the slope of the micrometer fiducial line in relation to the camera movement and L is the nominal length.

The magnification factor c_x is the relation between camera pixels and scale division lines at the thimble. By multiplying the slope a (pixel mm^{-1}) in equation (1) by the movement L (mm) the result is a correction for the alignment error (in pixels). The corrected position of the thimble (in pixels), relative to the fiducial line, is then multiplied by the scale factor c_x (μm/pixel).

The error E_x of a micrometer is obtained from the relationship

$$E_x = l_{ix} - l_s + \delta l_{ap} + \delta l_{ay} + \delta l_c + \delta l_p + \delta l_m + \alpha L \Delta t \qquad (2)$$

where E_x is the error of the micrometer; l_{ix} is the micrometer reading; l_s is the reference position; δl_{ap}, δl_{ay} are corrections for the Abbe error, due to offset between the measurement axis of the micrometer and the length transducer, with angular errors of translation stage; δl_c is the correction for cosine error between the micrometer and the length transducer; δl_p is the correction for flatness of the measuring surface of the micrometer; δl_m is the correction for repeatability errors (includes for example variations in measuring force and temperature); α is the thermal expansion coefficient of steel; L is the nominal length and Δt is the temperature difference of the micrometer from 20 °C.

Cosine error, δl_c

The alignment error or cosine error δl_c between the micrometer and the length transducer is tested to be easily adjustable within $\pm 0.4^\circ$. Most of the error sources are assumed to have a rectangular distribution and the standard uncertainty is calculated by dividing the variation by $\sqrt{3}$. The standard uncertainty for alignment is

$$\frac{0.4^\circ}{\sqrt{3}} = 0.23^\circ = 4 \text{ mrad}.$$

Magnification factor, c_x

The scale factor is calibrated using an interferometrically calibrated line-scale [8] the uncertainty of which is less than 0.1 μm/50 mm. The result of the calibration is a scale factor of 7.24 μm/pixel and a standard error of 0.03 μm/pixel. Here the main error source is in the focusing and vertical position adjustment of the lens. When a typical micrometer thimble is slightly turned an angle matching one 10 μm scale line the camera sees it as a displacement in the image of roughly 1 mm (see figure 3). This magnification increases the sensitivity of the above scale parameters by the factor 100. Therefore the 'micrometer-reading to pixel' magnification factor c_x is 0.0724 μm/pixel.

Found position, x_i

In machine vision systems used in laboratories the lens errors are typically about 0.1% of the field of view or roughly about ± 1 pixel. The errors of the pattern-matching algorithm are typically about 1/8 pixel. The errors in the developed machine vision system were evaluated using an accurate line-scale. Although lines of the glass scale are of better quality than the lines of a micrometer, the measurement is very similar to the measurement of the position of micrometer scale lines because the same algorithm is used. Now the typical error of a single scale line was ± 0.2 pixel in the image and assuming a rectangular distribution the corresponding standard uncertainty for x_i is 0.12 pixel.

Slope, a

The slope is determined from measurements of the fiducial line. The straightness of these measurements corresponds to errors in the movement of the translation stage of the camera. The standard uncertainty for the slope is estimated to be 0.008 pixel mm^{-1}.

Position of the fiducial line, x_o

The offset of the fiducial line is evaluated from linear regression together with the slope a. The standard uncertainty for this position is found to be typically 0.07 pixel.

Reference position, l_s

The accuracy of the length transducer is ± 0.5 μm, according to the manufacturer. However, the length transducer has been calibrated against a laser interferometer over several years and a systematic error, which is found to be stable, can be largely compensated. The remaining error is approximated to ± 0.2 μm, which corresponds to a standard uncertainty of 0.12 μm assuming a rectangular distribution.

Abbe error, δl_{ap}, δl_{ay}

Ideally when length scales are compared, they should be on the same axis. If the scales are not on the same axis, this offset multiplied by the sine of any angular deviation in the linear movement along the scale gives the Abbe error. The length transducer is vertically 6 mm and horizontally 18 mm from the centre of the micrometer screw axis (see figure 5). This gives an Abbe error δl_{ap} due to the pitch and δl_{ay} due to the yaw of the translation stage. The pitch is within ± 0.03 mrad and the yaw is within ± 0.02 mrad according to measurements made with an autocollimator. Assuming rectangular distributions the corresponding standard uncertainties are 0.0173 mrad for the pitch and 0.0115 mrad for the yaw.

Flatness of measuring faces, δl_p

The flatness of the measuring faces of a micrometer should be within ± 0.5 μm according to ISO 3611. Assuming a rectangular distribution the corresponding standard uncertainty would be 0.29 μm. In the developed equipment only the middle of the measuring surface is contacting the ball. Therefore, the standard uncertainty for the correction for flatness of the measuring surface is much smaller and it is approximated to be 0.1 μm.

Temperature difference, Δt

The equipment is operated in a temperature-controlled room. The temperature difference of the micrometer from 20 °C is estimated to be $\pm 1^\circ$ under typical conditions when performing calibrations, and assuming a rectangular distribution the standard uncertainty is 0.58°. As effective length for thermal expansion 20 mm is assumed. The rest of the temperature related uncertainties sources are supposed to be seen at repeatability test.

Repeatability errors, δl_m

The pooled standard uncertainty for repeatability errors, such as variations in measurement force and temperature, is approximated to 0.2 μm based on repeatability tests.

In table 1 the standard uncertainties are combined. The estimates in the second column in table 1 are only shown as an example. The sensitivity factors are found in the fifth column. Because of the formulation of the measurement model, the

Table 1. Uncertainty budget for the calibration of a micrometer with the developed instrument.

Quantity	Estimate	Distribution	Standard uncertainty	Sensitivity factor	Uncertainty contribution
Independent of length					
x_i	400 pixels	Rectangular	0.115 pixel	0.072 μm/pixel	0.008 μm
x_o	390 pixels	Normal	0.070 pixel	0.072 μm/pixel	0.005 μm
c_x	0.072 μm/pixel	Normal	0.0003 μm/pixel	5 pixels	0.002 μm
l_s	24.9995 mm	Normal	0.115 μm	1	0.115 μm
δl_{ap}	0 mrad	Rectangular	0.017 mrad	6 mm	0.104 μm
δl_{ay}	0 mrad	Rectangular	0.012 mrad	18 mm	0.208 μm
δl_p	0 μm	Normal	0.100 μm	1	0.100 μm
δl_m	0 μm	Normal	0.200 μm	1	0.200 μm
Length dependent					
Δt	0 K	Rectangular	0.580 K	0.0115 1/K L[a]	0.007 μm L
a	0.25 pixel mm^{-1}	Normal	0.008 pixel mm^{-1}	0.072 1/pixel L	0.001 μm L
δl_c	0 mrad	Rectangular	4.000 mrad	0.002 1/mrad L	0.008 μm L
L	20 mm				
E_x	0.86 μm		Independent of length		0.343 μm
			Length dependent (uncertainty)		0.010 μm L
			Expanded uncertainty ($k = 2$)		Q [0.685; 0.021L] μm
			Expanded uncertainty, $L = 20$ mm ($k = 2$)		0.802 μm

[a] L is length in mm.

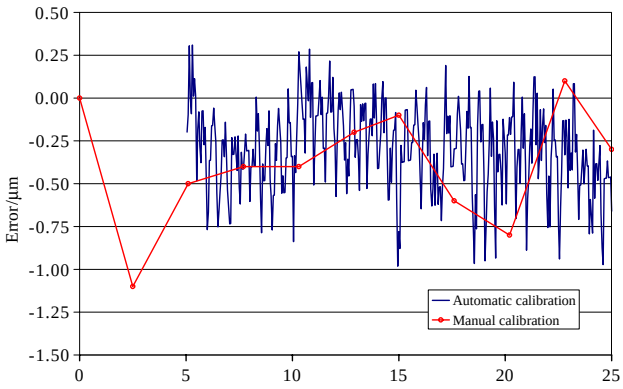

Figure 6. Calibration result using ten gauge blocks and using the automatic system.

(This figure is in colour only in the electronic version)

magnification factor c_x has a sensitivity factor which actually is the reading of the micrometer (see equation (1) and figure 3) and the value 5 pixels is shown as an example of a reading of 0.36 μm. The uncertainty budget shows that the error sources on the machine vision system are very small. The uncertainty contribution from the found position (x_i), magnification factor (c_x) and fiducial line (x_o and a) is only 0.05 μm ($k = 2$).

6. Results

Results from a manual calibration (ISO 3611) performed by an experienced technician together with results from an automatic calibration are shown in figure 6. The result from the automatic calibration gives a much more detailed picture of the errors of the micrometer than a manual calibration. In figure 6 there are fluctuations in the error curve which correspond to one revolution of the thimble, probably due to the flatness error in the measuring face of the micrometer. The slower fluctuation in the error curve might be due to the either pitch error in the screw or the Abbe error in the developed instrument. However, in this case the micrometer seems to be quite good with small errors of the screw. The agreement between different methods of calibration of a micrometer is acceptable. The differences can be explained by the uncertainties for each result.

7. Conclusion

Using machine vision in a normal routine calibration makes it possible to check hundreds of points on the scale of a micrometer. If a micrometer is used for quality checking at a production line in a factory measuring the same dimension thousands of times each year the result might be wear and errors at this single point of the scale of the micrometer. If manually calibrated this wear would probably not be revealed and the result would be quality problems when the micrometer gives wrong dimensions to the part at the production line.

The accuracy of the automatic calibration of a micrometer screw is better than the manual calibration because image processing works on a magnified image, and the variations in turning force are smaller than with a human operator. The purpose of this paper was to show the feasibility of traceable calibration of micrometers using machine vision. Although both machine vision methods and mechanical design of the equipment could be improved, the main conclusion is that the presented new approach has the potential to produce more than ten times more calibration results at an uncertainty which is less than 10% compared to the uncertainty of a manual calibration. In future improvements of the instrument the Abbe error should be minimized, more sophisticated machine vision methods could be used and the speed of the measurement program should be optimized.

References

[1] ISO 3611 1978(E) 1978 Micrometer callipers for external measurements 6 pp

[2] Tsai R Y A 1987 versatile camera calibration technique for high-accuracy 3d machine vision metrology using

off-the-shelf TV cameras and lenses *IEEE J. Robot. Autom.* **3** 323–44
[3] Robinson M *et al* 1995 The accuracy of image analysis methods in spur gear metrology *Meas. Sci. Technol.* **6** 860–71
[4] Yi S, Haralick R and Shapiro L 1993 Error propagation in machine vision *Mach. Vis. Appl.* **7** 93–114
[5] ISO (International Organization for Standardization) 1993 *Guide to the Expression of Uncertainty in Measurement* (Geneva, Switzerland: ISO) 110 pp
[6] Hemming B and Lehto H 2002 Calibration of dial indicators using machine vision *Meas. Sci. Technol.* **1** 45–9
[7] Wade A and Fitzke F 1998 A fast, robust pattern recognition system for low light level image registration and its application to retinal imaging *Opt. Express* **3** 190–7
[8] Lassila A, Ikonen E and Riski K 1994 Interferometer for calibration of graduated line scales with a moving CCD camera as a line detector *Appl. Opt.* **33** 3600–3